TESTING, EVALUATION AND SENSITIVITY ANALYSIS OF AN IN-SITU BIOREMEDIATION MODEL

A Thesis

Presented to the Faculty of the Graduate School

of Cornell University

in Partial Fulfillment of the Requirements for the Degree of

Master of Science

by

Brian L. Dosa

May 1994

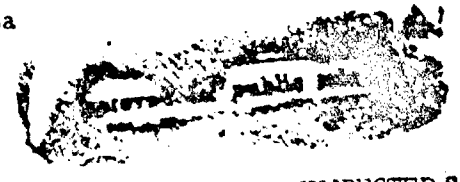

ABSTRACT

The testing, evaluation, and sensitivity analysis of an in-situ groundwater bioremediation model is presented. BIO2D is a two-dimensional, areal finite element model that incorporates oxygen limited Monod kinetics. It is validated using the International Groundwater Modeling Center's Level 1 Testing Protocol for its ability to model flow and transport of a conservative pollutant. Level 2 Testing is done for four hypothetical cases involving the cleanup of a phenol-contaminated aquifer. Predicted phenol concentrations are shown to be very close and slightly greater than solutions from the better known and tested model BIOPLUME II. It is shown that BIO2D outperformed BIOPLUME II in the final test, which involved an injection-extraction well doublet, due to greater mass balance errors and numerical dispersion in BIOPLUME II. Two potential improvements to BIO2D are presented. It is demonstrated that using an iterative solution technique is preferable to the linearized method. The proposed changes to the kinetic formulation need further testing however. A thorough sensitivity analysis of BIO2D is presented. The focus is on how the predicted concentrations change with uncertainty in the often unknown biological parameters. It is demonstrated that individual sensitivity alone is not sufficient. A technique of combined sensitivity called 2^k factorial design is applied to these parameters. It is shown that BIO2D is most sensitive to the Monod half saturation constant, K_s.

Biographical Sketch

Brian L. Dosa was born on January 5, 1963 in Ilion, New York. After attending high school in Delaware and Maryland, he entered the United States Military Academy at West Point. He received his B.S. degree in Civil Engineering in May, 1985. He was then commissioned as an officer in the U.S. Army Corps of Engineers. After serving in Army troop units he was selected for advanced schooling. In August 1992 he entered the M.S. program in the Department of Civil and Environmental Engineering at Cornell University, where his research was in the area of groundwater remediation modeling. After completion of the M.S. program he will return to West Point where he will teach civil engineering. He is a registered professional engineer in the state of Delaware.

For my wife Roberta, and my children Brian Jr., Philip, Rachel Mae and Emily.

Acknowledgements

I would like to thank my Lord Jesus, to whom belongs any praise I receive for my work. Without Him, all would be meaningless. I am also very thankful for my family and the invaluable support they provide.

I would like to thank my advisor, Professor Christine Shoemaker for her guidance and help in this research. I also thank Professor Gossett for serving on my committee and for the helpful comments on this thesis. Professors Liu, Liggett, and Brutsaert also provided valuable help along the way.

I was very fortunate to have the assistance of Warren Swanson in this research. His hard work and long hours on the computer were crucial to the success of this work. I am also grateful for very encouring and helpful officemates: Barbara Minsker, Chris Mansfield, Greg Whiffen, and Beth Eschenbach.

Finally, I am thankful for the help I received from Stewart Taylor, who wrote the biodegradation model studied. He also provided helpful comments on this thesis. Hanadi Rifai was also very helpful in my understanding of BIOPLUME II and the Method of Characteristics.

Financial support for this work came primarily from the U.S. Army and the

United States Military Academy. Computing resources were provided by the Cornell National Computing Facility (CNCF) through a Strategic User Award to Professor Shoemaker. The CNCF is funded inpart by the National Science Foundation, the State of New York, the IBM Corporation, and the Centers's Corporate Research Institute.

Table of Contents

List of Tables

List of Figures

Chapter 1

Introduction

The purpose of this research is to test and evaluate an in-situ groundwater bioremediation model named BIO2D. It was selected as the base model for ongoing optimization research at Cornell University. This work will scrutinize the model, subjecting it to rigorous and thorough validation and comparison testing, with the ultimate objectives of proving the model's validity, gaining valuable insights into its performance, and observing its sensitivity to the often uncertain biological parameters required as input.

Motivation for Research It is estimated that there are currently over 30,000 contaminated waste sites in the U.S. identified on the Comprehensive Environmental Response, Compensation and Liability Act (CERCLA) list *[Legrega et al., 1994]*. The Resource Conservation and Recovery Act (RCRA) list contains more than 5000 additional hazardous waste facilities. The extent of this national problem is enormous considering that a significant number of the 7 million underground storage tanks in the U.S. are estimated to be leaking *[Baker and Herson, 1994]*. The U.S. Army alone has identified over 10,000 individual potentially contaminated sites in 1265 active and closing installations. It is estimated that of these over 5000 require remedial action

[National Research Council, 1992].

Bioremediation The need to cleanup these sites has motivated the development of many new and innovative technologies. In 1986 CERCLA was ammended to encourage the use of remediation technologies that would result in permanent solutions *[Charbeneau et al., 1992].* One very promising method that often results in the detoxification and destruction of the contaminant (rather than the conventional approach of disposal) is bioremediation. Bioremediation is the use of microorganisms or microbial actions to detoxify and destroy environmental pollutants *[Baker and Herson, 1994].* Bioremediation is not a new tec' :ogy; rather, it is a new application of the same methods used to treat and trans .. .n domestic wastewater for the last 100 years. Both activated sludge and fixed-film processes are based on the exploitation of microorganisms in engineered systems. The application of bioremediation to the cleanup of hazardous waste sites offers the advantages of:

- on-site remediation, avoiding transport costs and liabilities
- elimination of the problem rather than merely moving it elsewhere
- reduction of costs and cleanup times in many cases
- utilizing an ecologically sound technology that applies natural processes

Bioremediation techniques have successfully been applied to a wide range of pollutants including polyaromatic hydrocarbons, volatile organics (benzene, toluene, ethylbenzene, and xylene - often noted as BTEX), pentachlorophenol, and phenols *[Charbeneau et al., 1992].* In addition, ketones, esters and chlorinated solvents (TCE, PCE) have been biodegraded *[Baker and Herson, 1994].*

This work focuses on the mathematical modeling of in-situ bioremediation, or biostimulation, of polluted aquifers where the existing subsurface microorganisms are

stimulated to accomplish the work of degrading the pollutants. This is accomplished by controlling their environment, and providing an electron acceptor (often in the form of O_2 or NO_3^-) to assist these organisms in "eating" the waste. This application of bioremediation has been successfully applied to numerous waste sites in the U.S. *[U.S. EPA, 1992a,b and Charbeneau et al., 1992]*. It has been estimated that the use of in-situ bioremediation in the cleanup of polluted aquifers has reduced the cleanup time and costs by a factor of 100 in some cases *[Lagrega et al., 1994]*. See *Lee et al. [1988], Baker and Herson [1994], and Charbeneau et al. [1992]* for a more complete presentation of bioremediation.

1.1 Bioremediation Modeling

Groundwater models are among the most important scientific tools available for understanding groundwater processes. They have been used extensively as planning and management tools at numerous hazardous waste sites *[National Research Council, 1992]*. Bioremediation models use mathematical representations of the complex biodegradation processes and the more widely understood flow and transport processes that govern groundwater in the subsurface. Several bioremediation models have been developed and presented in literature (see Section 1.2). Some of these attempt to represent the degradation in a very thorough and complete way, but often sacrifice the ablity to apply the model to field-scale problems. Others employ greater simplifications of the complex processes in order to permit more efficient codes that can be more easily applied to real cleanups.

BIO2D The model studied in this work is called BIO2D. It is a two-dimensional, areal finite element model that makes several assumptions that allow it to be applied to realistic problems. It was written by Dr. Stewart Taylor *[Taylor, 1993]*, and adopted for current optimization research at Cornell University. The research cou-

ples differential dynamic programming algorithms with BIO2D to determine optimal treatment strategies for remediation of polluted aquifers. See *Minsker and Shoemaker [1994]* and *Culver and Shoemaker [1993]* for more details. BIO2D was chosen as the base simulation model chiefly because analytical derivatives can be derived from its finite element formulation.

BIOPLUME II The most widely used and recognized biodegradation model is BIOPLUME II *[Rifai et al., 1987b]*. It is another example of a model that makes several simplifying assumptions in order to obtain a field-useable code. BIOPLUME II is based on the USGS solute transport model MOC *[Konikow and Bredehoeft, 1978]*. BIOPLUME II has been successfully applied to at least two field sites where natural biodegradation was observed. *van der Heijde and Einawawy, [1993]* report that BIOPLUME II has received extensive verification and peer reviews of its theory. An informal survey of environmental consultants that use biodegradation models conducted in the summer of 1993 by the author revealed that BIOPLUME II is the most commonly used and recognized. Although this may be due in part to the paucity of field scale biodegradation models available, BIOPLUME II is really the industry standard for bioremediation modeling. BIOPLUME II is used in this work as a basis of comparison for bioremediation testing of BIO2D.

Model Validation Testing Before a groundwater model can be used as a planning and decision making tool, its credentials must be established through systematic testing and evaluation of the model's performance *[van der Heijde and Einawawy, 1992]*. The International Groundwater Modeling Center (IGWMC) has formulated a model review, verification and validation procedure *[van der Heijde et al., 1985]* that it recommends for all groundwater models. IGWMC presents a three-level testing strategy:

1. *Level 1:* Verification by testing against analytical solutions for simple cases.
2. *Level 2:* Verification using more complex cases or simplified real-world systems specifically designed to test specific types of models or code features.
3. *Level 3:* Validation against independently obtained field or lab data.

Huyakorn, et al. [1984] and *Beljin [1988]* present the application of this procedure to groundwater transport models. Specific test cases and specifications are recommended for Level 1 tests. Examples of Level 2 and 3 tests are also presented. *Beljin* gives results from model testing and comparisons of USGS Method of Characteristics (MOC) model, Random Walk, and a finite element model called SEFTRAN. This work applies the first two levels of the IGWMC protocol in the evaluation of BIO2D drawing upon the work of *Huyakorn, et al.* and *Beljin.*

Sensitivity Analysis An important characteristic of a model is its sensitivity to changes or uncertainty in the required input parameters. Biodegradation models typically involve the use of several physical and biological parameters. This study will address the sensitivity of BIO2D to variations in biological parameters. The overall objective will be to discover which of the parameters are most important to know with some certainty, and which may be assumed from literature.

1.2 Literature Review

An excellent review of groundwater bioremediation modeling was recently published by *Bedient and Rifai [1992].* It contains a brief overview of the bioremediation technology for contaminated groundwater, a review of current models, and an application of BIOPLUME II to an aviation spill site in Michigan. This article is somewhat biased toward its authors' model, BIOPLUME II, but it does provide an excellent history of the development of biodegradation models.

BIO2D is an unpublished model, although *Taylor* did publish results of a sensitivity analysis using it in 1993. Much of this work is based upon handwritten notes from, and personal conversations with *Taylor*.

1.3 Specific Goals of this Research

The specific goals of this work are:

1. To test the ability of BIO2D to correctly model the processes of flow and transport of a conservative pollutant. This is presented in Chapter 3, where IGWMC Level 1 testing is applied to BIO2D. Here model predictions are compared to analytical solutions.

2. To test the ability of BIO2D to model the more complex processes of biodegradation. IGWMC Level 2 testing is applied to BIO2D, but here no analytical solutions are available. Chapter 4 presents this work, where several test cases are evaluated and model predictions are compared to BIOPLUME II.

3. To present and evaluate two potential improvements to BIO2D. These are included as Chapter 5.

4. To conduct a thorough sensitivity analysis of BIO2D to the input biological parameters. This includes the demonstration of a more complete technique than is commonly used. Chapter 6 presents these results.

Chapter 2 will begin this study with a review of the governing equations and a presentation of the ways that BIO2D and BIOPLUME II solve them.

Chapter 2

Model Descriptions

2.1 Introduction

BIO2D and BIOPLUME II take very different approaches to the problem of mathematically modeling the complex processes involved in biodegradation of contaminated groundwater. This chapter will examine these two models in some detail, looking closely at how they numerically estimate the solution to the governing partial differential equations, and laying the foundation for later comparisons and analysis. A summary of the major differences between these models is included.

BIOPLUME II (referred to hereafter as BIOPLUME) *[Rifai et al., 1987b]* is a relatively well known and widely used model. The model uses the finite difference method to predict steady-state or transient hydraulic heads and the method of characteristics to predict contaminant and oxygen concentrations resulting from transport and degradation. It is based on the USGS solute transport model MOC *[Konikow and Bredehoeft, 1978]*. BIOPLUME models biodegradation as an instantaneous reaction between contaminant and oxygen. Microbial biomass is assumed non-limiting; thus, the model does not include biomass growth nor transport.

BIO2D *[Taylor, 1993]* is a newer model that has not been well tested or validated.

It was selected as a base model for ongoing optimization research at Cornell University. The model predicts the steady-state hydraulic heads and contaminant, oxygen and microbial biomass concentrations resulting from transport and degradation. The rate of substrate degradation is modeled using the Haldane variant of Monod kinetics.

The two models differ fundamentally with respect to how each solves the governing equations. In addition, BIOPLUME's assumption of instantaneous kinetics greatly simplifies the problem and in general permits faster computations.

2.2 Governing Equations

The two-dimensional, depth averaged, flow and transport equations for a confined aquifer are as follows, where all variables are defined in Appendix A. These are the governing partial differential equations (PDEs) that describe the biodegradation problem. Both BIO2D and BIOPLUME approximate the solutions to them through the use of numerical techniques.

Flow in a confined aquifer:

$$\bar{S}\frac{\partial h}{\partial t} = \nabla \cdot (T \nabla h) + Q_w \tag{2.1}$$

Transport of Substrate:

$$R_s bn\frac{\partial S}{\partial t} = \nabla \cdot (bD \nabla S) - bV \cdot \nabla S - bn\lambda_{RS} + (\mathrm{S_w} - \mathrm{S})\mathrm{Q_w} \tag{2.2}$$

Transport of Oxygen:

$$R_o bn\frac{\partial O}{\partial t} = \nabla \cdot (bD \nabla O) - bV \cdot \nabla O - bn\lambda_{RO} + (\mathrm{O_w} - \mathrm{O})\mathrm{Q_w} \tag{2.3}$$

Transport of Biomass:

$$R_b bn\frac{\partial B}{\partial t} = \nabla \cdot (bD \nabla B) - bV \cdot \nabla B + bn\lambda_{RB} + (\mathrm{B_w} - \mathrm{B})\mathrm{Q_w} \tag{2.4}$$

Darcy's Law:

$$V = -K\nabla h \tag{2.5}$$

Hydrodynamic Dispersion:

$$D_{ijmn} = \alpha_{ijmn}\frac{V_m V_n}{V} + D_0 \tag{2.6}$$

In equations 2.2 - 2.4, the left hand side represents the time rate of change of substrate, oxygen and biomass. The right hand side represents the changes due to hydrodynamic dispersion, convective transport, microbial degradation and fluid sources/sinks respectively, for substrate, oxygen and biomass. BIO2D assumes steady-state flow conditions, and the left hand side of equation 2.1 equals zero. BIOPLUME, however, does not impose this restriction and can thus solve transient flow problems.

Dispersion Coefficients In both models, it is assumed that hydrodynamic dispersion dominates over molecular dispersion, and that the aquifer is isotropic. Thus the dispersivity tensors can be defined in terms of the longitudinal and transverse dispersivities of the aquifer, α_L and α_T. They are related to the dispersion coefficients by

$$D_L = \alpha_L V \tag{2.7}$$

$$D_T = \alpha_T V \tag{2.8}$$

It follows that the components of the dispersion coefficent for two-dimensional flow in an isotropic aquifer are *[Bear, 1979]*:

$$D_{xx} = \alpha_L\frac{V_x^2}{V} + \alpha_T\frac{V_y^2}{V} \tag{2.9}$$

$$D_{yy} = \alpha_T\frac{V_x^2}{V} + \alpha_L\frac{V_y^2}{V} \tag{2.10}$$

$$D_{xy} = D_{yx} = (\alpha_L - \alpha_T)\frac{V_x V_y}{V}. \tag{2.11}$$

Table 2.1: Physical Parameters Used in BIO2D and BIOPLUME

Parameter	Units	Description
n	[1]	Effective porosity. Assumed constant in BIOPLUME, but $n = n(x, y)$ in BIO2D.
b	$[L]$	Aquifer thickness. $b = b(x, y)$ for both models.
R_s	[1]	Contaminant retardation factor: linear isotherm: $R_s = \left(1 + \frac{\rho_b K_D}{n}\right) = constant$
K_D	$[\frac{cm^3}{g}]$	Distribution coefficient.
T_{xx}	$[\frac{L^2}{T}]$	Transmissivity: $T_{xx} = K_{xx} b$
T_{yy}	$[\frac{L^2}{T}]$	Transmissivity: $T_{yy} = K_{yy} b$ $T_{xx} = T_{xx}(x, y)$; $T_{yy} = T_{yy}(x, y)$ for both models.
K	$[\frac{L}{T}]$	Hydraulic conductivity.
α_L	$[L]$	Longitudinal dispersivity.
α_T	$[L]$	Transverse dispersivity. $\alpha_L = \alpha_L(x, y)$; $\alpha_T = \alpha_T(x, y)$ for both models.
S	[1]	Storativity of aquifer. Required for transient problems in BIOPLUME only.

Retardation Effects Both BIO2D and BIOPLUME assume a linear isotherm for substrate (contaminant) adsorption. The contaminant retardation factor is calculated by

$$R_s = \left(1 + \frac{\rho_b K_D}{n}\right). \tag{2.12}$$

Both models assume that the oxygen is not retarded. Microbial retardation is addressed in Section 2.3.

Physical Parameters In order to use either BIO2D or BIOPLUME several physical parameters characterizing the polluted aquifer must be specified. These are summarized in Table 2.1.

Biodegradation In equations 2.2 - 2.4, λ_{RS}, λ_{RO}, and λ_{RB} represent the rate of change of substrate, oxygen and biomass due to biodegradation. BIO2D and BIOPLUME differ in their formulation of these degradation terms. Since BIOPLUME does not model biomass, equation 2.4 and λ_{RB} are unique to BIO2D. Detailed explanations of these terms follows in Sections 2.3 and 2.4.

Boundary Conditions Equations 2.1 - 2.4 do not completely define the biodegradation problem; boundary and initial conditions are required as well. The values of the initial concentrations, boundary conditions for hydraulic head, and appropriate concentrations along the entire perimeter of the two-dimensional domain must be specified by the user of either model. The three types of possible boundary conditions are:

1. *Type 1.* Specified head or concentration boundaries (Dirichlet conditions) for which heads and/or concentrations are given.
2. *Type 2.* Specified flow boundaries (Neumann conditions) for which the derivative of the head or concentration is given. A no-flow boundary condition is set by specifying flux to be zero.
3. *Type 3.* Head or concentration dependent flow boundaries (Cauchy or mixed boundary conditions) for which flux across the boundary is calculated given a boundary head and/or concentration value. This type of boundary condition is often called mixed because it relates boundary heads/concentrations to boundary flows.

See *Anderson and Woessner [1992] or Bear [1979]* for a more detailed description of these boundary conditions.

2.3 BIO2D

BIO2D uses the Galerkin finite element method in space with a variably weighted finite difference approximation in time to find approximate solutions to equations 2.1 - 2.4.

Finite Element Method The following is a brief description of the finite element method (FEM) used to solve the problem of flow, transport and biodegradation in BIO2D. It is not meant as a complete coverage or derivation of the method. Rather, it is meant to give the reader a general background of how BIO2D uses FEM to estimate the solution of the governing equations. See *Remson et al. [1971], Pinder [1977], Pinder and Gray [1977], Huyakorn and Pinder [1983] and Segerlind [1984]* for more complete coverage of FEM applied to groundwater problems.

For convenience equations 2.1 - 2.4 may be redefined in linear differential operator form as follows (see Appendix A for variable definitions):

$$L_1 = \nabla \cdot (T \nabla h) + Q_w \tag{2.13}$$

$$L_2 = R_s bn \frac{\partial S}{\partial t} - \nabla \cdot (bD \nabla S) + bV \cdot \nabla S + bn\lambda_{RS} - (\mathrm{S_w} - \mathrm{S})\mathrm{Q_w} \tag{2.14}$$

$$L_3 = R_o bn \frac{\partial O}{\partial t} - \nabla \cdot (bD \nabla O) + bV \cdot \nabla O + bn\lambda_{RO} - (\mathrm{O_w} - \mathrm{O})\mathrm{Q_w} \tag{2.15}$$

$$L_4 = R_b bn \frac{\partial B}{\partial t} - \nabla \cdot (bD \nabla B) + bV \cdot \nabla B - bn\lambda_{RB} - (\mathrm{B_w} - \mathrm{B})\mathrm{Q_w} \tag{2.16}$$

where $L_1 = L_2 = L_3 = L_4 = 0$.

The first step in applying the FEM is to subdivide the domain into nfe elements, with *nds* nodes. It is assumed that the solution to the governing partial differential equations can be approximated by the sum of a series of interpolating basis functions. The objective is to approximate the solution functions $h(x,y,t)$, $S(x,y,t)$, $O(x,y,t)$, and $B(x,y,t)$ from equations 2.1 - 2.4. The basis functions provide the

approximations, h^*, S^*, O^*, and B^* as follows:

$$h(x,y,t) \approx h^*(x,y,t) = \sum_{i=1}^{nds} h_i(t) w_i(x,y) \tag{2.17}$$

$$S(x,y,t) \approx S^*(x,y,t) = \sum_{i=1}^{nds} S_i(t) w_i(x,y) \tag{2.18}$$

$$O(x,y,t) \approx O^*(x,y,t) = \sum_{i=1}^{nds} O_i(t) w_i(x,y) \tag{2.19}$$

$$B(x,y,t) \approx B^*(x,y,t) = \sum_{i=1}^{nds} B_i(t) w_i(x,y) \tag{2.20}$$

where $h_i(t)$, $S_i(t)$, $O_i(t)$, and $B_i(t)$ are the values of the hydraulic head, and the concentrations of substrate, oxygen and biomass at node i, respectively. The term $w_i(x,y)$ is the basis function for node i, which is a function of space only. The terms $h_i(t)$, $S_i(t)$, $O_i(t)$, and $B_i(t)$ are functions of time only.

The basis function is an interpolation function equal to any value between 0 and 1; it will have a value of 1 if (x,y) is at node i, and a value of 0 for all other nodes. $w_i(x,y)$ will be between 0 and 1 in all elements that include node i, and 0 throughout any element that does not contain node i. There are many possible basis functions that meet this requirement. BIO2D uses linear basis functions, and the nodes correspond to the corners of the elements. In general, two-dimensional elements may be triangular or quadrilateral, but BIO2D uses quadrilateral only.

Because h^*, S^*, O^*, and B^* are approximations of h, S, O, and B respectively, the differential operators evaluated using the approximate solutions define residual, non-zero errors, i.e.,

$$R_1 = L_1(h^*) \tag{2.21}$$

$$R_2 = L_2(S^*) \tag{2.22}$$

$$R_3 = L_3(O^*) \tag{2.23}$$

$$R_4 = L_4(B^*) \tag{2.24}$$

These residuals are minimized when they are orthogonal to a set of weighting functions. In the Galerkin method the weighting functions are chosen to be the same as the basis functions $w_i(x,y)$. Residual errors are mininized by imposing the following conditions:

$$\int_D w_i(x,y)L_1(h^*)dD = 0 \tag{2.25}$$

$$\int_D w_i(x,y)L_2(S^*)dD = 0 \tag{2.26}$$

$$\int_D w_i(x,y)L_3(O^*)dD = 0 \tag{2.27}$$

$$\int_D w_i(x,y)L_4(B^*)dD = 0 \tag{2.28}$$

for $i = 1, 2, ...nds$ and where D is the domain of the region.

Green's theorem is applied to equalize the interelement continuity requirements for the weighting and basis functions, and a variably weighted finite difference scheme approximates the time derivatives. The integrals may then be evaluated, and the elemental coefficients calculated element by element and summed to create the global coefficient matrices. The result is the following system of equations:

$$[A]\{h\} = [P_h]\{Q_w\} + \{F_h\} \tag{2.29}$$

$$\begin{aligned}\left([M_s] + \Delta t\theta\left[[N] + [R_s^{t+1}] + \textstyle\sum_{i=1}^{m} Q_{w_{t,i}}[P_c]^i\right]\right)\{S\}^{t+1} \; = \\ \left([M_s] - \Delta t(1-\theta)\left[[N] + [R_s^t] + \textstyle\sum_{i=1}^{m} Q_{w_{t,i}}[P_c]^i\right]\right)\{S\}^t \; + \\ \textstyle\sum_{i=1}^{m} Q_{w_{t,i}}[P_c]^i S_w + \Delta t\theta\{F_s\}^{t+1} + \Delta t(1-\theta)\{F_s\}^t\end{aligned} \tag{2.30}$$

$$\begin{aligned}\left([M_o] + \Delta t\theta\left[[N] + [R_o^{t+1}] + \textstyle\sum_{i=1}^{m} Q_{w_{t,i}}[P_c]^i\right]\right)\{O\}^{t+1} \; = \\ \left([M_o] - \Delta t(1-\theta)\left[[N] + [R_o^t] + \textstyle\sum_{i=1}^{m} Q_{w_{t,i}}[P_c]^i\right]\right)\{O\}^t \; + \\ \textstyle\sum_{i=1}^{m} Q_{w_{t,i}}[P_c]^i O_w + \Delta t\theta\{F_o\}^{t+1} + \Delta t(1-\theta)\{F_o\}^t\end{aligned} \tag{2.31}$$

$$\left(\theta[M_b]^{t+1} + (1-\theta)[M_b]^t + \Delta t\theta\left[[N] + [R_b^{t+1}] + \sum_{i=1}^{m} Q_{w_{t,i}}[P_c]^i\right]\right)\{B\}^{t+1} = \quad (2.32)$$
$$\left(\theta[M_b]^{t+1} + (1-\theta)[M_b]^t + \Delta t(1-\theta)\left[[N] + [R_b^t] + \sum_{i=1}^{m} Q_{w_{t,i}}[P_c]^i\right]\right)\{B\}^t +$$
$$\sum_{i=1}^{m} Q_{w_{t,i}}[P_c]^i B_w + \Delta t\theta\{F_b\}^{t+1} + \Delta t(1-\theta)\{F_b\}^t$$

where { } denotes vectors and [ ] denotes matrices. The coefficients of these matrices are defined in Appendix B. Observe that 2.30 - 2.32 are nonlinear equations because of $[R_s]$; $[R_o]$; and $[M_b]$ and $[R_b]$.

Equation 2.29 is solved first for values of the hydraulic head at each node. The Darcy velocities and dispersion coefficients are then calculated by 2.5 and 2.6. The solutions for 2.30 - 2.32 are obtained by uncoupling and linearizing these equations, using a sequential procedure. Equations 2.30 - 2.32 are solved in sequence with matrices and vectors calculated explicitly using the solution from the previous time step. Equation 2.29 is resolved only when the pumping rates or locations are changed.

Taylor [1993] reports that numerical testing of this sequential, linearized solution against the fully-coupled, nonlinear solution has proven its accuracy and efficiency. This will be further addressed and tested in Chapter 5.

Stability Criteria The finite difference approximation in time used by BIO2D for solving the solute transport equations is unconditionally stable for the implicitness factor (see Appendix B), $\theta \geq 0.5$. For $\theta < 0.5$, the solution is conditionally stable. It is important to note that in BIO2D the user is responsible to select the appropriate value for θ.

Accuracy Criteria The finite element method is subject to numerical errors, including artificial dispersion sometimes called "numerical dispersion". Numerical errors often called "overshoot" and "undershoot" can also occur, particularly for ad-

vective dominated problems. Numerical dispersion arises from errors associated with the discretization of time and space. To minimize these errors *Anderson and Woessner [1992]* recommend that the grid should be designed so that the Peclet number (P_e) is less than or equal to one. However, acceptable solutions are possible with P_e as high as ten *[Huyakorn and Pinder, 1983]*. By aligning the element sides with the direction of flow, transverse numerical dispersion can virtually be eliminated *[Kinzelbach, 1986]*. Imposing such Peclet number conditions also eliminates overshoot and undershoot. The Peclet condition is given by:

$$P_{e_x} = \frac{\Delta x}{\alpha_x} \leq 1.0 \tag{2.33}$$

$$P_{e_y} = \frac{\Delta y}{\alpha_y} \leq 1.0. \tag{2.34}$$

Similarly the time discretization should satisfy the accuracy criteria that the Courant number (C_r) is less than or equal to one. The Courant condition is given by:

$$C_r = \frac{V\Delta t}{\Delta x} \leq 1.0. \tag{2.35}$$

Equations 2.33 - 2.35 are the accuracy criteria for BIO2D.

Monod Kinetics BIO2D models the biodegradation of substrate using a Haldane variant of the Monod equation where,

$$\lambda_{RS} = BR_b \frac{\mu_{max}}{Y} \left[\frac{S}{K_s + S + \frac{S^2}{K_i}}\right] \left[\frac{O}{K_o + O}\right] \tag{2.36}$$

$$\lambda_{RO} = BR_b F \frac{\mu_{max}}{Y} \left[\frac{S}{K_s + S + \frac{S^2}{K_i}}\right] \left[\frac{O}{K_o + O}\right] \tag{2.37}$$

$$\lambda_{RB} = BR_b \left\{\mu_{max} \left[\frac{S}{K_s + S + \frac{S^2}{K_i}}\right] \left[\frac{O}{K_o + O}\right] - r_b\right\} + C_c Y k_c \tag{2.38}$$

All variables are defined in Appendix A.

Microbial Inhibition The inhibition coefficient decreases the microbial growth rate at high substrate concentrations, allowing toxicity effects to be modeled when appropriate. As $K_i \rightarrow \infty$ or $S \rightarrow 0$, inhibition effects are negligible.

Microbial Retardation The partitioning of biomass between water and solid phase is critical to modeling the degradation of contaminant in the aquifer. It is modeled with the Freundlich isotherm *[Lagrega et al., 1994]* given by:

$$B^* = K_b B^{\frac{1}{N_b}} \tag{2.39}$$

The corresponding biomass retardation factor is defined by

$$R_b = \left(1 + \frac{1-n}{n} \rho_b K_b B^{\frac{1}{N_b}-1}\right) \tag{2.40}$$

where K_b is the Freundlich constant, N_b is the Freundlich exponent and B^* is the amount of bacteria absorbed per unit weight of soil. $N_b = 1$ for a linear isotherm. Figure 2.1 shows an example of the Freundlich isotherm. Note that $N_b < 1$ often has no physical-chemical basis.

Biological Parameters The Monod kinetics represented by equations 2.36 - 2.38 include eleven biological parameters that must be specified to parameterize BIO2D. These parameters can be determined by collection and analysis of field data or by laboratory study. Because these parameters are site specific, and they often vary considerably from the lab to the field, the values are often not known with much certainty. Chapter 6 will address sensitivity analysis of these parameters. A brief description of each is found at Table 2.2.

Assumptions Several assumptions are made in the formulation of BIO2D:

1. Darcy's Law is valid and hydraulic head gradients are the only driving mechanism for aquifer flow.

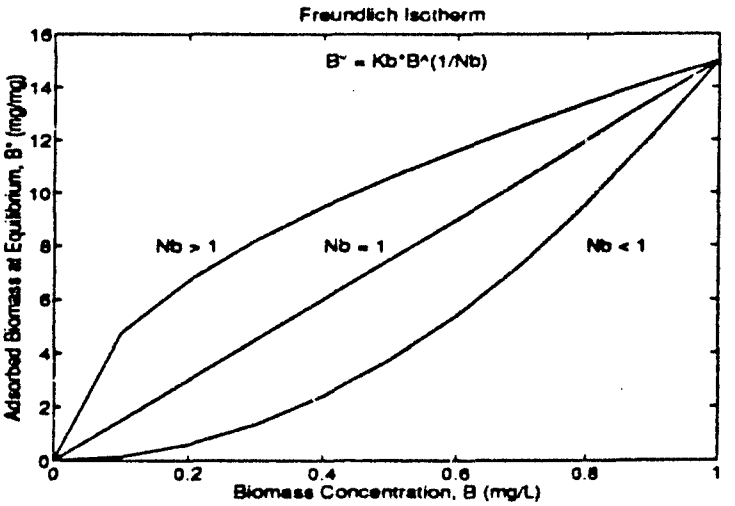

Figure 2.1: Freundlich Isotherm for Microbial Retardation

2. Steady-state flow conditions: the model assumes that the aquifer heads respond very quickly to pumping rates, so that the heads in period T depend only upon pumping within period T, and/or that the time horizon for pumping is relatively long.

3. The aquifer is isotropic with respect to the longitudinal and transverse dispersivities. $\alpha_L = \alpha_L(x, y)$ and $\alpha_T = \alpha_T(x, y)$ in BIO2D.

4. Ionic and molecular diffusion are negligible as compared with hydrodynamic dispersion.

5. Oxygen and substrate are the only rate limiting factors in microbial growth; nitrogen, phosphorus and other trace organics are available in sufficient quantities.

6. As in *Borden and Bedient [1986]*, equilibrium partitioning of biomass between the solid and water phase is assumed. This effect is modeled in equations 2.4, and 2.36 - 2.38 by a retardation factor, R_b, found using a Freundlich isotherm (equation 2.40).

7. There are no changes in porosity, permeability or dispersivity as a result of biological growth within the pore space. BIO2D assumes that these physical parameters are constant with time. See *Molz et al. [1986]* or *Taylor and Jaffe [1991]* for more complex models that consider these effects.

8. The complex subsurface bacterial population can be represented as consisting of a single facultative, heterotrophic bacterial type. In the absence of hydrocarbon they maintain a constant background concentration by aerobically or anaerobically consuming the background carbon found in the aquifer. In the presence of oxygen and a more easily degradable carbon source they preferentially consume the hydrocarbon. It is also assumed that the yield coefficient, Y and death rate, r_d are constant for aerobic and anaerobic consumption of substrate contaminant and background carbon.

9. Background carbon, C_c, remains constant in the aquifer. It may change form through fermentation, but carbon mass remains constant.

10. Background carbon utilization is given by a first order rate constant, k_c.

11. Oxygen is recharged at a rate necessary to offset O_2 consumed in the aerobic degradation of background carbon.

12. Oxygen is not retarded.

13. Vertical variations in head and concentration of substrate, oxygen and biomass are negligible, and a depth averaged model is justified.

Table 2.2: Biological Parameters Used in BIO2D

Parameter	Units	Description
F	$[\frac{mg}{mg}]$	Stoichiometric ratio of oxygen to substrate consumed in degradation. Determined from balanced reaction. Neglects substrate used for net microbial growth.
μ_{max}	$[\frac{1}{day}]$	Maximum specific growth rate of bacteria.
K_s	$[\frac{mg}{L}]$	Monod substrate half-saturation constant. Substrate concentration at one half the maximum growth rate.
K_i	$[\frac{mg}{L}]$	Substrate inhibition constant. Accounts for substrate toxicity effects.
K_o	$[\frac{mg}{L}]$	Monod oxygen half-saturation constant. Oxygen concentration at one half the maximum growth rate.
Y	$[\frac{mg}{mg}]$	Yield coefficient. Defined as the ratio of mass of biomass formed to the mass of substrate consumed.
r_b	$[\frac{1}{day}]$	Endogenous decay coefficient. Accounts for energy required for cell maintenance, death and predation that reduce the growth rate of biomass.
R_b	[1]	Microbial retardation factor, Freundlich isotherm: $R_b = \left(1 + \frac{1-n}{n}\rho_b K_b B^{\frac{1}{N_b}-1}\right)$
K_b	$[\frac{L}{mg}^{\frac{1}{N_b}}]$	Freundlich isotherm constant.
N_b	[1]	Isotherm exponent. $N_b = 1$ for linear isotherm.
C_e	$[\frac{mg}{L}]$	Background carbon concentration in aquifer. (e.g., humic, fulvic acids)
k_e	$[\frac{1}{day}]$	First order decay rate of background carbon.

Table 2.3: BIO2D Input Files

Input File	Purpose
data	User specifies timing data, physical and biological parameters, well data, output control and other options.
mesh	User specifies spatial discretization data.
ibc	User specifies boundary and initial conditions for problem.

Input/Output Files The simulation of contaminant transport and bioremediation in groundwater using BIO2D requires the use of the three input files shown in Table 2.3.

2.4 BIOPLUME

BIOPLUME is a two-dimensional, depth averaged biodegradation model. It uses the finite difference method to predict hydraulic heads and the method of characteristics (MOC) to predict contaminant and oxygen concentrations resulting from transport and degradation. BIOPLUME is built on the MOC model *[Konikow and Bredehoeft, 1978]*, maintaining the same numerical techniques, but solving the transport equation for both substrate and oxygen.

Method of Characteristics The following is a brief description of the method of characteristics (MOC) used to solve the problem of transport and biodegradation in BIOPLUME. It is taken from *Konikow and Bredehoeft [1978] and Rifai et al. [1987b].* It is not meant as a complete coverage or derivation of the method; rather, it is meant to give the reader a general background of how the MOC estimates the solution of the governing equations. See *Garder et al. [1964] or Konikow and Bredehoeft [1978]* for a more complete description.

Flow Equation BIOPLUME uses an iterative alternating-direction implicit (ADI) procedure to solve a finite difference approximation of the flow equation (2.1) *[Konikow and Bredehoeft, 1978].* After the head distribution has been completed for a given time step, the velocity of the groundwater flow is estimated at each node using an explicit, finite difference form of equation 2.5. See *Pinder and Bredehoeft [1968]* or *Trescott, Pinder and Larson [1976]* for a more complete coverage of the ADI procedure.

Transport Equations The technique used by BIOPLUME is not to solve partial differential equations 2.2 and 2.3 directly, but to solve a nearly equivalent system of ordinary differential equations (ODEs). In order to do this the substantial or material

derivative is used. For example, the *substantial derivative* of substrate is defined as:

$$\frac{DS}{Dt} = \frac{\partial S}{\partial t} + \frac{\partial S}{\partial x}\frac{dx}{dt} + \frac{\partial S}{\partial y}\frac{dy}{dt} \tag{2.41}$$

The second and third terms of equation 2.41 correspond to the advective part of equation 2.2. Thus equation 2.2 can be replaced by the following system of ODEs:

$$\frac{dx}{dt} = V_x \tag{2.42}$$

$$\frac{dy}{dt} = V_y \tag{2.43}$$

$$R_s bn\frac{dS}{dt} = \nabla \cdot (bD\,\nabla S) - bn\lambda_{RS} + (\mathrm{S_w} - \mathrm{S})\mathrm{Q_w} \tag{2.44}$$

The solutions of this system of equations may be given as:

$$x = x(t)\,;\; y = y(t)\,;\; S = S(t) \tag{2.45}$$

Similarly equation 2.3 may be replaced by the following:

$$\frac{dx}{dt} = V_x \tag{2.46}$$

$$\frac{dy}{dt} = V_y \tag{2.47}$$

$$bn\frac{dO}{dt} = \nabla \cdot (bD\,\nabla O) - bn\lambda_{RO} + (\mathrm{O_w} - \mathrm{O})\mathrm{Q_w} \tag{2.48}$$

where solutions of this system of equations may be given as:

$$x = x(t)\,;\; y = y(t)\,;\; O = O(t) \tag{2.49}$$

The solutions given by equations 2.45 and 2.49 are called the characteristic curves of partial differential equations 2.2 and 2.3 respectively.

Given the solutions to equations 2.42 - 2.44 and 2.46 - 2.48, a solution to the partial differential equations (2.2 and 2.3) may be obtained by following the characteristic curves. This is accomplished numerically by introducing a set of moving points or particles that can be traced within the finite difference grid. Every particle then

corresponds to one characteristic curve, and the values of x, y, S and O are obtained as functions of time for each characteristic *[Garder et al., 1964]*. Each point has a concentration and position associated with it and is moved within the flow field in proportion to the velocity at its location. This may be visualized as tracing fluid particles through a flow field and noting changes in concentration as they move.

The method of characteristics uses particle tracking to solve for changes in concentration due to advective transport, and an explicit finite difference approximation to solve for changes in concentration due to dispersion, pumping, divergence of velocity, changes in saturated thickness and biodegradation.

The changes in concentrations due to advective transport are calculated in BIOPLUME as follows. The first step is to distribute a geometrically uniform pattern of traceable particles in the finite difference grid. The user of BIOPLUME must specify between four and seven particles per cell, as *Konikow and Bredehoeft [1978]* found this to produce satisfactory results in most two-dimensional problems. In general, using more particles results in greater accuracy, but requires more computations and longer run times. Each particle is assigned as its initial concentration the initial concentration of the node of the cell containing the particle.

In each time step of the model simulation, all particles are moved a distance proportional to the size of the time step and the velocity at the location of the particle. The new position of each particle is computed using a finite difference approximation of equations 2.42 - 2.43 and 2.46 - 2.47. The x and y velocities for any particular particle are computed using a bilinear interpolation over the area of half a cell. After all points have been moved, the concentration at each node is temporarily assigned the average of the concentrations of all points then located within the area of the cell.

The changes in concentrations due to hydrodynamic dispersion, fluid sources/sinks, divergence of the velocity, changes in the saturated thickness of the aquifer and

biodegradation are calculated using an explicit finite difference approximation of equation 2.44 and 2.48. The resulting approximate solution completes the definition of the characteristic curves of 2.2 and 2.3.

Because the processes of hydrodynamic dispersion, advective transport, mixing and biodegradation are occuring continuously and simultaneously, equations 2.42 - 2.44 and 2.46 - 2.48 should be solved simultaneously. However, equations 2.42 - 2.43 and 2.46 - 2.47 are solved by particle movement based on *implicitly* computed heads, while equations 2.44 and 2.48 are solved *explicitly* with respect to concentrations. This source of error is minimized using a two-step explicit procedure in which the finite difference approximation of equations 2.44 and 2.48 are solved at each node; equal weight is given to concentration gradients computed at the previous time level and to concentration gradients computed from the particle movements.

Stability Criteria The explicit numerical solution of the solute transport equations have a number of stability criteria associated with them as discussed in *Konikow and Bredehoeft [1978].* These criteria restrict the allowable size of the time step based on the grid size, dispersion coefficients, pumping rates, and calculated velocities. In BIOPLUME the stability criteria are calculated by the program. The user must specify the overall time period of interest and the program determines the minimum required time step and number of particle moves necessary to satisfy stablity.

Instantaneous Kinetics *Borden and Bedient [1986]* reported that microbial kinetics had very little effect on the hydrocarbon (contaminant) distribution in the body of a plume, and on the time until contaminant breakthrough. They observed that the rate of oxygen delivery is much slower than the rate of microbial consumption, and that groundwater velocity dominates the rate of oxygen availability. Thus, they replaced the original Monod kinetics with an instantaneous reaction between

oxygen and substrate. BIOPLUME generates two sets of tracer particles (as described above) for tracking the change in oxygen and substrate with time. At every step, the solute transport equations (equations 2.2 and 2.3) are solved separately to estimate the concentrations of oxygen and substrate. The two plumes are combined using the principle of superposition to simulate the instantaneous reaction between them. In an explicit finite-difference form, this approximation is *[Rifai et al., 1987b]*:

$$\text{For } S_t > \frac{O_t}{F} \qquad \begin{aligned} S_{t+1} &= S_t - \frac{O_t}{F} \\ O_{t+1} &= 0 \end{aligned} \tag{2.50}$$

$$\text{For } S_t \leq \frac{O_t}{F} \qquad \begin{aligned} S_{t+1} &= 0 \\ O_{t+1} &= O_t - S_t F \end{aligned} \tag{2.51}$$

where S, O and F are defined in Appendix A. Thus, the only biological parameter that must be specified in BIOPLUME is F.

BIOPLUME Options BIOPLUME offers the user three additional options for contaminant transport and biodegradation modeling.

- First order contaminant decay.
- Biodegradation from anaerobic decay: modeled as first order decay of contaminant.
- Biodegradation from reaeration: modeled as first order decay of contaminant.

In each case the only required input is the coefficient of decay. These options are not addressed nor tested in this work.

Assumptions *Konikow and Bredehoeft [1978]* present the following assumptions for the MOC model:

1. Darcy's Law is valid and hydraulic head gradients are the only driving mechanism for aquifer flow.
2. The porosity and hydraulic conductivity of the aquifer are constant with time, and porosity is uniform in space.
3. Gradients of fluid density, viscosity and temperature do not affect the velocity distribution.
4. Ionic and molecular diffusion are negligible as compared with hydrodynamic dispersion.
5. Vertical variations in head and concentration of substrate, oxygen and biomass are negligible.
6. The aquifer is homogeneous and isotropic with respect to the longitudinal and transverse dispersivities.

In addition, *Rifai et al. [1987b]* include the following assumptions for BIOPLUME:

1. Instantaneous reaction between substrate and oxygen in the aquifer, thus microbial biomass, and all other nutrients are available in sufficient quantities.
2. Oxygen is not retarded.

Required Parameters for MOC/BIOPLUME In addition to the physical parameters given in Table 2.1, BIOPLUME requires some additional parameters which are associated with the method of characteristics (Table 2.4). See *Rifai et al. [1987b]* and *Konikow and Bredehoeft [1978]* for details and guidance in the use of these variables.

Table 2.4: Parameters Required by Method of Characteristics

Parameter	Description
NPMAX	Maximum number of particles.
NITP	Number of iteration parameters.
ITMAX	Maximum number of iterations in ADI procedure (used to solve flow equation).
TOL	Convergence criteria in ADI procedure.
NPTPND	Initial number of particles per node.
CELLIS	Maximum cell distance per particle move.

2.5 Summary of Differences in Models

Table 2.5 gives a summary of the major differences in how BIO2D and BIOPLUME approximate the solutions to the governing partial differential equations. An analysis of how these two models perform in validation testing is the subject of the following two chapters.

Table 2.5: Summary of Differences in BIO2D and BIOPLUME

	BIO2D	BIOPLUME
Procedure used to solve PDEs	Finite Element Method	Method of Characteristics
Types of Flow Problems Solved	steady-state only	transient or steady-state
Flexibility in Element Sizes	great, can use various sizes and combinations to match problem	none, must use equally sized rectangular cells.
Kinetics Used	Monod	Instantaneous
Biological Parameters Req'd	11 (see Table 2.2)	1 (must specify F)
Stability	unconditionally stable for $\theta \geq .5$	calculated internally
Numerical Errors	prone to numerical dispersion, but can be controlled by finer discretization	minimal numerical dispersion except at wells (see Section 3.7).
Units Used	any consistent units	English
Additional Options	none	first order decay degradation by reaeration anaerobic degradation

Chapter 3

Validation Testing

3.1 Introduction

The first step in evaluating BIO2D was to test its ability to model solute transport. This was done using the International Ground Water Modeling Center's Level 1 verification protocol *[Huyakorn et al., 1984; Beljin, 1988].* The objectives of this process were to check the ability of its algorithms to solve the governing equations of flow and solute transport under a variety of physical conditions, and to check the accuracy of the computer code.

Five test problems with analytical or semi-analytical solutions were used, ranging from a simple one-dimensional problem to a relatively complex problem involving two pumping wells. The specific test problems applied in the validation were:

- Transport in a semi-infinite column, Type 1 inlet boundary condition
- Transport from a continuous point source in a uniform flow field
- Transport of a solute slug in a uniform flow field
- Transport in a radial flow field caused by an injection well

- Transport in a non-uniform flow field caused by an injection - extraction well doublet

3.2 Basis of Comparison

In order to evaluate the performance of BIO2D against the analytical solution, and compare it to BIOPLUME, the following criteria were used:

- Root Mean Square Error, calculated as a percent of the analytical solution:

$$\frac{\sum_{i=1}^{n} \sqrt{(observed_i - analytic_i)^2}}{\sum_{i=1}^{n} (analytic_i)} \tag{3.1}$$

- Qualitative comparisons such as "good", "reasonable", and "unacceptable" based on experience and intuition.

3.3 Validation Test 1: Transport in a Semi-Infinite Column

The first validation test considered one-dimensional flow and transport in a semi-infinite column. A uniform flow field with a constant concentration boundary condition was specified (Figure 3.1). The grid Peclet number, P_e was 2.0 and the initial Courant number, C_r was 0.4. A complete problem statement, input specifications, the analytical solution and timing results are included at Appendix C.

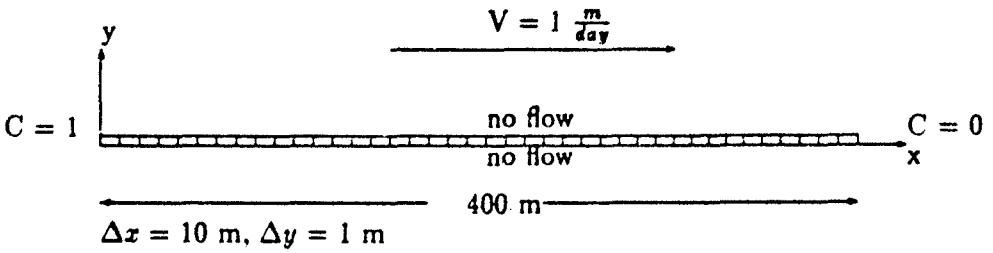

Figure 3.1: Schematic Sketch of Validation Test 1

Results from this test are shown at Figures 3.2 - 3.4. They indicate an acceptable match to the analytic solution was attained using BIO2D for both a retarded and non-retarded solute. The greatest source of error was numerical dispersion, which can be damped by reducing the time step or by varying the time weighting or implicitness factor, θ. At the prescribed time step of 2.5 days, it is necessary to vary the θ to 0.55

to obtain a good fit (Figure 3.2).

It is desirable for on-going optimization research to have the implicitness factor equal to one. In this case it is necessary to reduce the time step to 0.5 day to achieve comparable results (Figure 3.3). As shown in Table 3.1, further refinement in the solution can be attained by reducing the time step and/or adjusting θ. For unconditional stability, the implicitness factor must be greater than or equal to 0.5. Figure 3.4 shows the results for a retarded solute, where the RMSE was only slightly greater than for the non-retarded case.

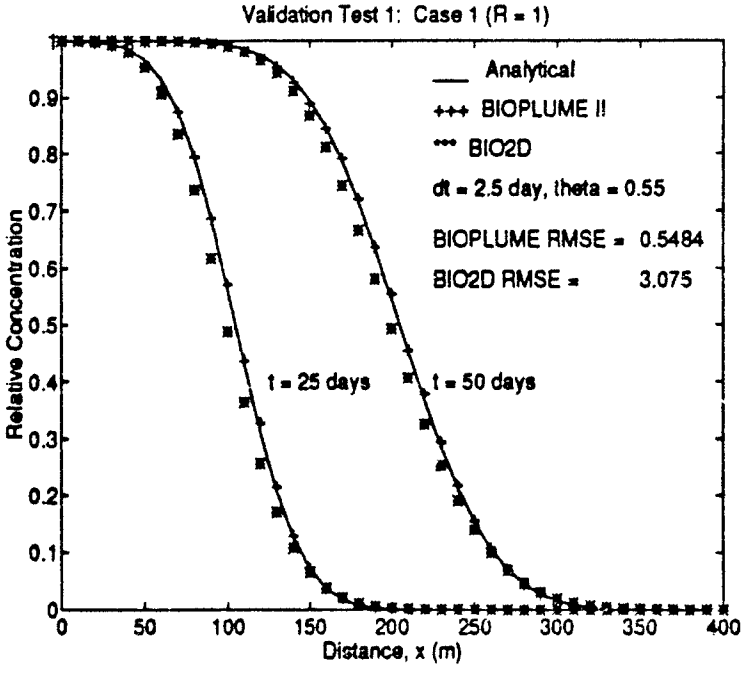

Figure 3.2: Validation Test 1, Case 1 at 25 and 50 days for $\Delta t = 2.5\ days$, $\theta = 0.55$

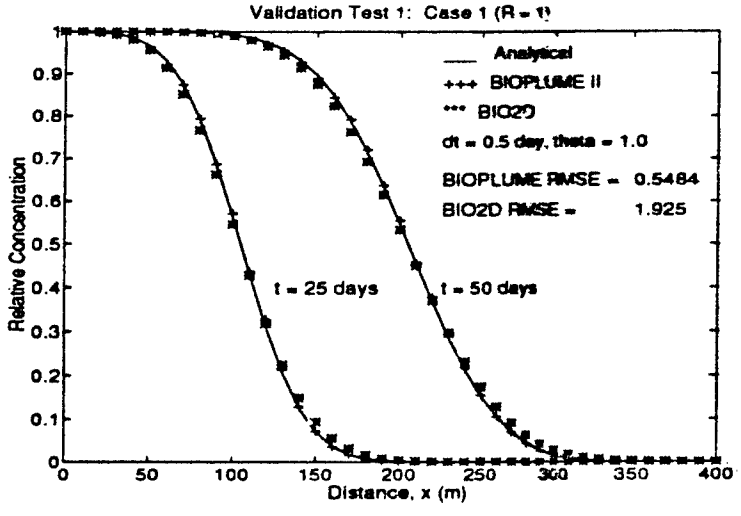

Figure 3.3: Validation Test 1, Case 1 at 25 and 50 days for $\Delta t = 0.5\ days,\ \theta = 1.0$

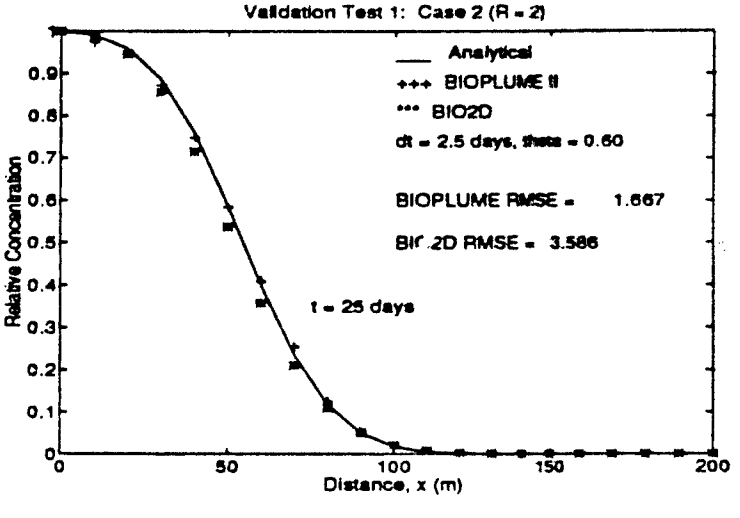

Figure 3.4: Validation Test 1, Case 2 at 25 and 50 days for $\Delta t = 2.5\ days,\ \theta = 0.60$

Table 3.1: Validation Test 1 Results, BIO2D

Case 1: $R_s = 1$			*Case 2:* $R_s = 2$		
Δt	θ	RMSE	Δt	θ	RMSE
2.5	1.0	8.05	2.5	1.0	7.21
2.5	0.55	3.08	2.5	0.60	3.59
1.0	1.0	3.63	1.0	1.0	3.11
0.5	1.0	1.92	0.5	1.0	2.01
0.1	1.0	1.01			
1.0	0.55	1.19			
0.5	0.55	0.29			

3.4 Validation Test 2: Transport From a Continuous Point Source

The second test applied to BIO2D was transport in a uniform flow field from a continuous point source. The continuous point source was modeled as an injection well with $QC_0 = 704\frac{g}{m-day}$ (Figure 3.5). The analytical solution assumes that the source is small enough that it doesn't alter the flow field; this was accomplished by specifying a small Q and large C_0. Fine, medium and coarse grids were used to evaluate the model's sensitivity to spatial discretization. A complete problem statement, input specifications, the analytical solution and timing results are included at Appendix C.

For case 1 (Δx = 60 m, Δy = 15 m), the best attainable match is possible when the implicitness factor is equal to 0.85 (Figure 3.6), although the solution with the implicitness factor equal to 1.0 is only slightly worse (by 0.3%). At either value BIO2D produces acceptable results at 1000 and 2000 days. As in Test 1, numerical dispersion causes the greatest error and can be damped by the use of finer discretization, as demonstrated by case 2 vs. case 3 (Table 3.2).

Figure 3.7 shows the results at 2000 days for a transverse cut of the plume at 180 and 900 meters from the source. The solution compares favorably to the analytical solution.

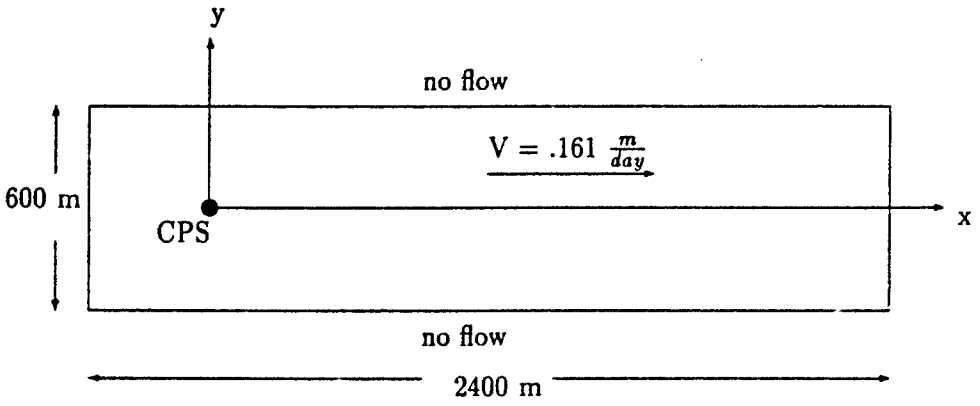

Selected Grid	Δx	Δy	P_{e_x}	P_{e_y}	C_r
Fine	10 m	10 m	0.47	2.32	1.61
Medium	60 m	15 m	2.8	3.5	0.27
Coarse	60 m	30 m	2.8	7.0	0.27

Figure 3.5: Schematic Sketch of Validation Test 2

Table 3.2: Validation Test 2 Results, BIO2D

Case	Δx (m)	Δy (m)	Δt (days)	θ	RMSE
1a	60	15	100	1.0	7.9
1b	60	15	100	0.85	7.6
2	60	30	100	1.0	18.5
3	10	10	100	1.0	7.8

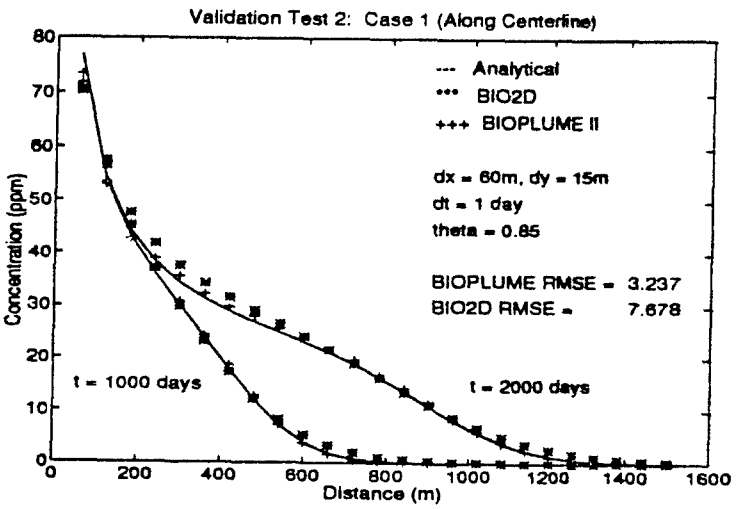

Figure 3.6: Validation Test 2, Case 1 Centerline Concentrations for Case 1

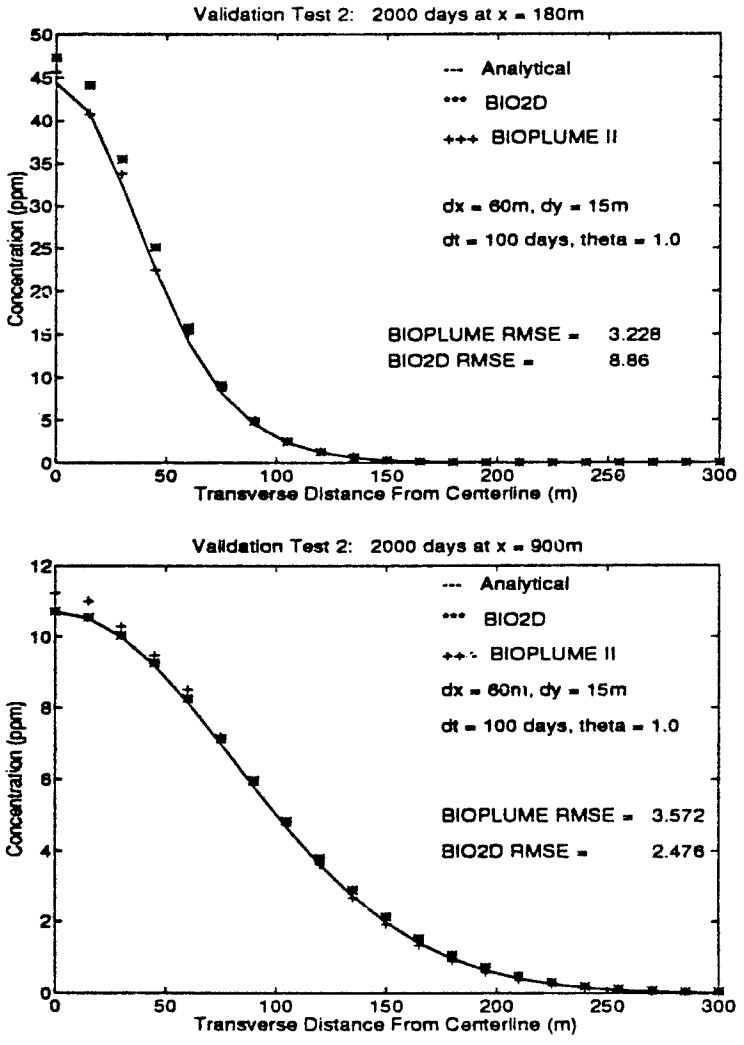

Figure 3.7: Validation Test 2, Case 1 Concentrations at x = 180 m and 900 m

3.5 Validation Test 3: Transport of a Solute Slug

This test considered the transport of a contaminant slug released at t=0 in a uniform flow field. The slug was modeled using an initial concentration at the origin of 3500 mg (Figure 3.8). The Peclet number was 1.25 in the x-direction and 5.00 in the y-direction. The initial Courant number was 0.4. A complete problem statement, input specifications, the analytical solution and timing results are included at Appendix C.

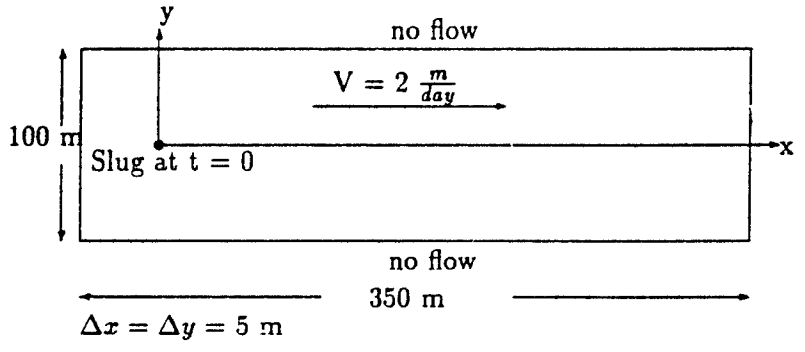

Figure 3.8: Schematic Sketch of Validation Test 3

Results from Validation Test 3 show a strong dependence on the time step and the implicitness factor (Table 3.3). For the specified time step of one day, the best results are found if $\theta = 0.65$ is used. As shown in Figure 3.9 this solution contains a 13.55% error. This error is greatest in early times and is reduced as the plume disperses. If a 0.1 day time step is used, however, it is possible to achieve a solution

with only 7% error and keep the implicitness factor at unity (Figure 3.10). As seen in Figure 3.11, the errors along two transverse sections of the plume were much less than along the longitudinal centerline. Table 3.3 shows a summary of results for this test.

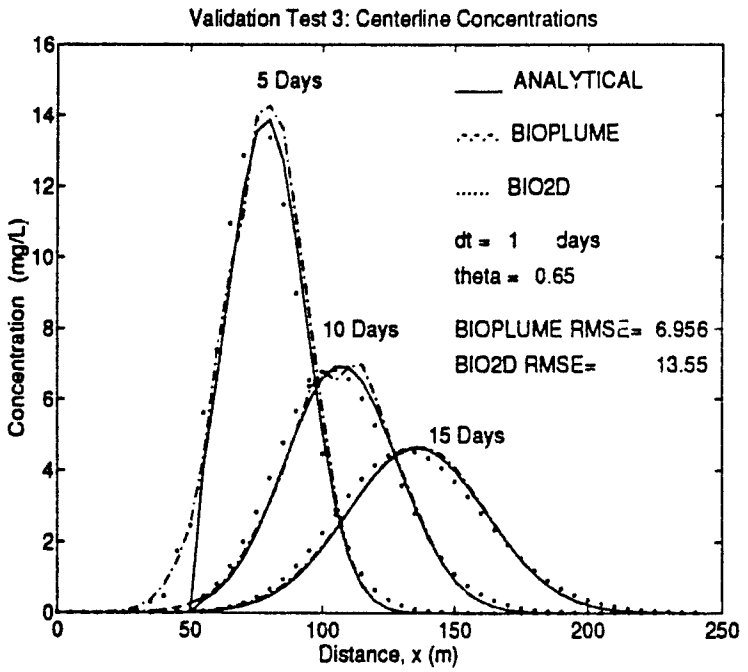

Figure 3.9: Validation Test 3 Centerline Concentrations, $\Delta t = 1$ day, θ =0.65

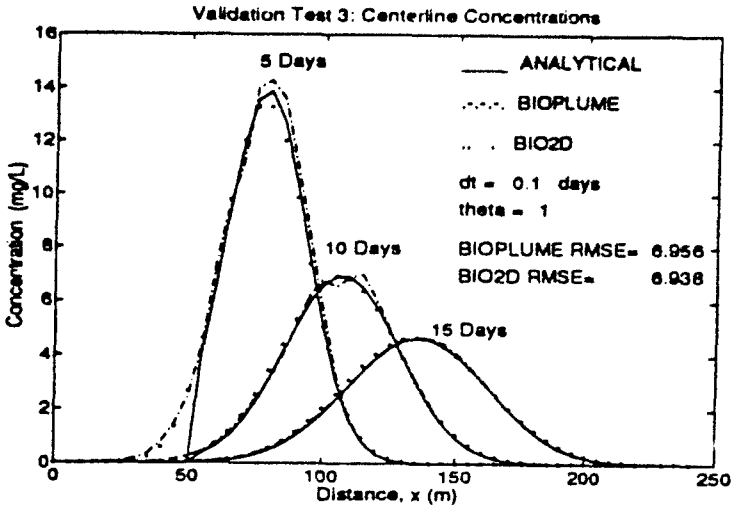

Figure 3.10: Validation Test 3 Centerline Concentrations, $\Delta t = 0.1$ day, $\theta = 1.0$

Table 3.3: Validation Test 3 Results, BIO2D

Δt(days)	θ	RMSE
1.0	1.0	33.96
1.0	0.65	13.55
0.5	1.0	20.24
0.25	1.0	12.2
0.1	1.0	6.9

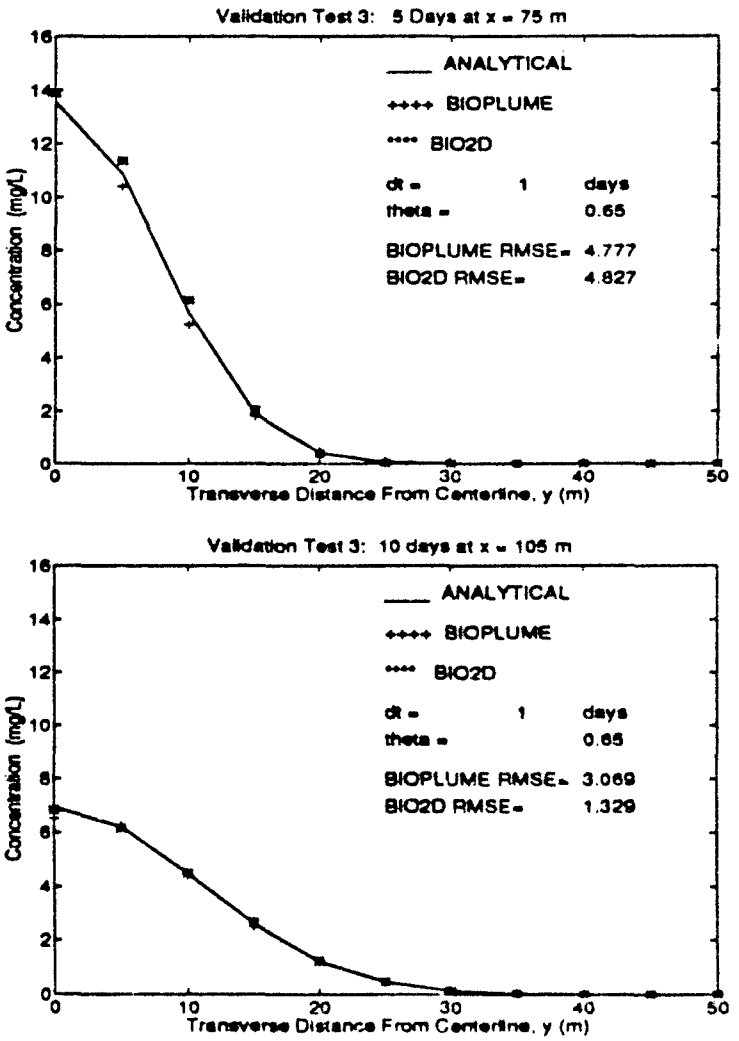

Figure 3.11: Validation Test 3 Concentrations at x = 75 m and 105 m

3.6 Validation Test 4: Transport in a Radial Flow Field

The fourth validation test used to evaluate BIO2D was transport in a radially diverging flow field resulting from an injection well (Figure 3.12). The strength of the injection well was specified as $25\frac{l}{day}$. The resulting flow field is largest near the well and decreases with distance away from the well. The flow field and resulting transport generated by BIO2D were checked against the analytical solution. The Peclet number for this problem was 3.33, and the Courant number was 0.40. A complete problem statement, input specifications, the analytical solution and timing results are included at Appendix C.

Results from this test demonstrate the complexity of transport in a non-uniform flow field. Even with a relatively fine spatial discretization ($\Delta x = \Delta y = 1$ m) and a small time step ($\Delta t = 1$ day) the best results were still 16% in error (Figure 3.13). In addition, the accuracy of the solution was not significantly improved by reducing the time step or altering the implicitness factor (Table 3.4). It is interesting to note that the results from BIOPLUME (MOC) were not any better!

Cross Section:

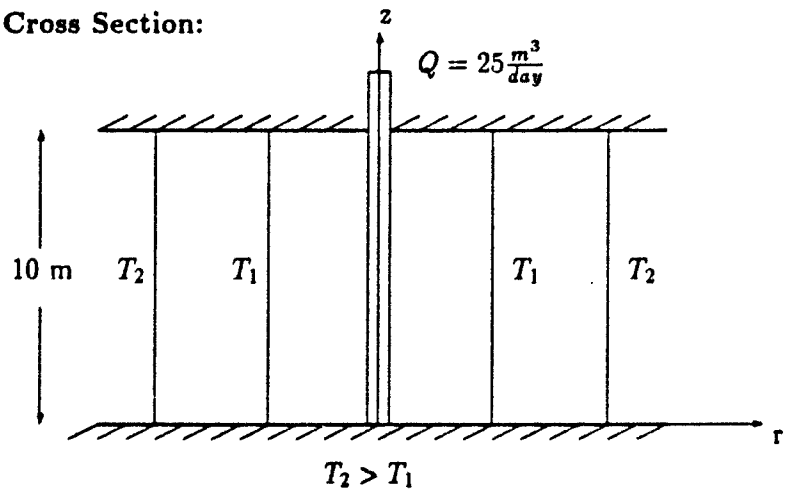

Plan View:

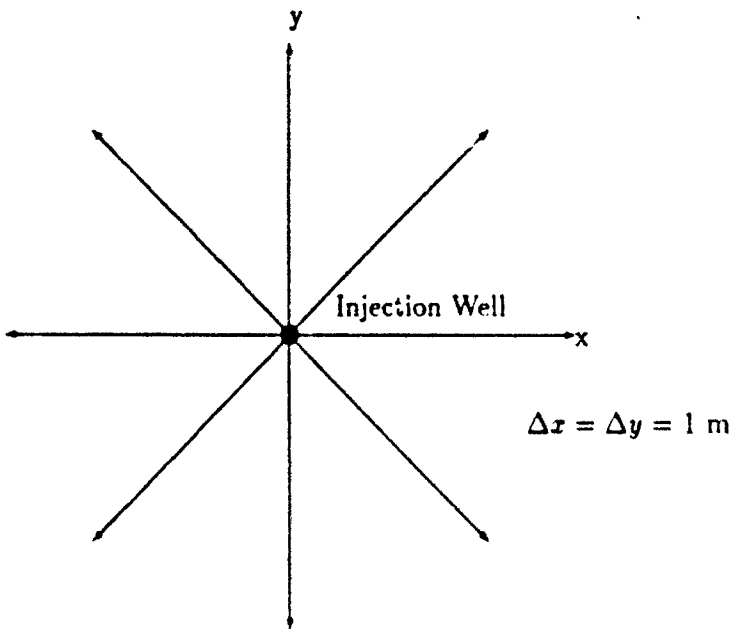

Figure 3.12: Schematic Sketch of Validation Test 4

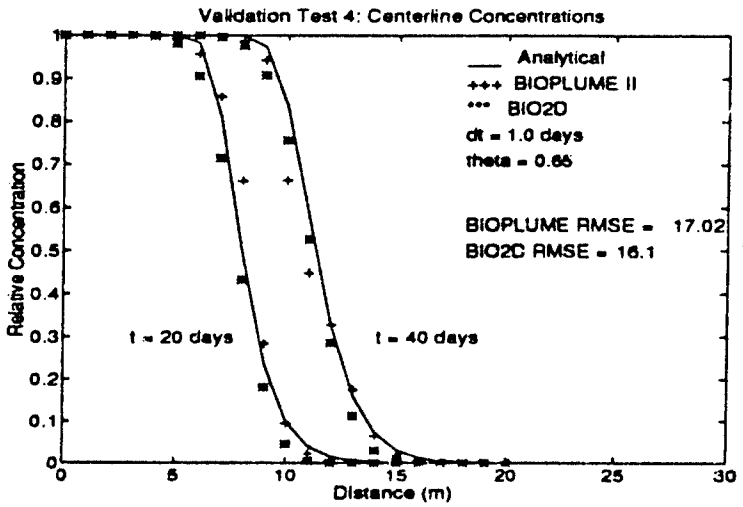

Figure 3.13: Validation Test 4 Radial Concentrations at 20 and 40 days

Table 3.4: Validation Test 4 Results, BIO2D

Δt (days)	θ	RMSE
1.0	1.0	16.15
1.0	0.65	16.19
0.5	1.0	16.11
0.1	1.0	16.05

3.7 Validation Test 5: Transport in a Non-Uniform Flow Field Caused by an Injection - Extraction Well Doublet

The final validation test used to evaluate BIO2D concerned solute transport between a pair of recharging and discharging wells operating at a constant flow rate (Figure 3.14). The objective was to test the ability of BIO2D to predict the concentration breakthrough curve at the extraction well. Both wells fully penetrate a uniform thickness, confined aquifer that is assumed as infinite, homogeneous and isotropic. The flow field is assumed as steady-state. Contaminated water at 100 $\frac{mg}{L}$ is injected at (60,0) at a flow rate of $Q = 2\ \frac{m^3}{d}$; and water is pumped out at (150,0) at the same rate. Five different cases, corresponding to increasing dispersion and lower P_e were considered. In each, a grid spacing $\Delta x = \Delta y = 5$ m was maintained.

For the most general case involving the combined influences of advection and dispersion, an analytical solution does not exist *[Huyakorn et al., 1984]*. For a more limited case of pure advection, a semi-analytical solution was developed and programmed by *Javandel et al. [1984]*. The model, called RESSQ, uses the complex velocity potential to estimate the concentration distribution in the aquifer. It is applicable to an aquifer meeting the above restrictions. Figure 3.15 shows the streamline pattern generated by RESSQ. A complete problem statement, input specifications, and a discussion the semi-analytical solution are included at Appendix C.

Figures 3.16 - 3.20 show the concentration breakthrough curves at the extraction well, as predicted by BIO2D and BIOPLUME. The semi-analytical solution obtained using RESSQ assumes pure advection. This case is shown in Figure 3.16 where $\alpha_L = \alpha_T = 0.01$ m and the corresponding P_e is 500. Observe that the breakthrough curve predicted by BIOPLUME demonstrated great fluctuations for which the semi-analytical solution represents the approximate upper envelope. These results are

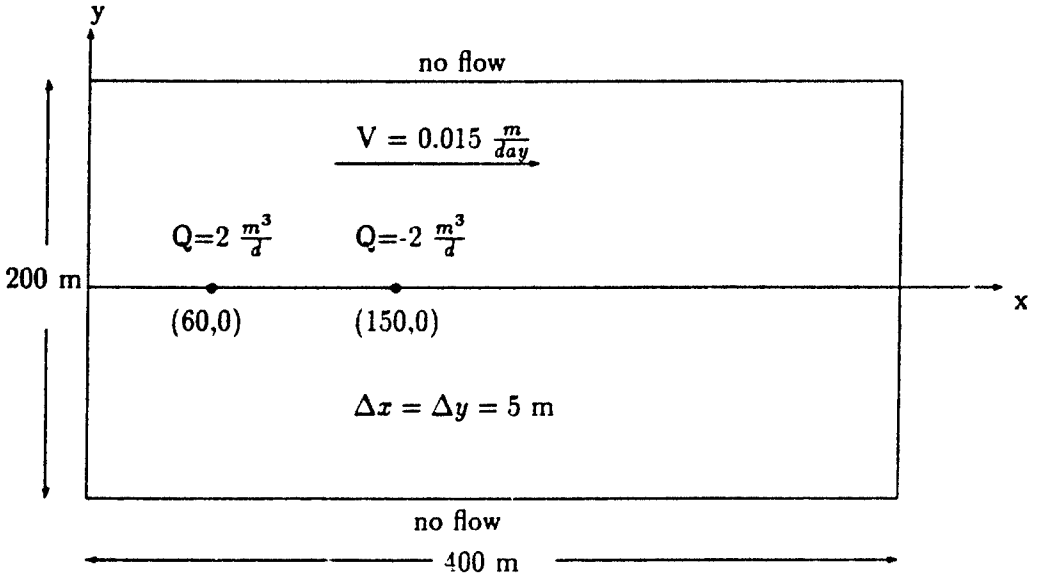

Figure 3.14: Validation Test 5 Schematic Sketch

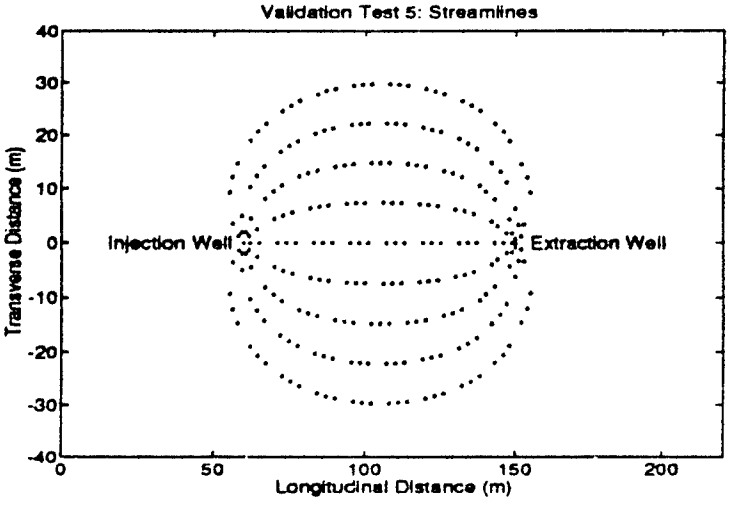

Figure 3.15: Validation Test 5: Streamlines

very similar to those reported by *El Kadi [1988]* for MOC. The solution predicted by BIO2D is quite poor as well. Numerical errors associated with such a high P_e are very visible.

In Figures 3.17 - 3.20 where both advection and dispersion are important observe the following:

- The magnitude of the fluctuations in BIOPLUME become smaller as the dispersion increases, and the P_e decreases.
- Numerical errors in BIO2D are no longer present for $P_e \leq 5$.
- It appears that BIOPLUME demonstrates more numerical dispersion than BIO2D, although there is no analytical solution to compare to.
- Case 5 (α_L = 9.1 m, α_T = 1.8 m) represents the dispersion in an aquifer that will be used extensively in Chapter 4. Observe in Figure 3.20 that BIOPLUME appears to demonstrate more numerical dispersion for this case.

These results show the difficulty of accurately representing the transport of a pollutant in a non-uniform flow field involving wells. *El Kadi* considers this test "severe", since it involves mainly radial flow and curved flow lines. However, in the application of BIO2D or BIOPLUME to an optimization model where numerous wells and changing pumping rates are likely, this test is an important one. No RMSE results were computed as the results from RESSQ did not lend themselves to a meaningful comparison.

The numerical problems of the MOC and wells are documented elsewhere *[El Kadi, 1988]* and *[Konikow and Bredehoeft, 1978]*, and are only summarized here. These errors are associated with the poor representation of the radial flow near wells; and by the method of estimating the solute mass removed from the aquifer at the extraction well and introduced into the aquifer at the injection well. For example, at the extraction well the MOC must regenerate particles after the particles representing

the pumped water are removed. The net effect is the artificial creation of mass, and hence, large mass balance errors.

Table 3.5 demonstrates these high mass balance errors. These errors were computed for a 1500 day simulation. For Case 1 (pure advection), the errors are based upon the RESSQ semi-anlytical solution. For Cases 2-5 the errors were computed based on the total mass injected minus the total mass extracted. The mass extracted was calculated by integrating the respective breakthrough curve over the 1500 day simulation. For Case 5, observe that BIOPLUME's mass balance error was approximately 5 times greater than the error in BIO2D. This will be important to recall in Chapter 4 when biodegradation of a similar case is considered.

The errors observed in BIO2D for the first two cases are a function of the very high P_e. In cases involving greater dispersion (and lower P_e) BIO2D outperforms BIOPLUME based on mass balance errors. In addition, it appears that numerical dispersion was greater for BIOPLUME.

Table 3.5: Validation Test 5 Mass Balance Errors (After 1500 Days)

CASE	Dispersivities	Error in Percent	
		BIOPLUME	BIO2D
1	$\alpha_L = \alpha_T = 0.01$ m	25.7	15.6
2	$\alpha_L = \alpha_T = 0.1$ m	18.5	17.1
3	$\alpha_L = \alpha_T = 1.0$ m	14.1	1.7
4	$\alpha_L = \alpha_T = 5.0$ m	7.9	0.1
5	$\alpha_L = 9.1$ m, $\alpha_T = 1.8$ m	5.6	1.1

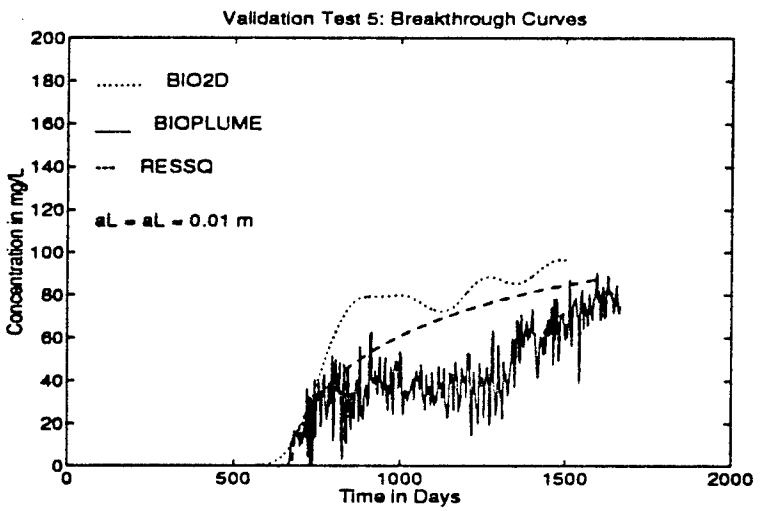

Figure 3.16: Validation Test 5: Pure Advection

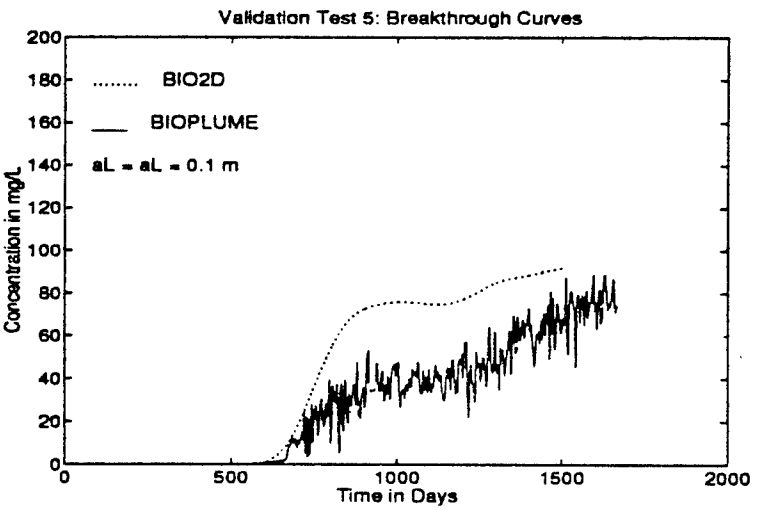

Figure 3.17: Validation Test 5: $\alpha_T = \alpha_L = 0.1$ m

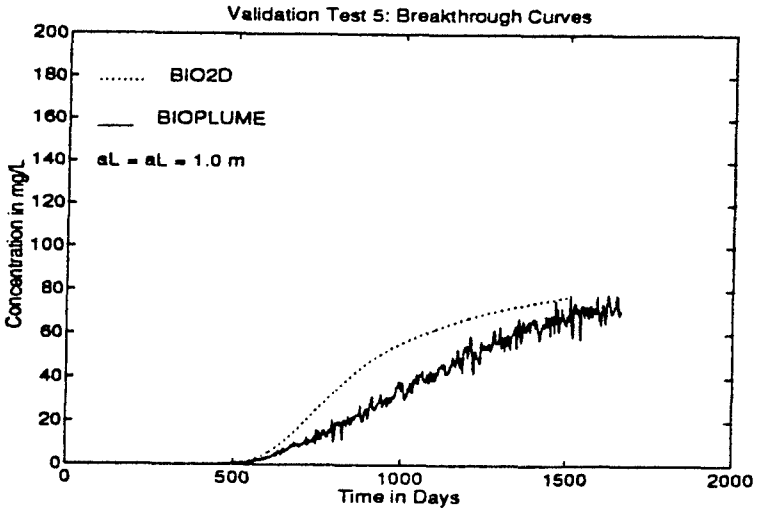

Figure 3.18: Validation Test 5: $\alpha_T = \alpha_L = 1$ m

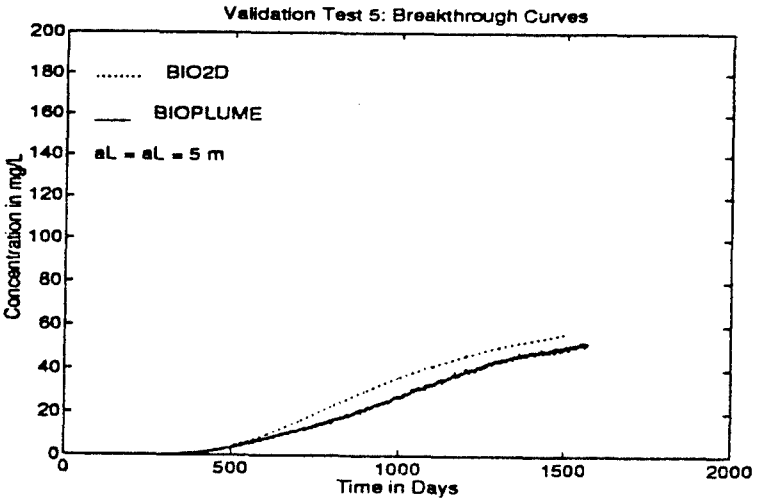

Figure 3.19: Validation Test 5: $\alpha_T = \alpha_L = 5$ m

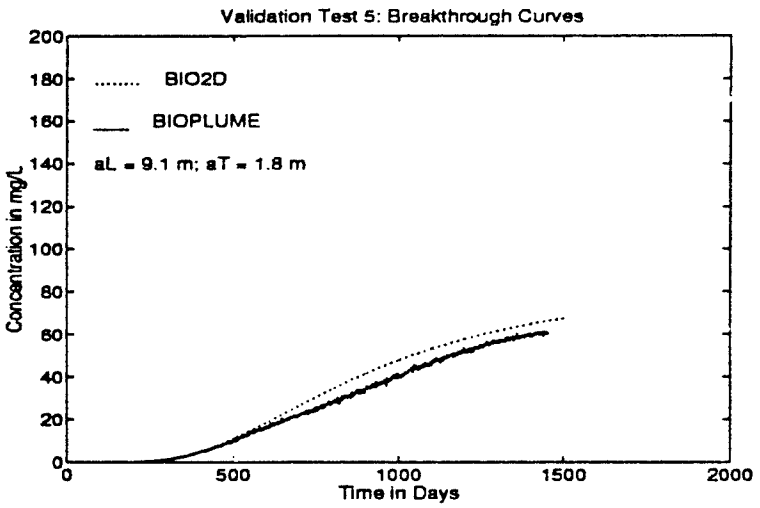

Figure 3.20: Validation Test 5: $\alpha_L = 9.1$ m, $\alpha_T = 1.8$ m

3.8 Summary

The application of these recommended tests to BIO2D verify its ability to satisfactorily solve the governing equations of flow and solute transport under several varied physical conditions. The accuracy of the computer code was established as well. The tests showed that BIO2D, as is common with Finite Element Models *[Anderson and Woessner, 1992]*, is prone to numerical dispersion. The user must be careful to specify a fine enough discretization to minimize this modeling error. This can be assured by following the accuracy criteria given by equations 2.33 - 2.35.

In addition, the effect of Δt and θ are significant. In order to keep $\theta = 1.0$, as is important for some optimization applications, the time step must be even smaller than might be necessary without this constraint.

Table 3.6 shows how BIO2D compared with BIOPLUME for the first four validation tests. BIOPLUME outperformed BIO2D by an average of 3%, largely because the Method of Characteristics is not prone to numerical dispersion *[Anderson and Woessner, 1992; Garder et al., 1964]* except at wells.

Validation Test 5 demonstrated the difficulty of accurately modeling flow in a non-uniform flow field involving well pairs. For this test BIO2D outperformed BIOPLUME based on greater mass balance errors in the latter model.

Table 3.6: Validation Testing Summary

	RMSE		
Validation Test	BIOPLUME	BIO2D	θ
1	0.55	3.08	0.55
2	3.24	7.68	0.85
3	6.95	13.55	0.65
4	17.02	16.10	0.65
Average	6.94	10.10	

Chapter 4

Bioremediation Testing

4.1 Introduction

After validating BIO2D's ability to accurately model the flow and transport of a conservative contaminant using the IGWMC's Level 1 Testing (Chapter 3), its ability to model the more complex processes of bioremediation was studied. This chapter utilizes the IGWMC's Level 2 Testing to accomplish this. Unfortunately, analytical solutions for oxygen limited biodegradation do not yet exist, therefore, the approach taken was to model four relatively simple, yet realistic problems and to compare the solutions predicted by BIO2D and by BIOPLUME. This resulted in some excellent insights into these models. The specific problems used were:

- Biodegradation of a hydrocarbon spill
- Natural degradation of an existing plume
- Remediated cleanup of an existing plume with a single injection well
- Remediated cleanup of an existing plume with an injection - extraction well doublet

Biodegradation Extremes BIO2D models biodegradation as limited by Monod kinetics (Equations 2.12 - 2.14). In order to evaluate the contaminant concentrations predicted by BIO2D, it is helpful to consider the bounds that it is subject to.

In an instantaneous model, degradation is limited only by the amount of contaminant and oxygen present; thus, it predicts the most optimistic or "best case" solution of substrate degradation. The concentrations predicted by an instantaneous model define a lower bound of what one should expect from a model that limits degradation. BIOPLUME is an instantaneous model, and insomuch that it can accurately describe flow and transport, defines a lower limit for BIO2D.

Modeling of a non-degrading substance defines the most conservative or pessimistic solution of substrate degradation. The concentrations predicted for a conservative contaminant define an upper bound for BIO2D.

Because BIO2D predicts slower than instantaneous kinetics, but more degradation than a conservative tracer, it should predict substrate concentrations that falls somewhere between these two extremes (Figure 4.1). As discussed in section 2.3 the solution predicted by BIO2D is a function of the input biological parameters; the selection of these parameters should change the predicted concentrations, moving them between these upper and lower bounds.

Test Aquifer The same hypothetical aquifer was used to test and compare the models for all four degradation tests. As seen in Figure 4.2, the aquifer consists of a two-dimensional, depth-averaged confined aquifer. Potential pumping locations are indicated at nodes (60,0) and (300,0). A background Darcy velocity of 0.015 $\frac{m}{day}$ was specified; this was the velocity reported by *Borden and Bedient [1986]* for the UCC aquifer in Conroe, Texas. Table 4.1 lists the physical parameters assumed for the degradation tests. A spatial discetization of $\Delta x = \Delta y = 5$ m was selected based on the Accuracy criteria given by (2.33 - 2.35). (Several trial runs demonstrated that a

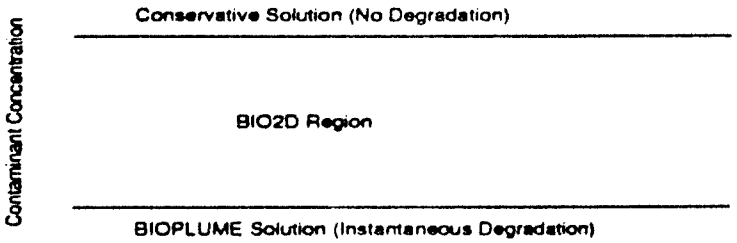

Figure 4.1: Biodegradation Regimes

$P_{e_y} = 2.78$ produced acceptable results.) An initial time step of $\Delta t = 1$ day was selected based on several trial runs and with consideration to the order of magnitude of the biological rate parameters. Note that for a conservative contaminant, application of the Courant criterion (2.35) requires a time step of approximately 30 days, based on the higher velocities found near pumping wells. Further analysis of the effects of time step size will be addressed.

The aquifer is axisymetrical with respect to the x-axis, so it was possible to model the upper half of the aquifer only, saving considerably on memory requirements and decreasing run-time. Thus, the domain was discretized into 1600 rectangular finite elements and 1701 nodes.

Boundary Conditions The flow boundary conditions specified for the degradation tests are Type 1 (constant head) along y = 0 and y = 400 m; and Type 2 (no flow)

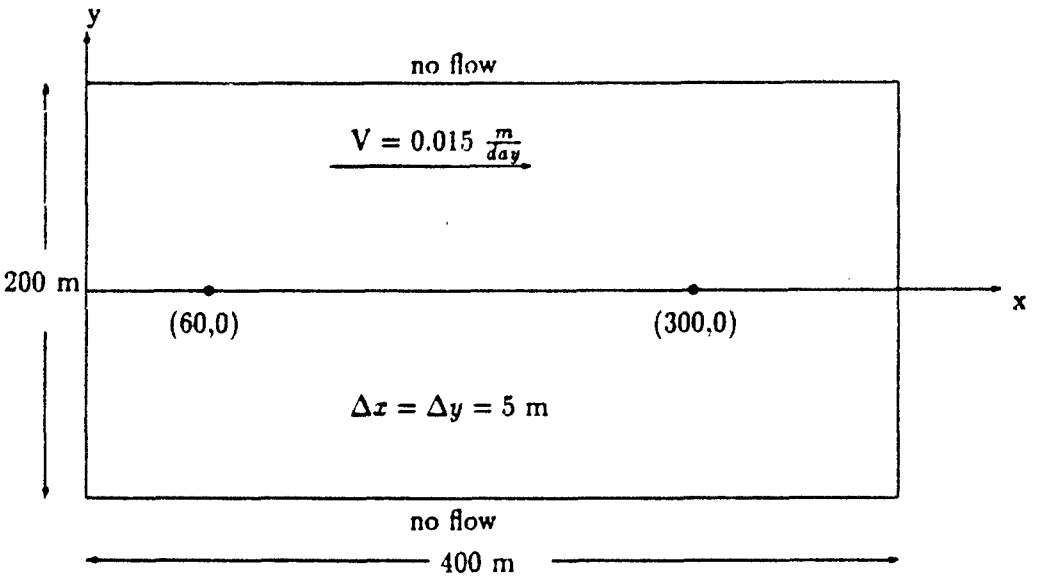

Figure 4.2: Biodegradation Testing Schematic Sketch

Table 4.1: Physical Parameters For Biodegradation Testing Problems

Parameter	Value
Darcy Velocity, V	0.015 $\frac{m}{d}$
Porosity, n	0.29
Longitudinal Dispersivity, α_L	9.1 m
Transverse Dispersivity, α_T	1.8 m
R_s	1.0
Aquifer Thickness, b	1.0 m
Δx	5.0 m
Δy	5.0 m
Δt	1.0 day
Implicitness Factor, θ	1.0
Peclet number (Pe_x)	0.55
Peclet number (Pe_y)	2.78
Courant number (Cr)	0.003

along x = 100 m and x = -100 m (Figure 4.2). Boundary conditions for transport are:

$$C(-60, y, t) = 0.0 \frac{mg}{L} \tag{4.1}$$

$$O(-60, y, t) = 3.0 \frac{mg}{L} \tag{4.2}$$

$$B(-60, y, t) = 0.001 \frac{mg}{L} \tag{4.3}$$

Choice of Contaminant The solution for BIO2D is a function not only of the code's ability to model transport, but also of the site-specific biological parameters (Section 2.3). For this study, the hypothetical pollutant chosen was *phenol*. It is a relatively common groundwater contaminant, and a large number of kinetic values are reported in literature.

Phenol is relatively mobile in soil-water systems. It is a common contaminant found in leachate from hazardous landfills, and is known to be a co-carcinogen *[La-Grega et al., 1994]*. Based on the intake of drinking water and aquatic organisms, the safe recommended level for human health is 3.5 $\frac{mg}{L}$. Several states, however, have established more stringent standards *[Oak Ridge National Laboratory, 1989]*.

The data required to conduct degradation testing and model sensitivity analysis were obtained from *Taylor [1993]* who compiled parameter ranges from literature, and fit approximate probability distributions for each of them. See *Rozich et al. [1983], Rozich et al. [1985], Chang and Rittmann [1987], Speitel et al. [1987], Hobson and Mills [1990], Lin [1992], and Wagner [1992]* for details of laboratory studies performed to get these values. Specific biological input parameters used are given in Table 4.2. The sample size refers to the number of different test results included, several from the same author. The mean values were used for biodegradation testing; the extremes will be used for the sensitivity analysis presented in Chapter 6. It is

Table 4.2: Values of Biological Parameters Used in Biodegradation Testing

Parameter	Units	Sample Size	Mean	Maximum	Minimum	Coefficient of Variation
μ_{max}	$[\frac{1}{day}]$	33	6.48	15.36	1.97	.55
K_s	$[\frac{mg}{L}]$	33	49.6	266	1	1.32
K_i	$[\frac{mg}{L}]$	33	356.8	1463	23	1.14
K_o	$[\frac{mg}{L}]$	3	1.0	2	0.1	1
Y	$[\frac{mg}{mg}]$	10	0.70	1.02	0.5	0.25
r_b	$[\frac{1}{day}]$	3	0.05	0.10	0.001	1
K_b	$[\frac{L}{mg}^{N_b}]$	3	15.26	22.97	7.55	0.50
N_b	[1]	3	1	1.1	0.9	0.10
F	$[\frac{mg}{mg}]$	Assumed $F = 3.0 = constant$				
C_c	$[\frac{mg}{L}]$	Assumed $C_c = 715 = constant$				
k_c	$[\frac{1}{day}]$	Assumed $k_c = 10^{-5} = constant$				

assumed that F, the ratio of oxygen to substrate used in degradation, is constant. It is based solely on stoichiometry, assuming complete oxidation of phenol to CO_2 and H_2O from:

$$C_6H_5OH + 7O_2 \longrightarrow 6CO_2 + 3H_2O \tag{4.4}$$

Bacterial Population It is assumed that the complex subsurface bacterial population can be represented as a single facultative, heterotrophic bacteria, such as *Bacillus*. In the absence of hydrocarbon they maintain a background concentration, B_b, by aerobically or anaerobically consuming the aquifer's naturally occurring organic carbon, such as humic or fulvic acid. In the presence of oxygen and the more easily degradable phenol, the microbes preferentially consume phenol. It is assumed that the yield coefficient, Y and death rate, r_b are constant for aerobic and anaerobic

consumption of phenol and background carbon.

The values for C_c and k_c were assumed to be constant at 715 $\frac{mg}{L}$ and 10^{-5} $\frac{1}{day}$ respectively. BIO2D assumes that the growth of bacteria on the background carbon occurs at a rate necessary to offset death and decay, so that

$$C_c k_c Y = R_b B_b r_b. \tag{4.5}$$

Thus, for assumed values of C_c, k_c, Y, R_b and r_b, the value of B_b, the background biomass, is fixed by equation 4.5. The corresponding value of B_b must be specified in the model as the initial condition for biomass. Failure to do this resulted in unstable results in degradation test runs. From equation 2.40 (Freundlich isotherm) for the assumed parameters of $K_b = 15.26$ $\frac{L}{mg}$ and $N_b = 1$, the microbial retardation factor R_b is 100. Finally, the background biomass concentration used for this baseline case from equation 4.5, using the mean values from Table 4.2, is 0.001 $\frac{mg}{L}$. Assuming the average cell weight of bacteria to be 10^{-11} $\frac{mg}{cell}$ *[Neiderhardt, 1990]*, this is equivalent to 10^5 $\frac{cells}{mL}$. This microbial concentration falls in the ranges reported as observed by *Borden and Bedient [1986].*

Basis of Comparison In order to compare the solutions generated by BIO2D and BIOPLUME the following criteria were used:

- Root mean square error (when analytical solution is available; from equation 3.1)
- Maximum substrate concentration, $S_{max}(\frac{mg}{L})$, in aquifer at any time
- Total substrate mass in aquifer, $S_{mass}(g)$, at any time
- Time to achieve a 1 ppm standard $(days)$
- CPU time to complete simulation run (min)

- Qualitative comparisons such as "good", "reasonable", and "unacceptable" based on experience and intuition.

In all cases, conservation of mass checks for both substrate and oxygen were performed.

4.2 Degradation Test 1: Biodegradation of a Hydrocarbon Spill

The first degradation test considered the spillage of a degradable contaminant into the hypothetical aquifer. This is a common scenario where leaky storage tanks discharge a hydocarbon pollutant into an aquifer for several months or even years before discovery. A spill rate of $QC_0 = 5\frac{g}{day}$ at (60,0) (Figure 4.2) was assumed. In order to make the problem realistic and ensure that the assumption of an unchanged velocity field (as required for the analytical solution) was met, a high concentration (16.7 $\frac{g}{L}$) and low flow rate (0.00015 $\frac{m^3}{day}$) were specified. The biological parameters were specified as the mean values from Table 4.2.

Initial Conditions The initial conditions are a clean aquifer (S = 0 $\frac{mg}{L}$), with a background oxygen concentration of 3.0 $\frac{mg}{L}$ and biomass concentration of 0.001 $\frac{mg}{L}$. It is assumed that the oxygen consumed by the facultative bacteria in degrading the background carbon is replenished from the vadose zone at a rate necessary to maintain the background concentration.

Conservative Tracer Comparison For a non-degradable contaminant, the analytical solution is given by Equations C.11 - C.15. Figure 4.3 depicts that both BIO2D and BIOPLUME do a good job of predicting the solution for this conservative case. The greatest error is found in the region closest to the source because the analytical solution at the well is infinity. A time step of 100 days is sufficient in BIO2D to achieve a good solution (5.61% RMSE), and the improvement in reducing the time step to 1 day is relatively insignificant (0.81% decrease in RMSE). This small time step is necessary for the satisfactory modeling of microbial degradation, however.

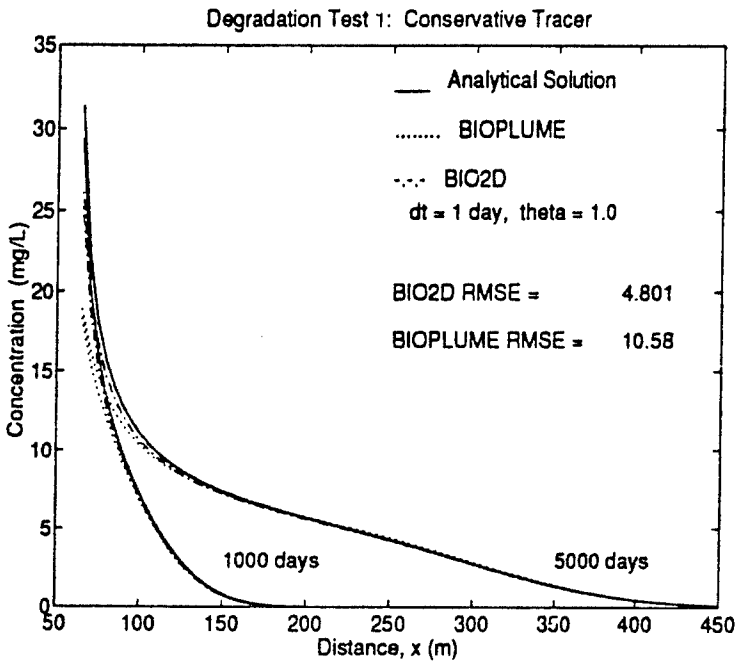

Figure 4.3: Degradation Test 1: Centerline Concentrations for Conservative Tracer

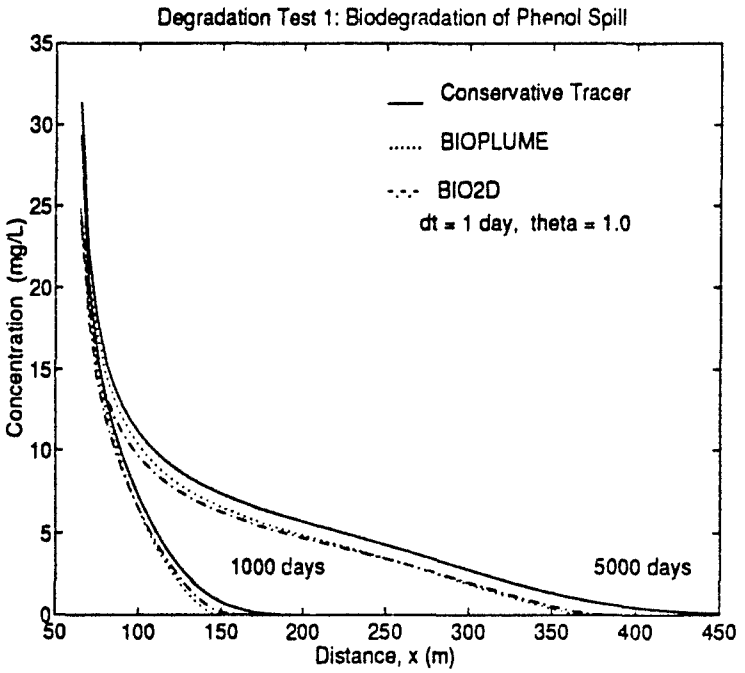

Figure 4.4: Degradation Test 1: Centerline Concentrations for Phenol Spill

Phenol Degradation Comparison Figure 4.4 compares the solutions from BIO2D and BIOPLUME for biodegradation of the phenol spill. The most conservative solution, as depicted by the upper curve, represents no degradation. The BIOPLUME solution represents a good estimate of the instantaneous, or most optimistic solution. The range that one would expect BIO2D solutions to fall is quite narrow, and the solution produced by BIO2D (using mean values from Table 4.2) is generally very close to BIOPLUME's solution. BIO2D does overpredict degradation near the source, but at the farthest extent of the plume predicts less degradation than BIOPLUME. Given the fundamental differences in the two models, and the uncertainty associated with the biological input parameters for BIO2D, the results are very reasonable.

4.3 Degradation Test 2: Natural Degradation of an Existing Plume

The second degradation test considered the natural cleanup of the hydrocarbon spill (modeled in Test 1) in the same hypothetical aquifer (Figure 4.2 and Table 4.1). It is assumed that the leaky storage tanks were discovered and the source of pollutant stopped after 2000 days. The cleanup is natural in that no oxygen was injected into the aquifer: biodegradation was limited by the oxygen remaining and oxygen recharged with flow into the aquifer. The biological parameters were specified as the mean values from Table 4.2.

Initial Conditions The oxygen and substrate initial plumes were those produced by BIO2D for Test 1 after 2000 days, and are shown in Figure 4.5. The initial biomass is assumed constant at a background concentration of 0.001 $\frac{mg}{L}$. As in Test 1, it is assumed that a background concentration of oxygen of 3 $\frac{mg}{L}$ is maintained everywhere (except in the phenol plume) by recharge with the vadose zone.

Conservative Tracer Comparison Before comparing the concentrations predicted by the two models for natural degradation, a comparison was done of their ability to model the transport of a identically shaped conservative plume. Figure 4.6 shows how BIO2D and BIOPLUME compare in their abilty to model the transport of the plume given in Figure 4.5 if it were a conservative tracer. The models predict nearly the same tracer plumes for all of the 3000 day simulation. BIOPLUME predicts a slightly higher maximum concentration at 1000 days (2.8% higher), but nearly the same at 2000 days and identical at 3000 days. Observe that the 1 ppm standard is achieved in 2650 days without any degradation. This is primarily due to the hydrodynamic dispersion of the plume, and no phenol is degraded. Mass is conserved in both models.

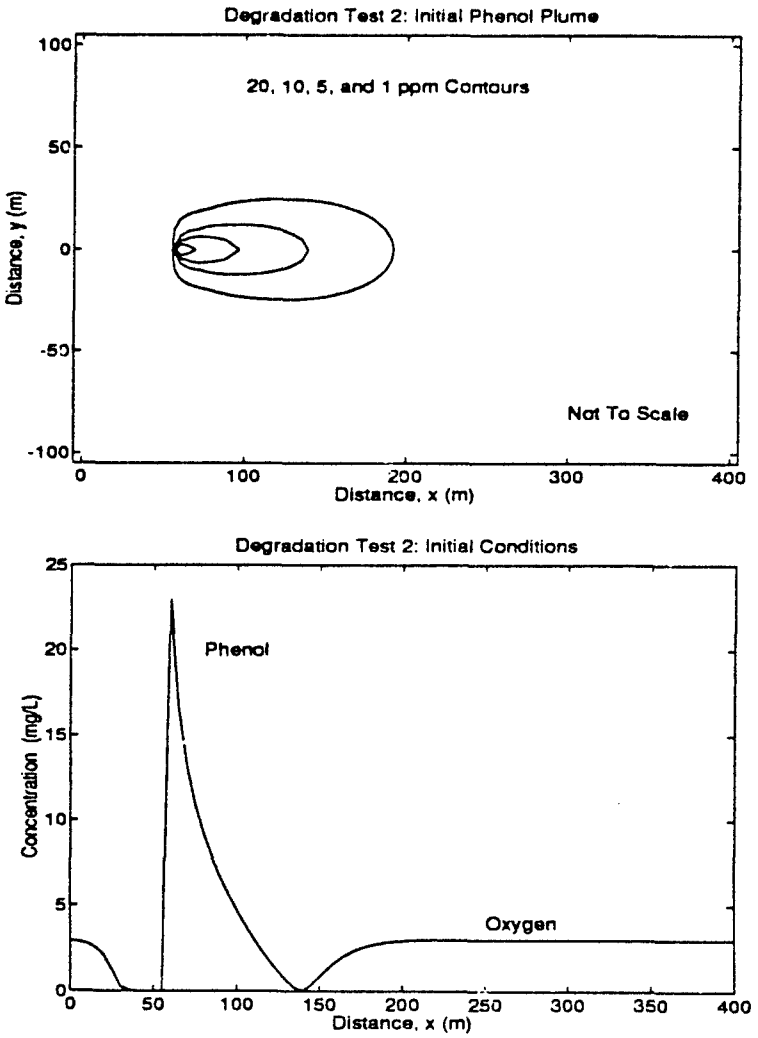

Figure 4.5: Degradation Test 2: Initial Conditions

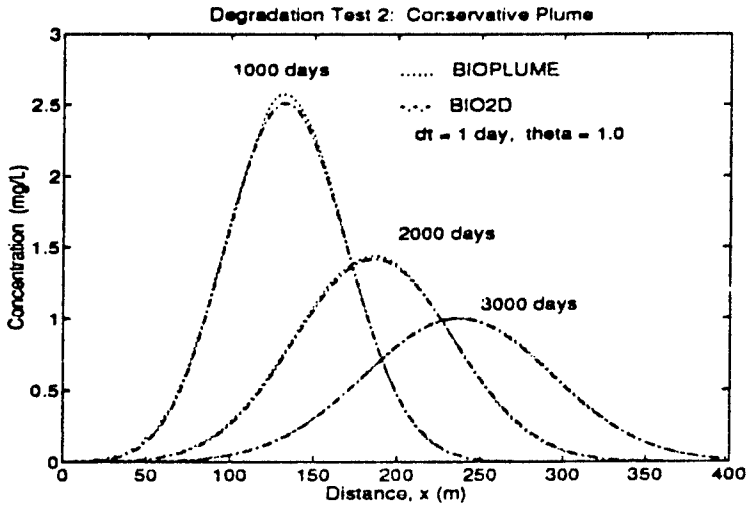

Figure 4.6: Degradation Test 2: Centerline Concentrations for Conservative Tracer

Phenol Degradation Comparison Figure 4.7 shows how the solutions for BIO2D and BIOPLUME compare for the natural biodegradation of the phenol plume given in Figure 4.5. Comparison of Figures 4.6 and 4.7 reveal the major effect of natural degradation to be at the leading edge of the plume, where oxygen is not yet depleted, and at the rear, where the effect of recharge oxygen is significant. The degraded plumes are narrower, but the peak concentrations are only slightly reduced. Figure 4.8 depicts the phenol concentrations along transverse cuts of the plume after 1000 days at x = 135 m, and after 2000 days at x = 190 m. Again, BIO2D and BIOPLUME predict very similar concentration profiles. Table 4.3 provides a summary of Degradation Test 2 results. The time to achieve a 1 ppm standard is 2230 days, which is 420 days quicker than without any biodegradation. at which the total plume mass remaining in the aquifer was less than 50% of the initial.

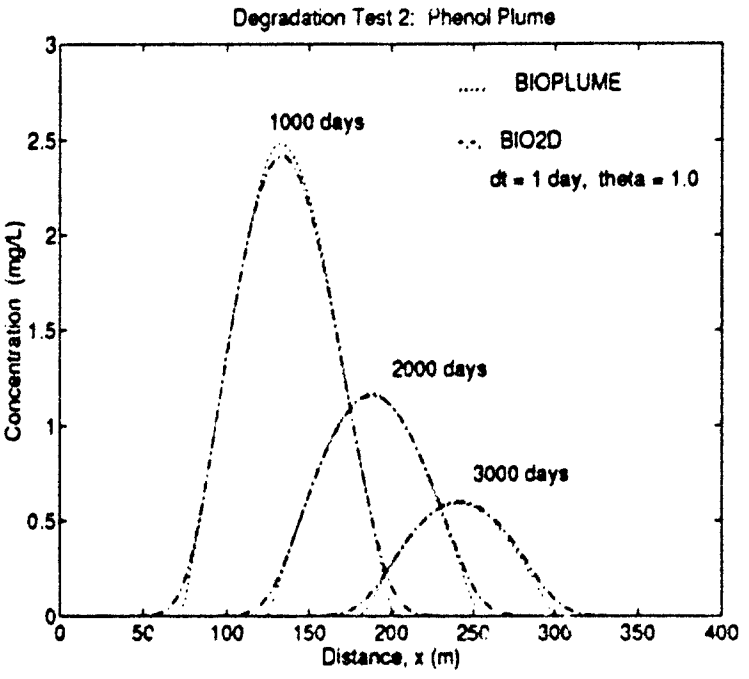

Figure 4.7: Degradation Test 2: Centerline Concentrations for Phenol Plume

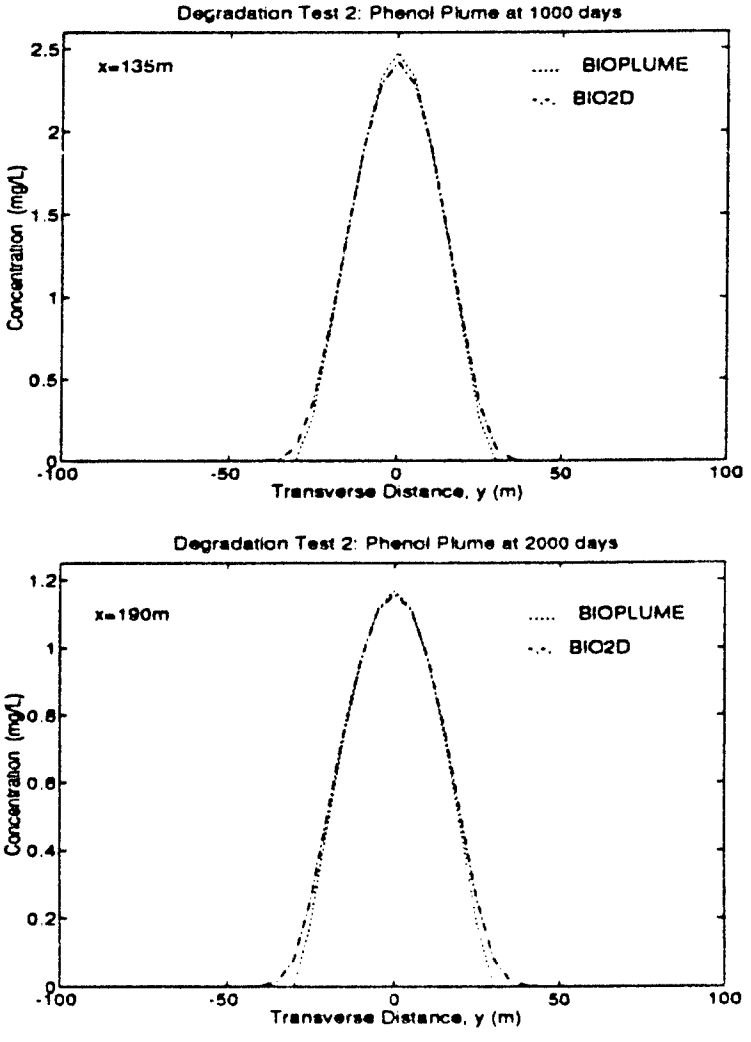

Figure 4.8: Degradation Test 2: Phenol Concentrations at x = 135 and 190 m

Table 4.3: Degradation Test 2 Results (Phencl)

TIME	MEASURE	BIO2D	BIOPLUME
Initial Conditions	S_{max} $(\frac{mg}{L})$	22.92	22.92
	S_{mass} (g)	2508	2508
500 days	S_{max}	4.10	4.23
	S_{mass}	2137	2032
1000 days	S_{max}	2.42	2.48
	S_{mass}	1667	1558
1500 days	S_{max}	1.63	1.66
	S_{mass}	1269	1156
2000 days	S_{max}	1.16	1.17
	S_{mass}	941	835
2500 days	S_{max}	0.84	0.83
	S_{mass}	675	576
3000 days	S_{max}	0.60	0.59
	S_{mass}	461	372
Totals for	*Time to 1 ppm stnd (days)*	2230	2230
3000 Days	*CPU Time (min)*	146	4.3

4.4 Degradation Test 3: Remediated Cleanup of an Existing Plume With a Single Injection Well

The third degradation test performed considered the remediated cleanup of the same plume and aquifer used used in Test 2. It is now assumed that the phenol spill was discovered and a remediation strategy designed. Specifically a fully-penetrating well was selected that injected oxygenated water at 8 $\frac{mg}{L}$ at a flow rate of 4 $\frac{m^3}{day}$ into the aquifer at (60,0) (see Figure 4.2). Again, the biological parameters were specified as the mean values from Table 4.2.

Initial Conditions The initial phenol plume was the same as for Test 2 (Figure 4.5). It is assumed that the facultative microbes maintain the assumed backgound concentration of 0.001 $\frac{mg}{L}$ by aerobic degradation of the background carbon, and that the O_2 used is replenished from the vadose zone.

Conservative Tracer Comparison The changes in the velocity field caused by pumping at a rate of 4 $\frac{m^3}{day}$ caused the plume to move and disperse more quickly than for Test 2 (no pumping). This is shown in Figure 4.9. After 1000 days, the plume has moved 40 meters further downgradient than in Test 2 (Figure 4.6), and the peak has also been reduced from 2.42 to 1.40 $\frac{mg}{L}$. Similar results are seen for 2000 and 3000 days. The time required to meet the 1 ppm standard was 1575 days. Thus, the effect of pumping is to wash the phenol out and increase hydrodynamic dispersion; however, no phenol is degraded. In both models, there is some error in the conservation of mass due to the difficulty of calculating the transport around the injection well *[El-Kadi, 1988]*. Table 4.5 shows that the error decreases with time for BIO2D, but remains approximately constant with time in BIOPLUME.

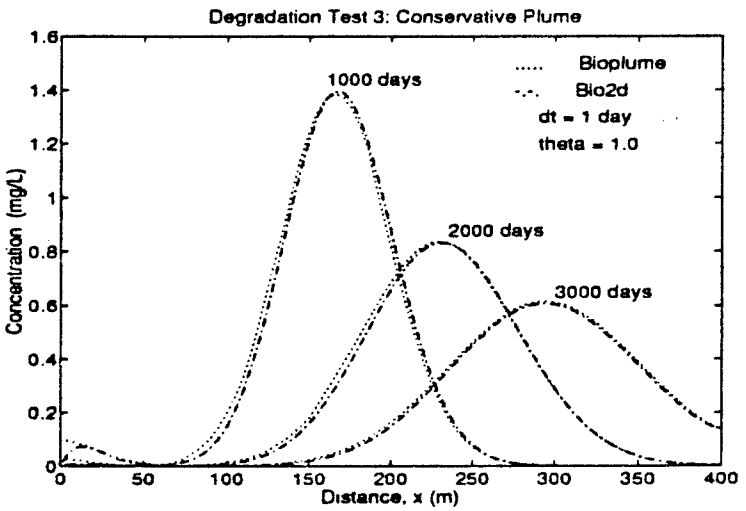

Figure 4.9: Degradation Test 3: Centerline Concentrations for Conservative Plume

Table 4.4: Degradation Test 3: Mass Balance Errors for Conservative Tracer

	BIO2D		BIOPLUME	
Time (days)	Mass (g)	Error (%)	Mass (g)	Error (%)
0	2508	0	2508	0
1000	2613	4.2	2539	1.2
2000	2581	2.9	2533	1.0
3000	2528	0.80	2443	1.4

Phenol Degradation Comparison The significant effect of stimulating the biodegradation of the phenol spill with oxygenated water is clearly seen in the results of this test. Table 4.5 provides a summary of results for this test. By injecting oxygenated water at a single well, BIO2D predicted that the 1 ppm standard was achieved in 805 days (as compared to 795 days predicted by BIOPLUME). This is about one third the time that was achieved by natural degradation alone, and one half that achieved by pumping without oxygen. Observe that of the original 2608 grams of phenol, BIO2D predicts that only 334 remain in the aquifer after 1000 days (as compared to 243 predicted by BIOPLUME). For the mean biological parameters used, BIO2D and BIOPLUME produced very similar results, Figure 4.10 shows the centerline concentrations predicted by BIO2D and BIOPLUME after 500, 1000 and 1500 days. Figure 4.11 shows the transverse concentrations predicted by BIO2D and BIOPLUME after 500 days at x = 140 m and after 1000 days at x = 180 m. The peak concentrations predicted are nearly identical, but BIOPLUME predicts more degradation at the phenol plume's edges.

Expanding the Time Step In order to reduce the length of the simulation, the time step may be increased. This may, however, result in unacceptable errors in the solution. For this degradation test, Δt was expanded to 2, 3, 4, 5 and 10 days to examine the trade off between a shorter simulation and accuracy. As seen in Table 4.6, the effect of changing the time step to 2, 3 and 4 days is minimal on the performance measures, but very significant in time savings. For Δt = 2, 3 and 4 days, the predicted values for all three measures of performance vary at most by 10 %, and less than 5% for most measures. Figure 4.12 shows the difference in centerline concentrations predicted by BIO2D when the time step is expanded from 1 to 4 days. In many applications, the small loss in accuracy may be more than compensated for by the time and money savings realized with the use of a larger Δt. Using a time

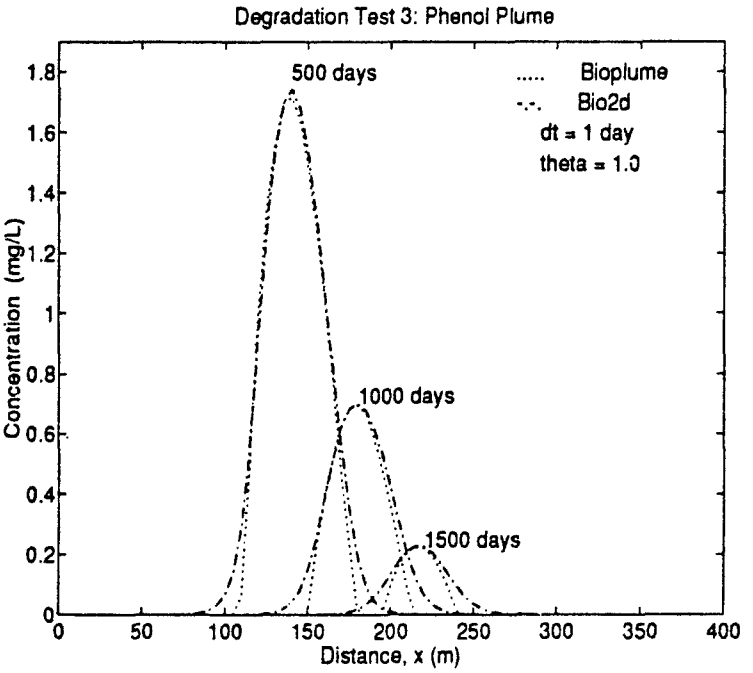

Figure 4.10: Degradation Test 3: Centerline Concentrations for Phenol Plume

step any larger than 4 days, however, results in consistent errors in excess of 10 %.

Table 4.7 shows the effect of varying the implicitness factor, θ. For $\Delta t = 1$ day, the effect is negligible. For $\Delta t = 5$ days, however, the solution is improved by adjusting θ. Unfortunately, no tested value of θ resulted in as good of a solution as was achieved by the use of a smaller time step.

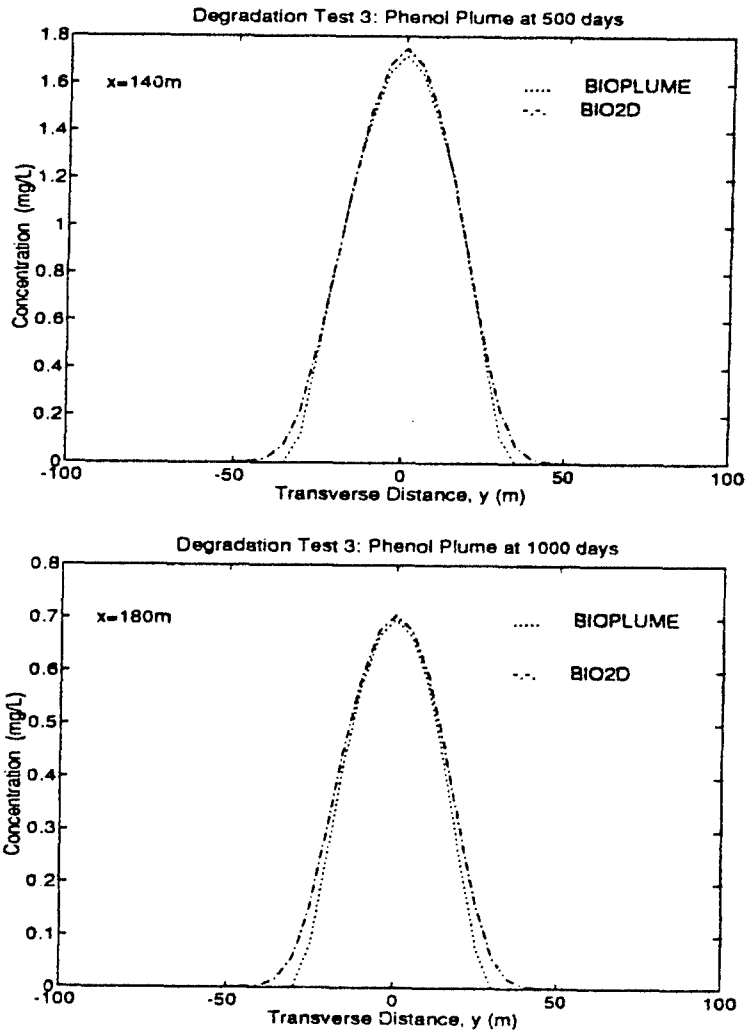

Figure 4.11: Degradation Test 3: Phenol Concentrations at x = 140 and 180 m

Table 4.5: Degradation Test 3 Results (Phenol)

TIME	MEASURE	BIO2D	BIOPLUME
Initial Conditions	S_{max} $(\frac{mg}{L})$	22.92	22.92
	S_{mass} (g)	2508	2508
500 days	S_{max}	1.74	1.72
	S_{mass}	879	756
1000 days	S_{max}	0.70	0.70
	S_{mass}	334	243
1500 days	S_{max}	0.23	0.22
	S_{mass}	84	41
Totals for	*Time to 1 ppm stnd (days)*	805	795
1500 days	*CPU Time (min)*	72	40

Table 4.6: Time Step Expansion in Degradation Test 3

		BIO2D With Δt (days) of:					
TIME	MEASURE	1	2	3	4	5	10
Initial Conditions	S_{max} $(\frac{mg}{L})$	22.92	22.92	22.92	22.92	22.92	22.92
	S_{mass} (g)	2508	2508	2508	2508	2508	2508
500 days	S_{max}	1.74	1.76	1.76	1.76	1.64	1.85
	S_{mass}	879	895	903	907	807	988
1000 days	S_{max}	0.70	0.71	0.72	0.72	0.64	0.80
	S_{mass}	334	345	351	353	295	416
1500 days	S_{max}	0.23	0.24	0.25	0.25	0.19	0.31
	S_{mass}	84	89	93	94	67	128
Totals for	*Time to stnd (days)*	805	812	816	816	765	870
1500 Days	*CPU Time (min)*	72	36	24	18	14.5	7.2

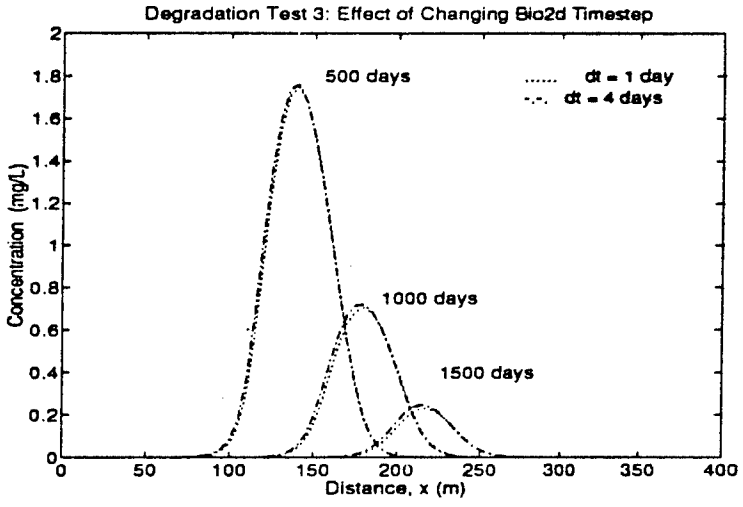

Figure 4.12: Degradation Test 3: Expanding Δt

Table 4.7: Time Step Expansion and Various Values of θ in Degradation Test 3

		$\Delta t = 1$ day			$\Delta t = 5$ days		
TIME	MEASURE	$\theta = 1.0$	$\theta = 0.75$	$\theta = 0.5$	$\theta = 1.0$	$\theta = 0.75$	$\theta = 0.5$
500 days	S_{max}	1.74	1.75	1.75	1.64	1.81	1.79
	S_{mass}	879	884	886	807	943	935
1000 days	S_{max}	0.70	0.71	0.71	0 .64	0.75	0.74
	S_{mass}	334	337	337	295	375	370
1500 days	S_{max}	0.23	0.23	0.23	0.19	0.27	0.26
	S_{mass}	84	86	86	67	105	103
Totals for	*Time to stnd (days)*	805	807	807	765	840	835
1500 Days	*CPU Time (min)*	72	72	72	14.5	14.5	14.5

4.5 Degradation Test 4: Remediated Cleanup of an Existing Plume With an Injection - Extraction Well Pair

The final degradation test performed considered the remediated cleanup of the same plume and aquifer used in Tests 2 and 3. It is now assumed that the remediation strategy included a doublet, with one injection well, pumping oxygenated water (8 $\frac{mg}{L}$) into the aquifer at (60,0), and one extraction well pumping water out of the aquifer at (300,0). (See Figure 4.2). Both wells are assumed to be fully-penetrating, and pump at a flow rate of 2 $\frac{m^3}{day}$. Thus, the total pumping effort remains the same as in Test 3. The biological parameters were specified as the mean values from Table 4.2.

Initial Conditions The initial phenol plume was the same as for Tests 2 and 3 (Figure 4.5). As before, it is assumed that the facultative microbes maintain a constant background concentration of 0.001 $\frac{mg}{L}$ by aerobic degradation of the background carbon, and that the O_2 used is recharged from the vadose zone.

Conservative Tracer Comparison The complexities of a non-uniform flow field caused by an injecection - extraction well doublet are seen in the results of this test. Recall Validation Test 5, which tested BIO2D and BIOPLUME under a very similar conditions, with a conservative contaminant. In that test we observed BIOPLUME's problems with wells that resulted in numerical dispersion and mass balance errors. Transport around the wells is dominated by radially convergent and divergent flow.

For a conservative tracer (Figure 4.13) the concentration profiles predicted by BIO2D and BIOPLUME are somewhat diff ·ו·. As in Test 3, the pumping results in mass balance errors in both models, although as *El-Kadi [1988]* reported, these errors are greater for the well doublet than for a single well. As seen in Table 4.8,

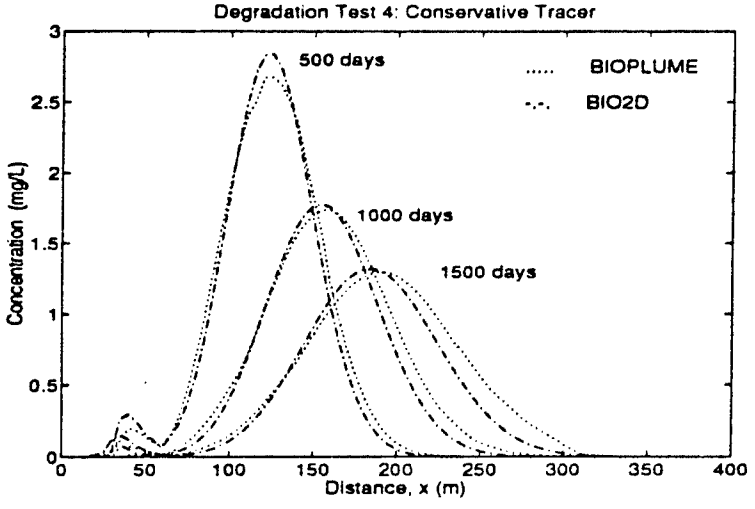

Figure 4.13: Degradation Test 4: Centerline Concentrations for Conservative Tracer

BIO2D overpredicted the tracer mass by about 6%, which remained approximately constant with time. BIOPLUME overpredicted the tracer mass by as much as 13.7 %, and this error increased with time. In this case, BIOPLUME actually demonstrated numerical dispersion. As seen in Figure 4.13, the numerical dispersion results in a lower peak concentration at 500 days. After 1000 and 1500 days, however, the additional mass artifically created by BIOPLUME results in a closer match of the peaks. These errors are due to BIOPLUME's difficulties in modeling transport near wells *[Konikow and Bredehoeft, 1978]* and *[El Kadi, 1988]*.

Phenol Degradation Comparison The results for phenol degradation are seen in Figure 4.15 and Table 4.9. Observe that BIO2D predicts greater degradation, or less total mass, than BIOPLUME using both S_{max} and S_{mass} as performance measures. In addition BIO2D predicts a 100-day faster cleanup. This may be due to

the fact that BIOPLUME artificially creates mass, as seen in the conservative case and in Validation Test 5. In addition, the O_2 injected into the aquifer as an electron acceptor is subject to numerical dispersion, resulting in less available at the plume for degradation. This effect was clearly seen in Validation Test 5 and is well documented as a weakness of the MOC when dealing with wells *[El Kadi, 1988]*. The combined effects of these two factors is more phenol mass, which is what we observed.

Table 4.8: Degradation Test 4: Mass Balance Errors for Conservative Tracer

	BIO2D		BIOPLUME	
Time (days)	Mass (g)	Error (%)	Mass (g)	Error (%)
0	2508	0	2508	0
500	2665	6.2	2676	7.0
1000	2673	6.6	2789	11.5
1500	2675	6.6	2819	13.7

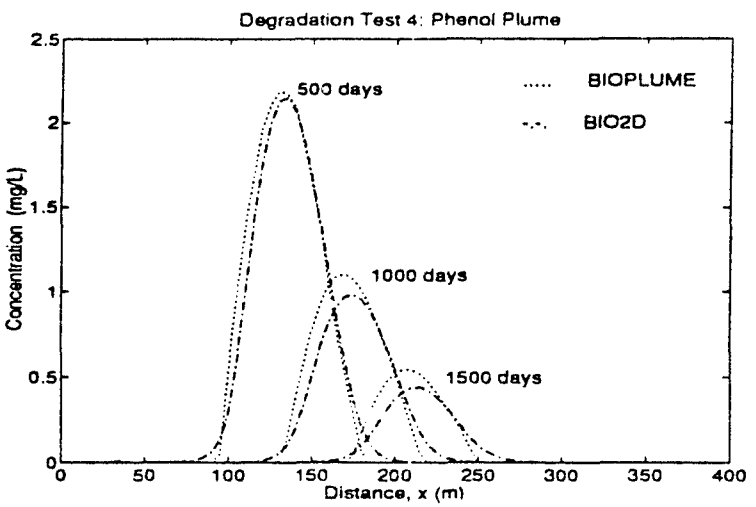

Figure 4.14: Degradation Test 4: Centerline Concentrations for Phenol Plume

Table 4.9: Degradation Test 4 Results (Phenol)

TIME	MEASURE	BIO2D	BIOPLUME
Initial Conditions	S_{max} $(\frac{mg}{L})$	22.92	22.92
	S_{mass} (g)	2508	2508
500 days	S_{max}	2.15	2.19
	S_{mass}	1138	1099
1000 days	S_{max}	0.98	1.10
	S_{mass}	543	544
1500 days	S_{max}	0.44	0.55
	S_{mass}	211	216
Totals for	*Time to 1 ppm stnd (days)*	987	1078
1500 days	*CPU Time (min)*	72	22

4.6 Summary

In this chapter, four bioremediation tests were performed on BIO2D, with comparisons made to BIOPLUME. Each considered a different problem involving the spill and cleanup of a phenol pollutant into a confined aquifer. BIO2D simulations were performed with the eleven biological parameters (Table 4.2) at their mean values.

For the first three tests, the two models predicted remarkably similar results. In each, BIOPLUME predicted slightly more degradation, which is consistent with what we expect. In Test 4, BIO2D predicted slightly more degradation that BIOPLUME. This is most likely due to errors associated with the MOC and wells.

These results can be summarized as follows:

- BIO2D predictions of contaminant concentrations were very reasonable, falling within the range expected in all tests except Test 4
- Although both models have difficulty representing flow and transport around wells, BIO2D appears to have outperformed BIOPLUME in a case involving injection and extraction
- In general BIOPLUME simulations were faster than BIO2D's. This is due to the small time step required by BIO2D during the early weeks of the cleanup when degradation is the dominant process. Chapter 5 will address an improvement that will permit much more competitive run times.
- The expansion of the Δt from 1 day to 2-4 days was found to be quite reasonable for Test 3. The loss of accuracy was relatively small and the run times were considerably faster. For many applications a larger time step may be justified.
- The adjustment of θ, the time implicitness factor was found to be insignificant to solution accuracy. This is due to the relatively small time step required by the degradation. For most applications taking $\theta = 1.0$ is satisfactory.

Chapter 5

BIO2D Program Improvements

The previous chapters have presented and evaluated the biodegradation model BIO2D as written by *Taylor*. It is the purpose of this chapter to propose and test two modifications to the model that may improve performance and better represent the processes involved in groundwater biodegradation.

5.1 Iterative Procedure

As discussed in Section 2.3, the solution technique for finding the approximate solutions to the governing partial differential equations (2.2 - 2.4) was to uncouple and linearize them. This procedure has the advantage of being computationally simple, but its accuracy must be further evaluated. An alternative technique is to solve these equations by the use of an iterative method. This method is presented as a way of checking the accuracy of a linearized approach, and as a potential refinement in the solution procedure.

Method of Solution Considering only substrate, equation 2.30 could be reformulated as:

$$\left([A_s] + [R_s]^{t+1}\right)\{S\}^{t+1} = \left([B_s] + [R_s]^{t}\right)\{S\}^{t} + [D_s] \tag{5.1}$$

where $[R_s]^{t+1}$ is a function of $\{S\}^{t+1}$. In the linearized method, $[R_s]^{t+1}$ is approximated by $[R_s]^t$ and the equation is solved in one step. In an iterative method, however, $[R_s]^{t+1}$ is updated after $\{S\}^{t+1}$ is found, and the equation is solved again. This procedure is continued until the solution converges to some acceptable tolerence. This can be represented by:

$$\left([A_s] + [R_s]_{i-1}^{t+1}\right)\{S\}_{i}^{t+1} = \left([B_s] + [R_s]^{t}\right)\{S\}^{t} + [D_s] \tag{5.2}$$

where i = the iteration number. This method is applied to the partial differential equations for substrate, oxygen and biomass.

The euclidean length, l_2 norm, was used as the basis for convergence of the iterative method. It is defined by:

$$\|x\| = \sqrt{|x_1|^2 + |x_2|^2 + \ldots + |x_n|^2} \tag{5.3}$$

The residual errors in substrate, oxygen and biomass convergence are given by:

$$\delta_S = \frac{\|S_i^{t+1} - S_{i-1}^{t+1}\|}{\|S_{i-1}^{t+1}\|} \tag{5.4}$$

$$\delta_O = \frac{\|O_i^{t+1} - O_{i-1}^{t+1}\|}{\|O_{i-1}^{t+1}\|} \tag{5.5}$$

$$\delta_B = \frac{\|B_i^{t+1} - B_{i-1}^{t+1}\|}{\|B_{i-1}^{t+1}\|} \tag{5.6}$$

The iterations continue until the following criteria are met:

$$\delta_S \leq \beta \tag{5.7}$$

$$\delta_O \leq \beta \tag{5.8}$$

$$\delta_B \leq \beta \tag{5.9}$$

where β is the convergence tolerence. As a matter of practicality, a maximum number of iterations, $mxitr$ can be set for the procedure.

The application of this procedure was made to Degradation Test 3, where a polluted aquifer is cleaned up using a single injection well (see Section 4.4). For this test, the solutions predicted by BIO2D and BIOPLUME were nearly identical.

For the baseline case (biological parameters assumed as the mean values from Table 4.2), a plot of residuals (equations 5.4 - 5.6) versus time is given by Figure 5.1. These residuals represent the error in the linearized solution. As seen in the figure, the residual errors begin relatively high, but level off to less than 0.05 after the first 20-30 days. It follows that the solutions obtained using iteration were not different than the linearized solution. Table 5.1 shows that the solutions for the linearized method, and the iterative method with $\beta = 0.05$ and 0.02 are virtually the same. The iterative procedure requires more computations, as reflected by the longer CPU times.

Using Iteration with Larger Time Steps Iteration can be exploited to reduce simulation run times by allowing the use of a larger time step. Runs were made with larger Δt to see if the desired accuracy could be obtained by using iterations. $\beta = 0.02$ was used for $\Delta t = 2$, 3, 4, and 5 days. As seen in Table 5.2, the use of iteration resulted in more acceptable solutions for time steps of 2, 3, and 4 days, as compared with the linearized solutions shown in Table 4.6. Any savings in the larger time step for $\Delta t = 3$ and 4 days were offset by the very high number of iterations required. For $\Delta t = 5$ days, even the use of iteration did not produce satisfactory results. Using the iterative technique with $\Delta t = 2$ days, however, resulted in significant CPU time savings and nearly identical results to the $\Delta t = 1$ day case. For this case it is clearly better to use $\Delta t = 2$ days with iteration, than to use a linearized method with $\Delta t = 1$ day, since the total run time is approximately 50% less.

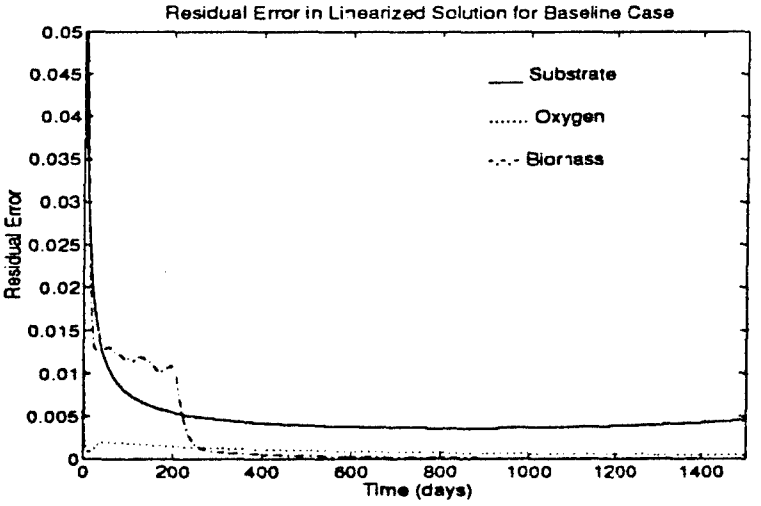

Figure 5.1: Residual Error in Linearized Solution of PDEs, Baseline Case

Table 5.1: Effect of Iteration on Baseline Case

		Δt = 1 day		
TIME	MEASURE	Linearized	$\beta = 0.05$	$\beta = 0.02$
500 days	S_{max}	1.74	1.74	1.74
	S_{mass}	879	879	878
1000 day.	S_{max}	0.70	0.70	0.70
	S_{mass}	334	334	333
1500 days	S_{max}	0.23	0.23	0.23
	S_{mass}	84	84	84
Totals for	*Time to stnd (days)*	805	803	802
1500 Days	*Total Iterations*	0	5	32
	CPU Time (min)	72	98	100

A Case Where an Iterative Solution is Necessary Consider a case where the value of K_s was taken at its minimum value of 1 $\frac{mg}{L}$ (Table 4.2). At this value, the degradation occurs at a much faster rate as seen by equations 2.36 - 2.38. As seen in Figure 5.2, the residual errors for substrate and oxygen are much greater than for the baseline case. The residual errors for biomass were *extremely* high, and were not even plotted on this graph. In this case, it is obvious that a linearized solution is not sufficient.

Figure 5.3 shows the residual errors for the solutions obtained using iteration ($\beta = 0.02$, $mxitr = 10$). In this case the error is still very high for the first 5-10 days, but quickly levels off to approximately 5% for the remainder of the 1500-day simulation. A summary of the linearized versus the iterative solutions is given in Table 5.3. Although this extreme example required a relatively high number of iterations (and long CPU time), the differences in the predicted concentrations were not trivial. In fact, the very high number of iterations was required to improve the residual from approximately 0.05 to 0.02. An alternative approach to maintaining accuracy in this case of faster kinetics would be to reduce the time step. As seen above, however, the iterative method is more efficient than the use of a smaller time step.

Summary The use of an iterative procedure offers a significant advantage over the linearized approach. In many cases it permits the use of a larger time step than would have been otherwise required. In other cases where the specified biological parameters result in fast kinetics, an iterative solution is required to avoid the use of a very small time step. Thus, it is recommended as an improvement to BIO2D. It will be used in all sensitivity analysis runs completed for Chapter 6.

Table 5.2: Using Iteration with Larger Time Steps

		Iteration ($\beta = 0.02$) and Δt (days) of:				
TIME	MEASURE	1	2	3	4	5
500 days	S_{max}	1.74	1.73	1.70	1.67	1.47
	S_{mass}	879	876	846	836	687
1000 days	S_{max}	0.70	0.70	0.67	0.65	0.53
	S_{mass}	334	331	314	304	233
1500 days	S_{max}	0.23	0.23	0.21	0.20	0.11
	S_{mass}	84	83	75	71	36
Totals for	*Time to stnd (days)*	805	800	783	772	690
1500 Days	*Total Iterations*	100	103	4500	2344	2188
	CPU Time (min)	100	53	140	110	102

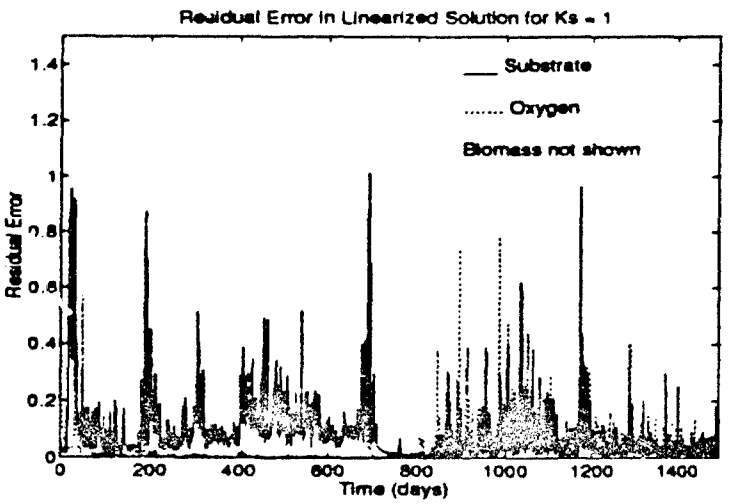

Figure 5.2: Residual Error in Linearized Solution of PDEs, $K_s = 1\ \frac{mg}{L}$

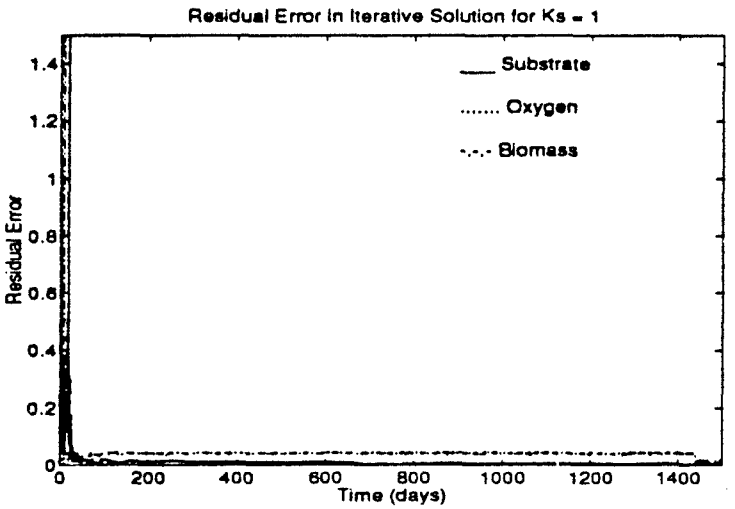

Figure 5.3: Residual Error in Iterative Solution of PDEs, $K_s = 1\ \frac{mg}{L}$

Table 5.3: Effect of Iteration on $K_s = 1\ \frac{mg}{L}$ Case

		Δt = 1 day		
TIME	MEASURE	Linearized	$\beta = 0.05$	$\beta = 0.02$
500 days	S_{max}	1.50	1.46	1.34
	S_{mass}	583	563	477
1000 days	S_{max}	0.54	0.52	0.43
	S_{mass}	160	150	104
1500 days	S_{max}	0.10	0.09	0.02
	S_{mass}	11	8	1
Totals for	*Time to stnd (days)*	697	686	636
1500 Days	*Total Iterations*	0	82	13,118
	CPU Time (min)	72	100	579

5.2 Modified Kinetics

The proposed changes to BIO2D presented in this section are the result of discussions with Dr. James Gossett, Cornell University. Some of the ideas that follow were taken from notes from Dr. Gossett's class on Environmental Engineering Processes.

A shortcoming in BIO2D as discussed and tested so far is that the governing PDE for oxygen fails to account for all oxygen sinks. Specifically, equation 2.37 neglects to account for substrate consumed in synthesis of net biomass and O_2 consumed in the aerobic degradation of background carbon. Equation 2.37 can be rewitten as:

$$\lambda_{RO} = BR_b F \frac{\mu_s}{Y} \tag{5.10}$$

where

$$\mu_s = \mu_{max} \left[\frac{S}{K_s + S + \frac{S^2}{K_i}} \right] \left[\frac{O}{K_o + O} \right] \tag{5.11}$$

Looking at each additional O_2 sink individually:

O_2 Consumed in Net Biomass Synthesis The following equations represent the production and use of energy in aerobic respiration and synthesis of new biomass, assuming that the contaminant substrate is used as the electron donor for both energy production and synthesis of net biomass:

Energy:

$$Substrate + O_2 \rightarrow CO_2 + H_2O + energy \tag{5.12}$$

Synthesis:

$$Substrate + NH_4 + energy \rightarrow C_5H_7O_2N \tag{5.13}$$

In essence, the substrate electron donor is oxidized and the O_2 electron acceptor is reduced. Energy is captured (e.g., as ATP) for use in biosynthesis, which involves

converting the substrate into cellular constituants ($C_5H_7O_2N$). In this case, when the same substrate is used for both energy and synthesis, a fraction of the substrate is used for synthesis, while the remainder is used for energy:

$$f_s + f_e = 1 \tag{5.14}$$

$f_s \equiv$ *fraction of substrate used for synthesis*

$f_e \equiv$ *fraction of substrate used for energy*

where f_e and f_s depend upon energetics (i.e., the energy available from the respiration reaction compared to that required by the synthesis reaction). In an activated sludge application, they also depend upon the solids retention time for the system.

In the governing equations used in BIO2D, F, the ratio of oxygen to substrate utilized, assumes that all substrate is used in an energy reaction (equation 5.12), and that none is used for synthesis (equation 5.13). They also neglect to account for O_2 used by the microorganisms as they consume dead biomass. An additional term that should be added to (equation 5.10) is proposed to account for these effects:

$$-1.42\left[\mu_s B - \frac{O}{K_o + O} r_b B\right] \tag{5.15}$$

where 1.42 is a conversion factor from grams biomass to grams oxygen, assuming a biomass composition of $C_5H_7O_2N$. Thus, when there is a net increase in biomass, the [ ] is positive, and the amount of O_2 utilized will be reduced by (equation 5.15) from the amount otherwise predicted. When there is a net decrease in biomass, however, the [ ] is negative, and there will be more oxygen consumed than in the present formulation. The term $\frac{O}{K_o+O}$ predicts a Monod-type consumption of oxygen as the microorganisms consume themselves.

O_2 Consumed by Background Carbon The second oxygen sink not accounted for by the governing PDEs is the O_2 consumed by the *aerobic* degradation of background carbon. Our simplifying assumption about the subsurface microorganisms

was that they could be represented by a single facultative bacterial population that maintained a constant background concentration by aerobically or anaerobically degrading the available carbon sources in the aquifer (Section 2.3, Assumption 8). In the presence of a contaminant substrate they preferentially consume it. BIO2D, however, neglects to account for any O_2 consumed by the biomass in the aerobic degradation of this background carbon. In the case where we assumed an initial, background concentration of O_2 in the aquifer, as in Degradation Tests 2-4, it follows that the microorganisms would *aerobically* degrade this carbon. An additional modification is proposed to account for this:

$$+ \frac{O}{K_o + O} F' C_c K_c \tag{5.16}$$

where F' is the stoichiometric ratio of oxygen to background carbon consumed in the aerobic degradation of background carbon.

Thus, the modified PDE for oxygen should include the following:

$$\lambda_{RO} = R_b \left\{ \frac{\mu_s F B}{Y} - 1.42 \left[\mu_s B - \frac{O}{K_o + O} r_b B \right] + \frac{O}{K_o + O} F' C_c K_c \right\} \tag{5.17}$$

Modification Testing The ultimate test of this proposed modification would be a comparison of predicted to observed concentrations from a field application. This, however, is beyond the scope of the present work. Tests were performed to investigate how these proposed changes affect the predicted contaminant concentrations for Degradation Test 3 (see Section 4.4). This scenario involved the cleanup of a aquifer polluted by a phenol spill. The aquifer cleanup was completed using a single injection well that introduced oxygenated water at a flow rate of 4 $\frac{m^3}{day}$. The predicted concentrations for this case were nearly the same for BIOPLUME and BIO2D.

Figure 5.4 shows the predicted centerline concentrations of phenol at 500, 1000 and 1500 days for the original kinetics and the modified kinetics. An initial oxygen concentration of 3 $\frac{mg}{L}$ was specified everywhere in the aquifer, except for anoxic

Table 5.4: Degradation Test 3: Modified vs Original Kinetics

		Initial Aerobic		Initial Anoxic	
TIME	MEASURE	Original	Modified	Original	Modified
500 days	S_{max}	1.74	1.91	1.79	1.91
	S_{mass}	879	1402	1210	1515
1000 days	S_{max}	0.70	1.05	0.87	1.06
	S_{mass}	334	1212	803	1310
1500 days	S_{max}	0.23	0.72	0.51	0.73
	S_{mass}	84	1161	574	1253
Totals for	*Time to stnd (days)*	805	1053	890	1070

conditions at the plume's location (see Figure 4.5). Mean values for all biological parameters were used (Table 4.2). Observe that the differences in the solutions of the governing equations are magnified with time. This is due in part to the consumption of the background O_2 by the facultative bacteria when modified kinetics are used. Very quickly, the background O_2 is consumed and anoxic conditions prevail. At 500 days, the initial O_2 is nearly gone, with the exception of O_2 recharged by the injection well, and O_2 recharged at the left boundary.

A more interesting comparison is seen in Figure 5.5. Again, the predicted centerline concentrations of phenol at 500, 1000 and 1500 days are depicted for the two different kinetic formulations. In this case, the initial background O_2 condition was taken as anoxic everywhere in the aquifer. Here, the differences between the predicted solutions were not as great as before, but still quite significant. The primary source of this difference is the additional O_2 sink given by equation 5.15, which accounts for O_2 consumed by the consumption of dead biomass.

Table 5.4 summarizes the results of these test runs.

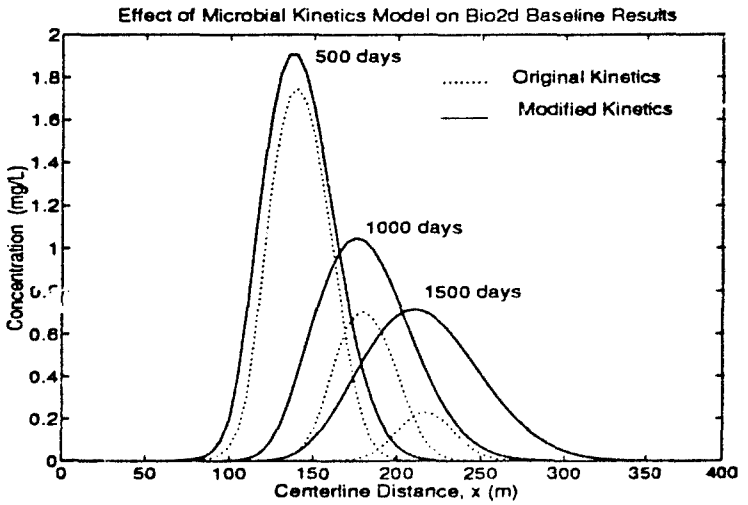

Figure 5.4: Original vs Modified Kinetics for Initial Aerobic Conditions

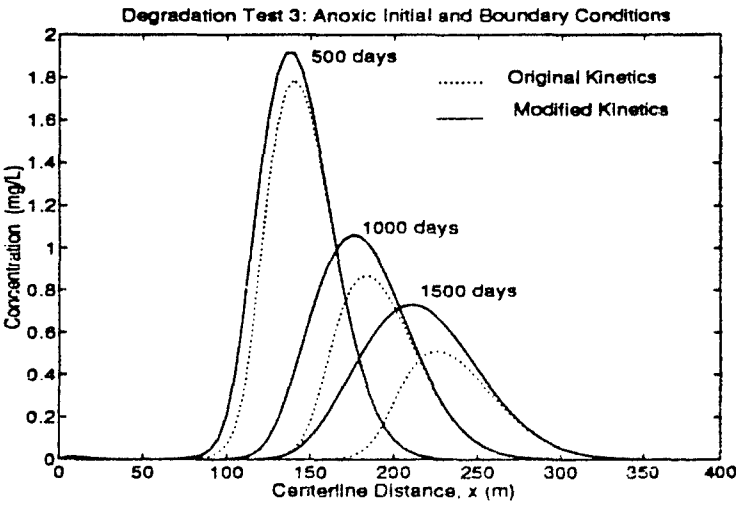

Figure 5.5: Original vs. Modified Kinetics for Initial Anoxic Conditions

5.3 Summary

In this chapter two modifications to the present formulation of BIO2D were presented and evaluated:

1. An iterative procedure to solve the nonlinear PDEs
2. Modified kinetics that more realistically account for O_2 consumed in microbial degradation

The first modification is highly recommended as a more efficient and accurate means of solving the problem. In some cases, where the biological parameters result in slow or moderate kinetics, the iterative solution will permit more efficient solution and shorter run times that the linearized method. In cases where the kinetics are fast, the use of an iterative solution is necessary to avoid the use of an extremely small time step.

The second modification needs further testing. The inclusion of additional O_2 sinks due to synthesis of net biomass and aerobic degradation of background carbon results in vastly different solutions. Although the modified kinetics seem to the author as a better representation of reality, model predictions must be compared to observed concentrations at a field site in order judge this modification's merits. Until this is completed, no change is warranted. It is recommended, however, that the initial and boundary conditions for O_2 in the aquifer be taken as anoxic everywhere, unless there is evidence to support another assumption. The assumption of a constant aerobic initial condition, in the presence of facultative bacteria, without recharge simply does not make sense.

Chapter 6

Model Sensitivity to Biological Parameters

6.1 Introduction

This chapter addresses sensitivity of BIO2D to changes in the often unknown *biological* parameters given in Table 2.2. The purpose is to quantify the uncertainty in the predicted concentrations of pollutant in an aquifer caused by uncertainty in the estimates of these constants. Sensitivity analysis is an essential step in all applications of groundwater modeling *[Anderson and Woessner, 1992]*, but it is especially important in degradation modeling because of the great number of unknown parameters. As discussed in Chapter 2, the predicted concentrations are a function of seven physical parameters (Table 2.1), eleven biological parameters (Table 2.2), and the initial and boundary conditions for the problem. It would be of great help to users of degradation models to gain a better understanding of which parameters are very important to know, and which parameters are not as important and might be assumed from literature. This will allow limited resources of time and money to be spent on determining the most important ones.

The basis for the sensitivity analysis performed was Degradation Test 3 (see Section 4.4). This scenario involved the cleanup of a phenol polluted aquifer using a single injection well that introduced oxygenated water at 8 $\frac{mg}{L}$. Recall that for this case predictions of contaminant concentrations were quite similar for BIO2D and BIOPLUME. A time step of $\Delta t = 1$ day was used. The iterative procedure, with original kinetics, presented in Chapter 5 was used for all runs, with iteration parameters of $\beta = 0.02$ and $mxitr = 10$.

Methodology The methodology used in this study of model sensitivity was to utilize existing parameter ranges for phenol degradation, observing predicted contaminant concentrations based on mean, maximum and minimum parameter values from published studies. This seems to be a much more rational approach to sensitivity than merely varying each parameter by the same percentage, as is often done. By using a realistic range the greater variablility of some parameters is accounted for. For example, it is much more useful to know how model predictions vary as K_s is changed from its minimum ($1\frac{mg}{L}$) to its maximum value ($266\frac{mg}{L}$), than it is to know how the predictions vary as K_s is perturbed by 5% from its mean value. The use of the parameter extremes also allows for the definition of bounds on the system performance ("best" and "worst" cases).

The ranges of the site-specific biological parameters assumed for this study are given in Table 4.2. These constants for phenol degradation were obtained from published laboratory and field studies. *[Rozich et al. ,1983; Rozich et al., 1985; Chang and Rittmann, 1987; Speitel et al., 1987; Hobson and Mills, 1990; Lin, 1992; and Wagner, 1992]* Of the eleven parameters, F, C_c, and k_c were considered as deterministic. F can be determined directly from the balanced reaction stoichiometry, assuming complete mineralization to CO_2 and H_2O from equation 4.4. Insufficient data were available to quantify variablity in C_c and k_c, and it was assumed that

growth rates on background carbon were small compared to growth on contaminant substrate. The remaining eight parameters were considered as unknown or stochastic. All eleven were assumed to be constant in time and space.

Both individual sensitivity and combined sensitivities were studied. The former is the more common approach where model output is observed as one parameter at a time is varied. In the latter approach all parameters are varied simultaneously. This is more thorough and accounts for parameter-parameter interactions.

Previous Work *Taylor* performed a sensitivity analysis using probability density functions for each of the unknown parameters. A Latin hypercube sampling scheme was used to obtain vectors of parameter distributions. These were input and the variations in model output measured. He used S_{max} as the measure of model sensitivity. This work differs from that of *Taylor* in the following ways:

- Both individual and combined sensitivities were studied
- Parameter extremes were used rather than assumed probability distributions
- Three measures of sensitivity were used: S_{max}, S_{mass}, and t_{stnd} as defined in Section 5.1
- A more realistic scenario was modeled: a larger aquifer (80,000 m^2) with a longer cleanup time (1500 days)

Preliminary Analysis A preliminary, qualitative analysis of how the predicted concentrations should be affected by changes in each of these biological parameters follows:

1. *F, the stoichiometric ratio of oxygen to substrate consumed in degradation:* As F increases, the amount of O_2 required for degradation increases per unit of

substrate. Thus, a higher F should result in less degradation given a finite amount of oxygen. In this work, however, F is considered deterministic.

2. μ_{max}, *the maximum specific growth rate of bacteria:* As μ_{max} increases, the biomass should grow more quickly and substrate consumption will procede at a faster rate, resulting in more degradation.

3. K_s, *the Monod substrate half-saturation constant:* As K_s decreases relative to S, the degradation should procede at a faster rate, resulting in more degradation. For $S >> K_s$, $\frac{S}{K_s+S} \rightarrow 1$.

4. K_o, *the Monod oxygen half-saturation constant:* As K_o decreases relative to O, the degradation should procede at a faster rate, resulting in more degradation. For $O >> K_o$, $\frac{O}{K_o+O} \rightarrow 1$.

5. K_i, *the substrate inhibition constant:* As K_i increases relative to S^2, the bacteria are less inhibited by the substrate, and degradation should be faster. For $S^2 << K_i$, $\frac{S^2}{K_i} \rightarrow 0$.

6. Y, *the yield coefficient:* As Y increases, more microbes are produced from a given amount of substrate. In addition, since Y is assumed constant for both degradation of substrate and of background carbon, the background biomass that can be supported will also increase with Y according to equation 4.5. Considering both effects, degradation should increase with higher values of Y.

7. r_b, *the endogenous decay coefficient:* As r_b increases, the bacteria decay at a faster rate. In addition, an increase in r_b will result in a lower background biomass concentration according to equation 4.5. The net effect is unclear; however, it is postulated that the amount of degradation will be reduced with increased r_b.

8. R_b, *the microbial retardation factor:* As R_b increases, more biomass is adsorbed to the solid matrix of the aquifer and more degradation should occur. However, according to equation 4.5, increases in R_b will be offset by lower background biomass concentrations, and this results in less degradation. The overall effect is unknown.

9. K_b, *the Freundlich isotherm constant:* As K_b increases, R_b increases, but the effect of increased R_b is unclear.

10. N_b, *the Freundlich isotherm exponent:* As N_b increases, R_b increases, but the effect of increased R_b is unclear. For $N_b \neq 1$, $R_b = R_b(B)$.

11. C_c, *the background carbon concentration in aquifer:* As C_c increases, the amount of background biomass that can be supported increases. Thus degradation will also increase. However, in this study C_c is considered deterministic.

12. k_c, *the first order decay rate of background carbon:* As k_c increases, the amount of background biomass that can be supported increases. Thus degradation will also increase, but as with C_c, k_c is considered deterministic.

6.2 Sensitivity to Uncertainty in Individual Biological Parameters

The first part of the sensitivity study was to determine the changes in model predictions given the uncertain biological parameters, considering *one parameter at a time.* This is the typical approach taken in sensitivity analysis *[Anderson and Woessner, 1992].* For the given scenario, simulations were performed with each biological parameter at its maximum and minimum value, holding all other parameters at their mean values (Table 4.2). This method has the advantage of being straightforward and relatively easy to perform. For the eight uncertain parameters, a total of 17 simulation runs were required. See Table D.1 for a complete listing of runs and parameter

combinations. This analysis provided a good initial estimate of what parameters were most significant.

The results of this analysis are summarized in Tables 6.1 and 6.2, and Figures 6.1 - 6.3. The contaminant concentrations predicted by BIO2D were most sensitive to the Monod half saturation constant K_s. The results were moderately sensitive to μ_{max}, r_b, and K_o. As seen in Table 6.2, the t_{stnd} was most sensitive to (in order of increasing sensitivity) low K_s, low K_o, low r_b, high μ_{max}, high K_s, and low μ_{max}. Sensitivity to all other parameter extremes was less than 1% of t_{stnd} for the baseline case, and it appears that at least for this initial study, the model results are not sensitive to Y, K_i, K_b, or N_b. The mean and standard deviation for all measures was computed, showing a reasonable match to the baseline run.

As seen in equations 2.36 - 2.38, the most sensitive extremes (low K_s, low K_o, low r_b, high μ_{max}) correspond to faster microbial kinetics. In these runs, the greatest number of iterations in the solution of the nonlinear PDEs were required for these cases with fast kinetics. Thus it appears that the degree of nonlinearity may be proportional to the rate of degradation. It particular, notice in Table 6.1 the extremely high number of iterations required for run #5, corresponding to $K_s = 1 \frac{mg}{L}$. In many of the 1500 times steps the iterative procedure did not converge to a 2% tolerance in the 10 iterations allowed. See Section 5.1 for a more complete analysis of this case.

Comparing these results to what was expected (preliminary analysis) it is seen that changes in K_s, μ_{max}, and r_b caused model predictions as anticipated. Changes in concentrations resulting from Y, K_i, K_b, and N_b were not evident, leading to the initial conclusion that the model predictions are insensitive to these parameters. Model results from K_o extremes were not as predicted. For $K_o = 0.1 \frac{mg}{L}$, less degradation was predicted than for the baseline case, however, the model predictions for $K_o = 2 \frac{mg}{L}$ were quite close to the baseline run. This was not well understood until further analysis of sensitivity changes with time was completed (see below).

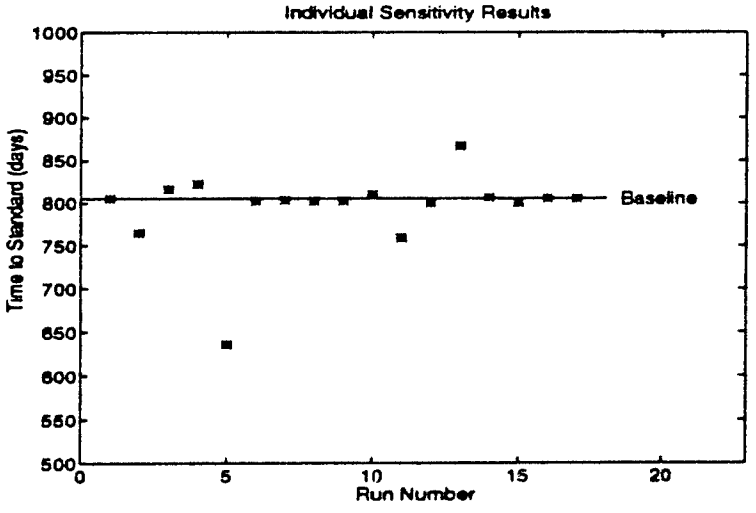

Figure 6.1: Individual Sensitivity: t_{stnd} versus Run (Runs Defined in Table D.1)

It is intersesting to note that of the seventeen runs, three predicted more degradation than BIOPLUME ($K_s = 1\ \frac{mg}{L}$, $\mu_{max} = 15.36\ \frac{1}{day}$, and $r_b = 0.001\ \frac{1}{day}$). One must conclude that either BIO2D is overpredicting degradation or that BIOPLUME is not accurately depicting instantaneous kinetics, due to numerical errors.

The sensitivity of the model output to K_s, μ_{max}, r_b, and K_o is further illustrated in Figures 6.4 - 6.7. These plots depict centerline concentration profiles at 500 and 1500 days for BIO2D as each parameter was varied from its minimum to its maximum value. Each plot also shows how these extremes compare with BIOPLUME. It is evident from these plots that using S_{max} as the only index of sensitivity may not be sufficient. It is important to measure sensitivity by both S_{max} and S_{mass}. For example, for run #4 where $K_s = 266\ \frac{mg}{L}$ (Figure 6.4), S_{max} at 500 days is only 2% greater than the baseline case; but S_{mass} is 56% greater. The estimate of total contaminant mass was more sensitive to K_s than was the estimate of S_{max}.

Table 6.1: Sensitivity To Changes in Individual Biological Parameters. (Runs Defined in Table D.1)

RUN	PARAMETER VALUE	500 days		1000 days		1500 days			*Iterations*
		S_{max}	S_{mass}	S_{max}	S_{mass}	S_{max}	S_{mass}	t_{stnd}	*required*
1	**Baseline**	1.74	879	0.70	334	0.23	84	805	100
2	$\mu_{max} = 15.36$	1.65	754	0.65	262	0.19	49	765	59
3	$\mu_{max} = 1.97$	1.77	1155	0.72	499	0.26	183	816	30
4	$K_s = 266$	1.78	1369	0.74	661	0.30	292	822	29
5	$K_s = 1$	1.34	477	0.43	104	0.02	1	636	13118
6	$K_i = 1463$	1.74	877	0.70	333	0.23	84	802	32
7	$K_i = 23$	1.74	879	0.70	333	0.23	84	803	32
8	$Y = 1.02$	1.74	877	0.70	333	0.23	84	802	32
9	$Y = 0.50$	1.74	877	0.70	333	0.23	84	802	32
10	$r_b = 0.10$	1.76	999	0.71	403	0.24	125	810	44
11	$r_b = 0.001$	1.62	687	0.64	228	0.20	35	759	25
12	$K_o = 2$	1.74	926	0.70	362	0.23	102	800	31
13	$K_o = 0.1$	1.78	964	0.83	459	0.39	172	867	50
14	$K_b = 22.97$ (R_b =150)	1.75	886	0.71	338	0.23	86	806	32
15	$K_b = 7.55$ (R_b =50)	1.74	874	0.70	331	0.22	83	800	32
16	$N_b = 1.1$ ($R_b = 99B^{\frac{1}{11}} + 1$)	1.75	883	0.70	336	0.23	85	805	0
17	$N_b = 0.9$ ($R_b = 99B^{\frac{1}{9}} + 1$)	1.75	883	0.70	336	0.23	85	805	0
	MEAN	1.71	897	0.69	352	0.23	101	794	
	STND DEV	0.10	185	0.08	117	0.07	65	47	
	BIOPLUME	1.72	756	0.70	243	0.22	41	795	

Table 6.2: Most Sensitive Parameters in Individual Study

RUN	PARAMETER VALUE	t_{stnd} (days)	% from BASELINE
5	$K_s = 1$	636	-21.0
13	$K_o = 0.1$	867	+7.7
11	$r_b = 0.001$	759	-5.7
2	$\mu_{max} = 15.36$	765	-5.0
4	$K_s = 266$	822	+2.1
3	$\mu_{max} = 1.97$	816	+1.4

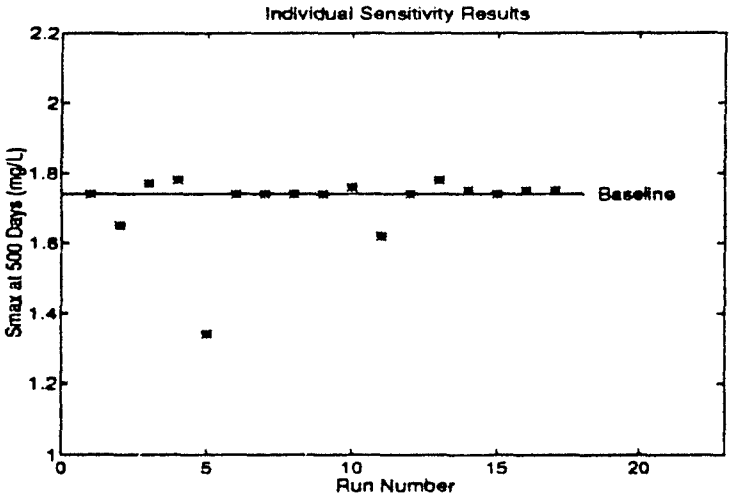

Figure 6.2: Individual Sensitivity: S_{max} versus Run (Runs Defined in Table D.1)

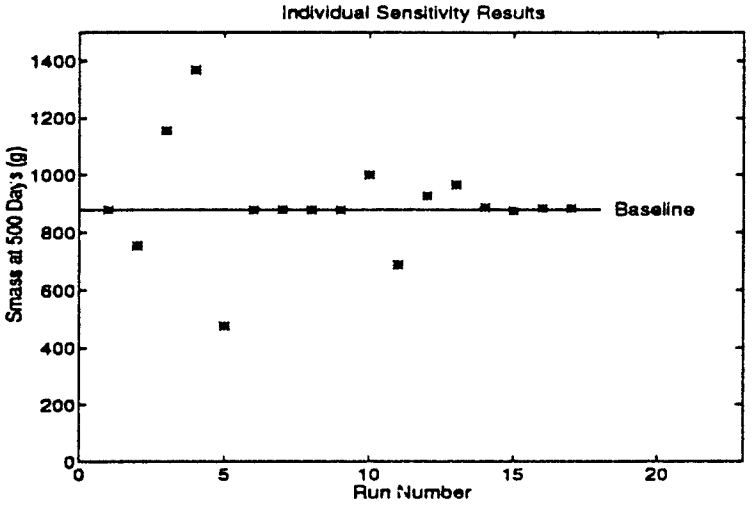

Figure 6.3: Individual Sensitivity: S_{mass} versus Run (Runs Defined in Table D.1)

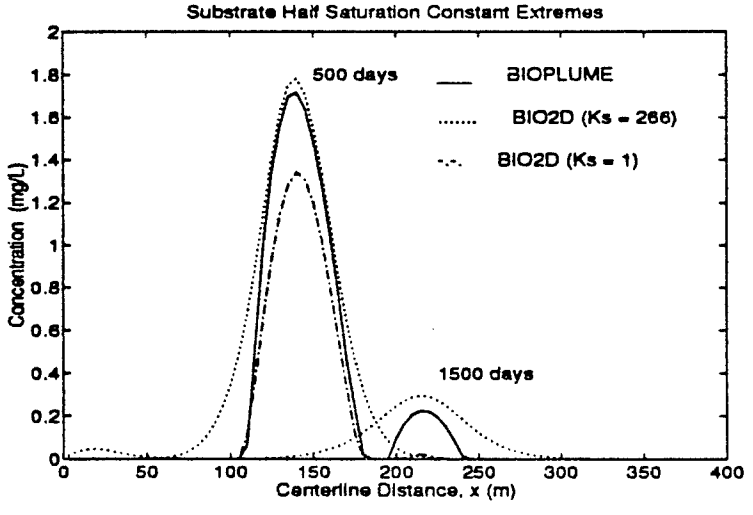

Figure 6.4: Sensitivity Analysis: Effect of K_s Extremes (Runs 4,5)

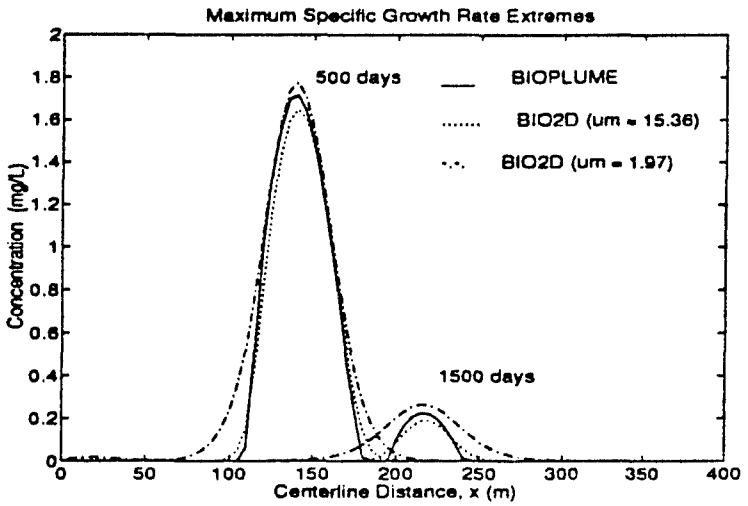

Figure 6.5: Sensitivity Analysis: Effect of μ_{max} Extremes (Runs 2,3)

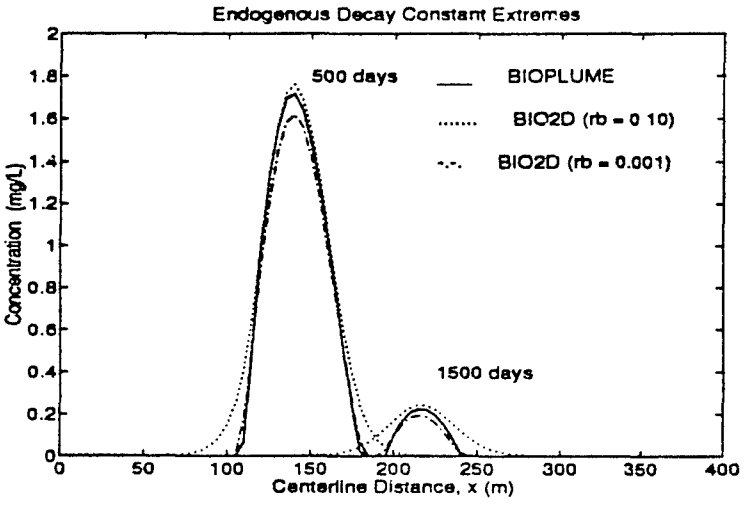

Figure 6.6: Sensitivity Analysis: Effect of r_b Extremes (Runs 10,11)

Sensitivity Over Time A sensitivity index as described by *Fjeld et al. [1989]* was used in order to further study the most sensitive parameters. This method involves using normalized measures of S_{max} and S_{mass} that emphasize changes on an absolute scale. Large percentage variations are not significant when $S \ll S_{stnd}$, whereas small percentage changes may be quite significant when $S \sim S_{stnd}$. The goal of this analysis was to investigate how sensitivity changes with time. Let η_t and γ_t be defined as follows:

$$\eta_t = \frac{S^{extreme}_{max_t} - S^{mean}_{max_t}}{S_{stnd}} \tag{6.1}$$

$$\gamma_t = \frac{S^{extreme}_{mass_t} - S^{mean}_{mass_t}}{S_{mass,ave}} \tag{6.2}$$

where $S^{extreme}_{max_t}$ is the maximum contaminant concentration in the aquifer at time t, found by a simulation with the parameter at its maximum or minimum value. $S^{mean}_{max_t}$ is the maximum contaminant concentration in the aquifer at time t, found by a simulation with all parameters at their mean values (baseline case). Similarly, $S^{extreme}_{mass_t}$ is the total contaminant mass in the aquifer at time t, found by a simulation with the parameter at its maximum or minimum value. $S^{mean}_{mass_t}$ is the total contaminant mass in the aquifer at time t, found by a simulation with all parameters at their mean values (baseline case). It is now possible to plot η_t and γ_t versus time to see *when* the model is especially sensitive. In this study S_{max} was normalized with respect to S_{stnd}, and S_{mass} was normalized with respect to the average mass in the aquifer, but in other applications different selections may be more appropriate.

Figures 6.8 - 6.15 show how the sensitivity indices η_t and γ_t vary with time for K_s, μ_{max}, K_o, and r_b extremes. A negative index indicates that the model prediction using the parameter extreme is smaller than the prediction made with all parameters at their mean values.

Summary Observations

- For η_t, the normalized sensitivity index of S_{max} in equation 6.1, the model predictions were not sensitive to low μ_{max}, high K_s, high r_b, nor high K_o. This was not true, however, for γ, the normalized sensitivity index of S_{mass} in equation 6.2. γ_t was sensitive to low and high values of μ_{max}, K_s, high r_b. This demonstrated that there are some significant differences in the sensitivities depending on the performance measure of interest.

- η_t sensitivity to high μ_{max}, low K_s, low r_b, and low K_o was very high initially and decreased with time. For high μ_{max} and low r_b, $\eta_t \rightarrow 0$ with increasing time. This is not true for low K_s, whose sensitivity is still significant at 1500 days.

- Sensitivity of η_t and γ_t to low K_o demonstrated a reversal at approximately 400 days. For the first 400 days, $\eta_t < 0$ and $\gamma_t < 0$, which is consistant with what was expected. After 400 days, the effect of low K_o was that $\eta_t > 0$ and $\gamma_t > 0$. This may be due to the fact that the value of K_o is really only significant relative to O. Thus, in the early stages of the cleanup $K_o < O$, but as the background oxygen is utilized, $K_o > O$. This results in a kinetic limitation and less degradation. This crossover effect is further illustrated in Figure 6.16. Observe that at 200 days the centerline profiles of phenol were as expected with the concentration predicted with $K_o = 2$ greater than the concentration predicted with $K_o = 0.1$. At 400 days the concentrations predicted for the two K_o extremes were approximately equal. At 600 days, however, the effect of K_o has reversed and the concentrations predicted with $K_o = 0.1$ were greater than with $K_o = 2$.

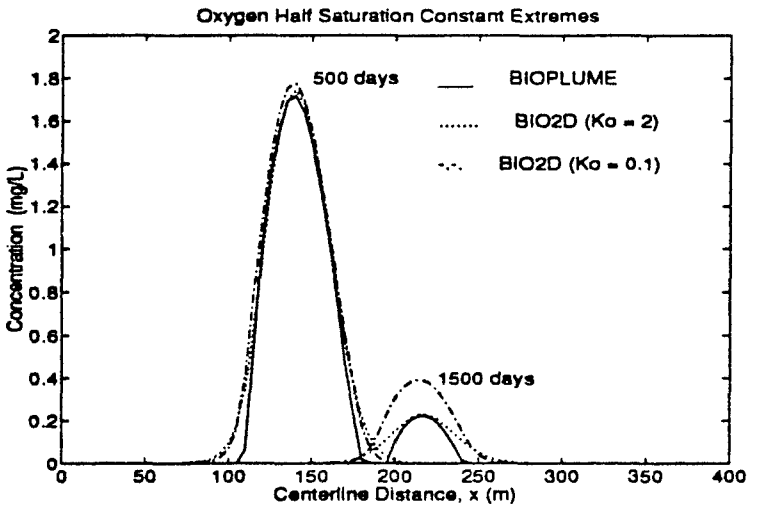

Figure 6.7: Sensitivity Analysis: Effect of K_o Extremes (Runs 12,13)

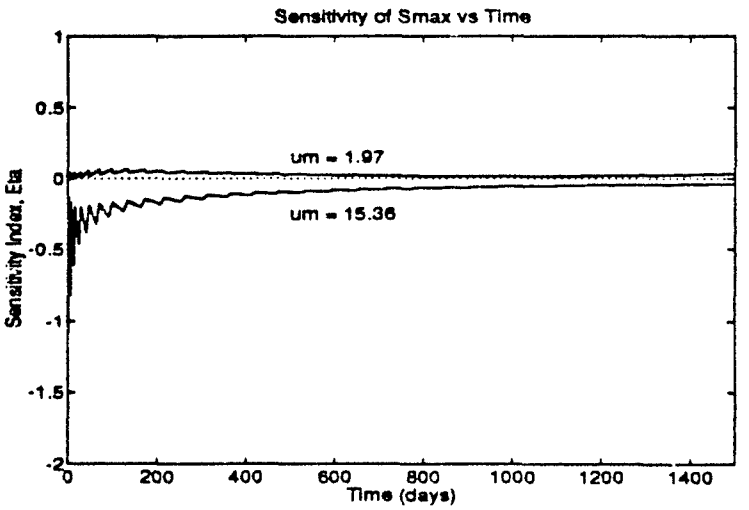

Figure 6.8: Sensitivity Index η_t (Equation 6.1) Versus Time for μ_{max} (Runs 2,3)

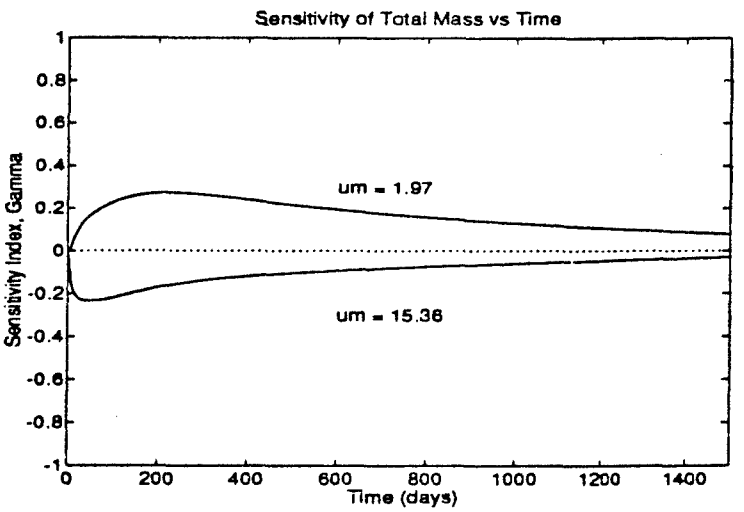

Figure 6.9: Sensitivity Index γ_t (Equation 6.2) Versus Time for μ_{max} (Runs 2,3)

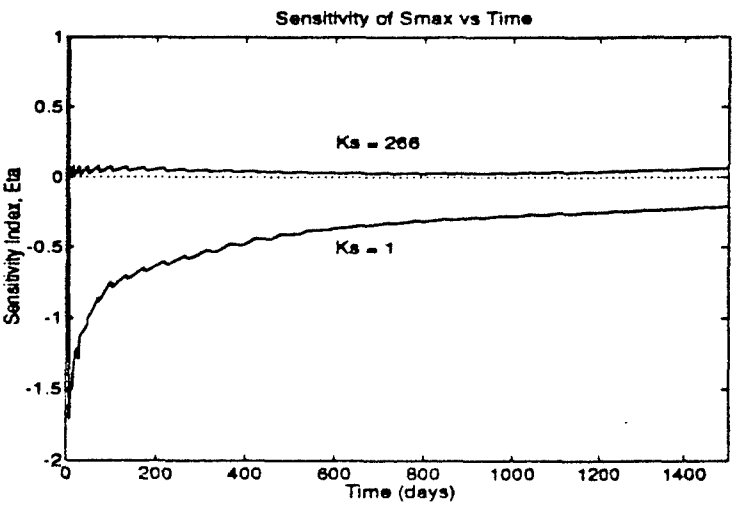

Figure 6.10: Sensitivity Index η_t (Equation 6.1) Versus Time for K_s (Runs 4,5)

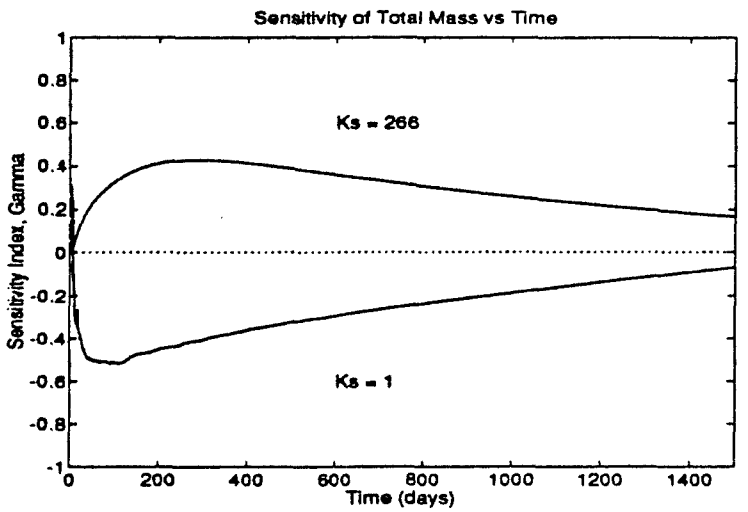

Figure 6.11: Sensitivity Index γ_t (Equation 6.2) Versus Time for K_s (Runs 4,5)

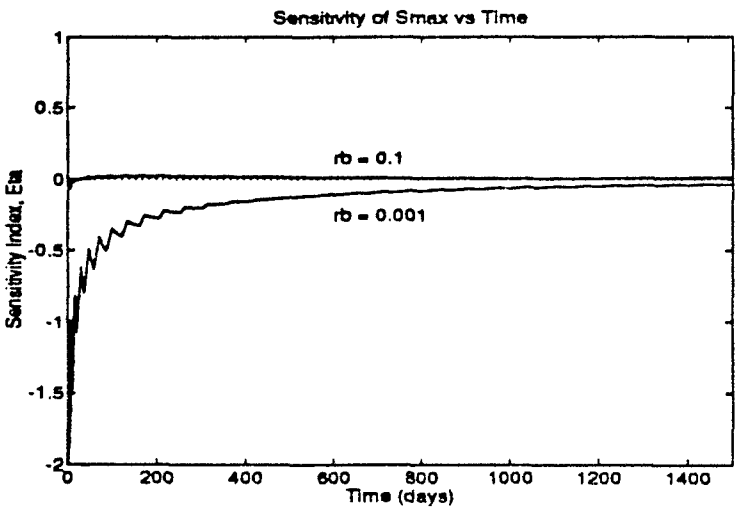

Figure 6.12: Sensitivity Index η_t (Equation 6.1) Versus Time for r_b (Runs 10,11)

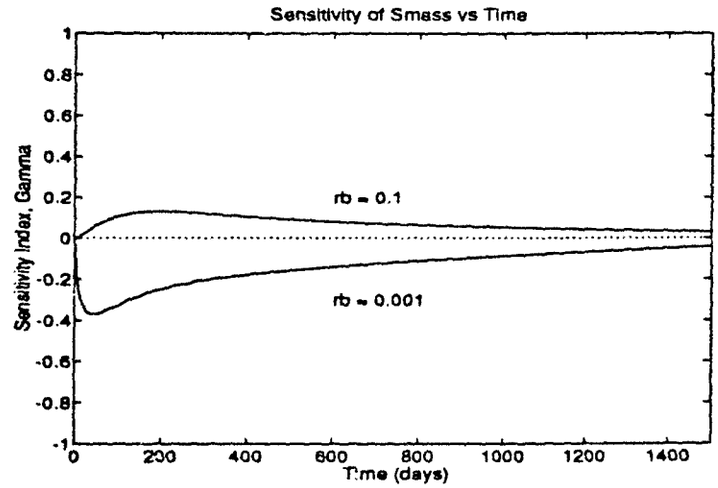

Figure 6.13: Sensitivity Index γ_t (Equation 6.2) Versus Time for r_b (Runs 10,11)

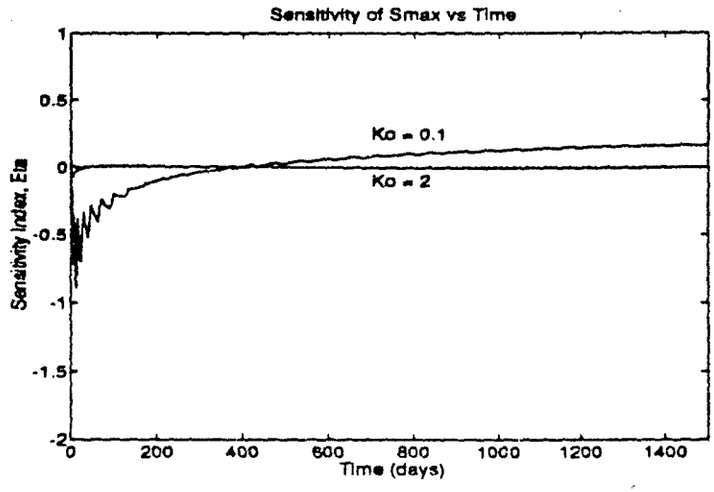

Figure 6.14: Sensitivity Index η_t (Equation 6.1) Versus Time for K_o (Runs 12,13)

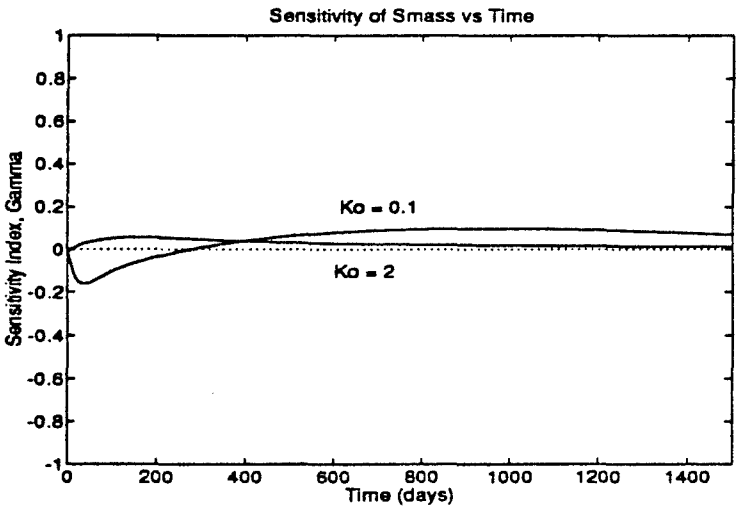

Figure 6.15: Sensitivity Index γ_t (Equation 6.2) Versus Time for K_o (Runs 12,13)

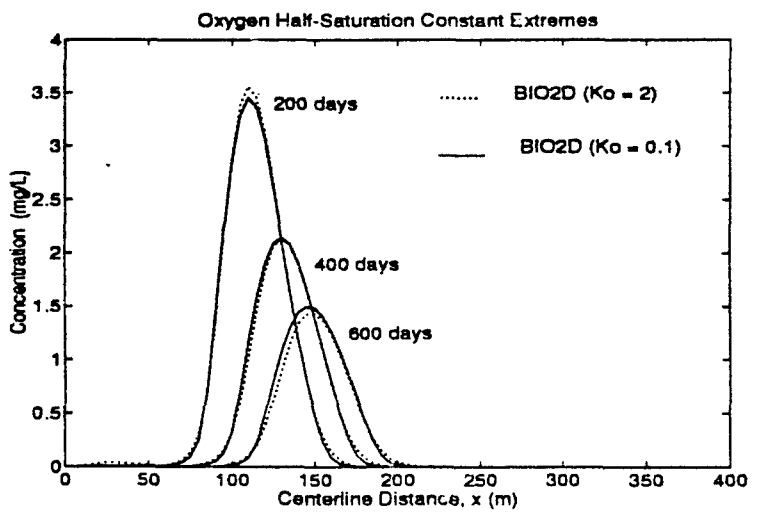

Figure 6.16: Combined Sensitivity: Changing Effects of K_o

6.3 Combined Sensitivity to Uncertainty in Biological Parameters

The analysis of BIO2D's sensitivity to uncertainty in *individual* biological parameters yielded some valuable information, but it was incomplete. The approach of varying one parameter at a time assumed no parameter-parameter interactions. But this is not realistic since there is uncertainty in all parameters. A more complete method is to consider joint or combined sensitivity.

2^k Factorial Design The method selected for the study of joint effects was borrowed from a field of Operations Research called Experimental Design and Optimization, as presented by *Law and Kelton [1991]*. They describe a computationally economical strategy to study the respones of a simulation model given possible decision levels or factors. The method is called 2^k *factorial design*. In the context presented by *Law and Kelton*, this is a decision making tool used to achieve optimal performance in a given system. Here managers or analysts are using a simulation model to assess the effects of two or more possible changes or improvements, and want to consider decision interactions.

2^k factorial design provides a systematic way of measuring model sensitivity where these interactions are important. The method is conceptually straightforward: for each decision level or factor k, two possible values or design points are selected, and a total of 2^k simulation runs are performed. *Law and Kelton* also define quantitative measures of the factor main effects and of two and three-way interactive effects.

The method of 2^k factorial design was directly applied to BIO2D and groundwater biodegradation modeling. The uncertain biological parameters were taken as the design factors (while their values are not controlled or designed, selection of reasonable values allow for application of the method). For each parameter the two possible

values were taken as the maximum and minimums for phenol (Table 4.2). The use of 2^k factorial design proved to be a very useful way of measuring and comparing the combined sensitivity of BIO2D to multiple changes in the biological parameters.

Assumptions As in the study of individual sensitivity, the parameters F, C_c, and k_c were considered deterministic. Based on the results of the individual sensitivity analysis, it was further assumed that microbial adsorption could be modeled with a linear isotherm ($N_b = 1$), and that inhibition effects were insignificant ($K_i \gg S$) so that K_i was taken as constant at its mean value. These assumptions were made in order to reduce the number of required simulations from 2^8 to 2^6, and were supported by results from the earlier study. Thus, a total of 64 runs were simulated, corresponding to the 64 different combinations of parameters. The runs were organized in a systematic manner so that run pairs were easily identified. A run pair corresponds to two runs where one parameter is varied from its minimum to its maximum value, while the other five parameters were held constant. Thus, there were a total of 32 run pairs for each parameter. A complete listing of runs and parameter combinations is found in Tables D.2 - D.3.

Results The results of the combined sensitivity runs are presented in Tables 6.3 - 6.5, and Figures 6.17 - 6.25. Tables 6.2 - 6.4 show the model predictions of S_{max} and S_{mass} for 500, 1000 and 1500 days and the total time required to achieve a 1 $\frac{mg}{L}$ standard (t_{stnd}) everywhere in the aquifer.

Model predictions of t_{stnd} and of S_{max} and S_{mass} for 500 days are presented as scatter plots in Figures 6.17 - 6.19. A close look at these plots reveals some definite patterns that correspond to specific parameter combinations. For example observe Figure 6.17. Here, the first 32 runs were made with $\mu_{max} = 1.97\ \frac{1}{day}$, and the last 32 with $\mu_{max} = 15.36\ \frac{1}{day}$. In runs 33-64, there is a definite downward shift of the even

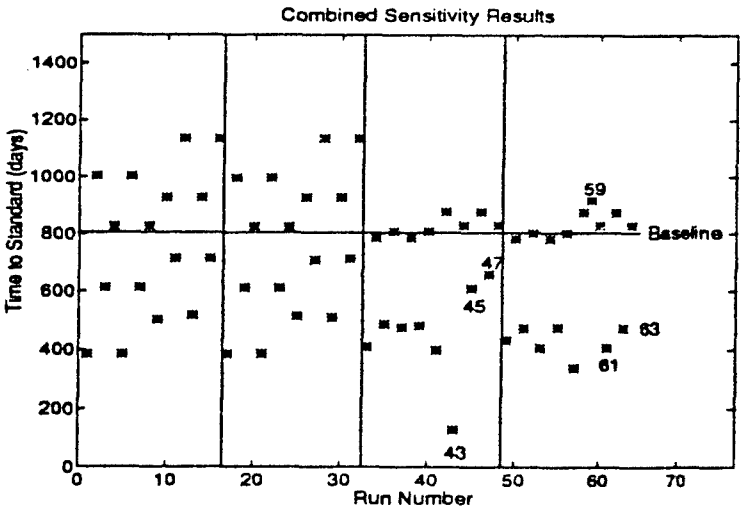

Figure 6.17: Combined Sensitivity: t_{stnd} versus Run (Runs Defined in Tables D.2 - D.3)

numbered runs (corresponding to $K_s = 266\ \frac{mg}{L}$) seen above the baseline, whereas the odd numbered runs ($K_s = 1\ \frac{mg}{L}$) do not shift as dramatically with the change in μ_{max}. Thus, low K_s appears to dominate over μ_{max} because the results for the the odd numbered runs do not change much with changes in μ_{max}. For high K_s, however, the effect of changes in μ_{max} were observed as more dramatic. This supports earlier observations that the model is most sensitive to K_s.

The low sensitivity of results to K_b can be seen by comparing runs 1-16 with runs 17-32, and runs 33-48 with 49-64. Observe in Figures 6.17 - 6.19 that there is almost no noticeable difference between the results from runs pairs 1,17; 2,18; 3,19; etc. The pattern in each quadrant repeats itself with only three exceptions (pairs 43,59; 45,61; and 47,63). Thus, it appears that the model is insensitive to K_b, especially at low values of μ_{max}.

Table 6.3: Combined Sensitivity To Changes in Biological Parameters for Runs 1-30 (Runs Defined in Table D.2 - D.3)

	500 days		1000 days		1500 days			*Iterations*
RUN	S_{max}	S_{mass}	S_{max}	S_{mass}	S_{max}	S_{mass}	t_{stnd}	*required*
1	0.555	78.54	0.000	0.00	0.000	0.00	385	1092
2	1.945	1176.86	1.002	670.05	0.573	347.11	1002	20
3	1.318	429.70	0.331	62.23	0.000	0.00	613	1372
4	1.794	885.05	0.734	331.27	0.248	79.54	826	18
5	0.555	78.54	0.000	0.00	0.000	0.00	385	1092
6	1.945	1176.86	1.002	670.05	0.573	347.11	1002	20
7	1.318	429.70	0.331	62.23	0.000	0.00	613	1372
8	1.794	885.05	0.734	331.27	0.248	79.54	826	18
9	1.003	309.33	0.261	55.23	0.000	0.00	502	13194
10	1.893	2136.50	0.911	1634.97	0.520	1253.95	927	48
11	1.541	635.51	0.547	182.35	0.105	17.21	713	13493
12	2.086	2377.51	1.139	2026.49	0.733	1721.10	1136	50
13	1.047	330.34	0.288	64.44	0.001	0.06	518	13500
14	1.893	2136.47	0.911	1634.94	0.520	1253.93	927	50
15	1.540	635.23	0.547	182.20	0.105	17.17	713	13493
16	2.086	2377.51	1.139	2026.48	0.733	1721.08	1135	50
17	0.551	77.51	0.000	0.00	0.000	0.00	385	1100
18	1.936	1166.65	0.996	662.45	0.568	341.62	996	20
19	1.314	427.34	0.328	61.35	0.000	0.00	611	1288
20	1.793	883.85	0.733	330.55	0.247	79.20	825	18
21	0.551	77.51	0.000	0.00	0.000	0.00	386	1100
22	1.936	1166.65	0.996	662.45	0.568	341.62	997	20
23	1.314	427.34	0.328	61.35	0.000	0.00	611	1288
24	1.793	883.85	0.733	330.55	0.247	79.20	825	18
25	1.036	325.07	0.279	61.27	0.000	0.00	514	13410
26	1.893	2136.46	0.911	1634.98	0.520	1253.97	927	50
27	1.526	625.89	0.538	177.31	0.099	15.80	707	13491
28	2.086	2377.50	1.139	2026.52	0.733	1721.12	1135	50
29	1.022	324.10	0.281	62.39	0.000	0.00	509	13467
30	1.893	2136.45	0.911	1634.95	0.520	1253.93	927	48

Table 6.4: Combined Sensitivity To Changes in Biological Parameters for Runs 31-60 (Runs Defined in Table D.2 - D.3)

	500 days		1000 days		1500 days			*Iterations*
RUN	S_{max}	S_{mass}	S_{max}	S_{mass}	S_{max}	S_{mass}	t_{stnd}	*required*
31	1.535	632.27	0.544	180.61	0.103	16.71	712	13492
32	2.086	2377.50	1.139	2026.49	0.733	1721.09	1135	48
33	0.683	125.72	0.000	0.00	0.000	0.00	409	1000
34	1.570	761.30	0.737	361.46	0.360	140.84	785	26
35	0.960	222.92	0.026	0.99	0.000	0.00	487	1437
36	1.741	786.11	0.713	279.27	0.241	54.27	808	20
37	0.922	217.32	0.003	0.09	0.000	0.00	475	908
38	1.570	761.30	0.737	361.46	0.360	140.84	785	26
39	0.942	215.11	0.019	0.65	0.000	0.00	481	1092
40	1.741	786.11	0.713	279.27	0.241	54.27	808	20
41	0.621	122.30	0.000	0.00	0.000	0.00	338	8424
42	1.854	1193.09	0.822	540.06	0.343	199.61	876	111
43	0.000	0.00	0.000	0.00	0.000	0.00	128	3847
44	1.784	1431.98	0.751	724.16	0.323	343.74	829	48
45	1.425	452.05	0.190	34.32	0.000	0.00	609	11684
46	1.853	1192.47	0.822	539.64	0.343	199.36	876	114
47	1.400	504.40	0.454	114.52	0.034	1.95	657	13496
48	1.784	1431.97	0.751	724.15	0.323	343.74	829	48
49	0.762	153.66	0.000	0.00	0.000	0.00	432	1052
50	1.563	754.24	0.998	500.00	0.732	356.72	782	26
51	0.916	205.02	0.008	0.20	0.000	0.00	472	1276
52	1.730	776.92	0.705	273.94	0.235	51.92	802	21
53	0.678	125.14	0.000	0.00	0.000	0.00	406	1070
54	1.563	754.24	0.998	500.00	0.732	356.72	782	26
55	0.925	208.49	0.015	0.42	0.000	0.00	475	1272
56	1.730	776.92	0.705	273.94	0.235	51.92	302	21
57	0.382	58.62	0.000	0.00	0.000	0.00	338	7125
58	1.852	1190.81	0.821	535.63	0.342	198.77	875	77
59	2.216	856.21	0.852	294.90	0.277	58.03	918	13500
60	1.784	1431.67	0.751	724.01	0.323	343.65	829	48

Table 6.5: Combined Sensitivity To Changes in Biological Parameters for Runs 61-64 (Runs Defined in Table D.2 - D.3)

	500 days		1000 days		1500 days			*Iterations*
RUN	S_{max}	S_{mass}	S_{max}	S_{mass}	S_{max}	S_{mass}	t_{stnd}	*required*
61	0.632	132.37	0.000	0.00	0.000	0.00	407	8489
62	1.851	1189.92	0.820	538.01	0.341	198.41	874	91
63	0.939	288.11	0.197	28.08	0.000	0.00	473	11599
64	1.784	1431.62	0.751	723.98	0.491	500.00	829	48

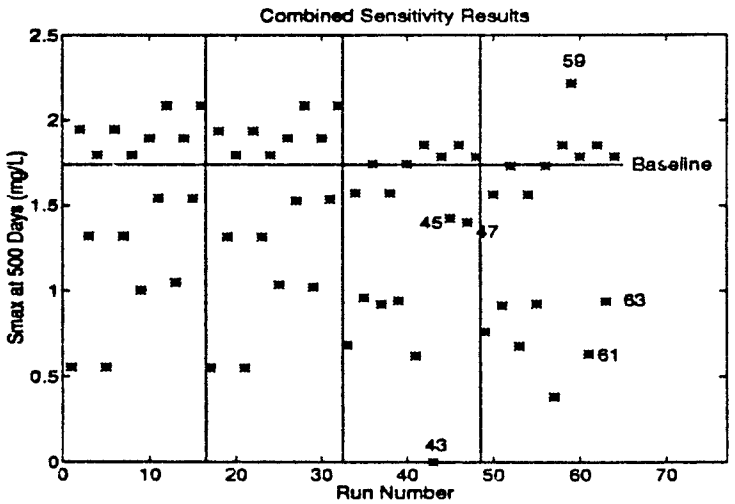

Figure 6.18: Combined Sensitivity: S_{max} versus Run (Runs Defined in Tables D.2 - D.3)

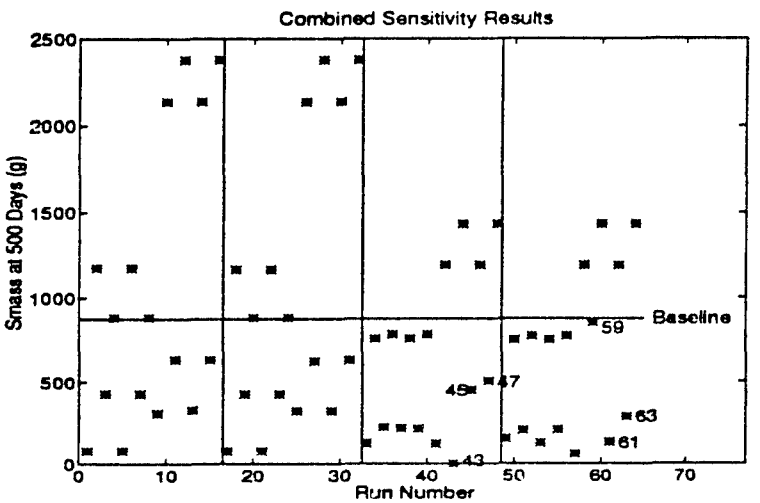

Figure 6.19: Combined Sensitivity: S_{mass} versus Run (Runs Defined in Tables D.2 - D.3)

Main Effects This qualitative analysis, however, is difficult, and can be somewhat misleading. *Law and Kelton* present a way of quantifying these results as follows. Let e_k be the *main effect* of parameter k. It is defined as the average change in model prediction due to changing parameter k from its minimum to its maximum value. This average is taken over all combinations of the other parameters in the problem. e_k can alternately be defined as the difference between the model predictions with k at its maximum value and the model predictions with k at its minimum value. It is possible to define $e_k^{S_{max}}$, $e_k^{S_{mass}}$, and $e_k^{t_{stnd}}$ using S_{max}, S_{mass} and t_{stnd} as the respective performance measures. For $e_k^{S_{max}}$ and $e_k^{S_{mass}}$ the main effect is averaged over the entire 1500 day simulation. For example, the main effect of K_s on t_{stnd} is defined as:

$$e_{K_s}^{t_{stnd}} = \frac{(t_{stnd}^2 - t_{stnd}^1) + (t_{stnd}^4 - t_{stnd}^3) + \cdots + (t_{stnd}^{64} - t_{stnd}^{63})}{32} \tag{6.3}$$

where $1, 2, 3, \cdots, 64$ refer to the simulation run number (Appendix D). Thus, for K_s the run pairs were $(2,1), (4,3), \cdots, (64,63)$. Similarly, the main effect of μ_{max} on S_{max} is defined as:

$$e_{\mu_{max}}^{S_{max}} = \frac{\sum_{t=1}^{1500} \left[\frac{(S_{max_t}^{33} - S_{max_t}^{1}) + (S_{max_t}^{34} - S_{max_t}^{2}) + \cdots + (S_{max_t}^{64} - S_{max_t}^{32})}{32} \right]}{1500} \tag{6.4}$$

The main effect of Y on S_{mass} is defined as:

$$e_Y^{S_{mass}} = \frac{\sum_{t=1}^{1500} \left[\frac{(S_{mass_t}^{5} - S_{mass_t}^{1}) + (S_{mass_t}^{6} - S_{mass_t}^{2}) + \cdots + (S_{mass_t}^{64} - S_{mass_t}^{56})}{32} \right]}{1500} \tag{6.5}$$

Using these and similar definitions, main effects of the six uncertain parameters on the three performance measures were calculated. As presented in Table 6.6, a positive effect can be explained as an increase in performance measure as the parameter is changed from its minimum to its maximum value. For example, as K_s is changed from 1 $\frac{mg}{L}$ to 266 $\frac{mg}{L}$, the main effect was an increase in predicted cleanup time of 383.7 days and an increase in the average S_{max} in the aquifer of 0.6023 $\frac{mg}{L}$.

Table 6.6: Combined Sensitivity: Main Effects (Given By Example in Equations 6.3 - 6.5)

PARAMETER	Main Effect:		
k	$e_k^{S_{max}}\ (\frac{mg}{L})$	$e_k^{S_{mass}}\ (g)$	$e_k^{t_{stnd}}\ (days)$
K_s	0.6023	848.2	384
μ_{max}	-0.0682	-334.8	-115
r_b	0.2992	459.9	81
K_o	0.2158	103.7	74
Y	-0.0259	13.3	13
K_b	0.0600	1.1	7

The main effects in Table 6.6 indicate that the predicted concentrations of contaminant are most sensitive to K_s, the Monod half saturation constant. The study results also indicate that the model is relatively insensitive to changes in Y and K_b. For μ_{max}, K_o, and r_b the results are moderately sensitive, and the order of sensitivity changes with the measure of interest. For t_{stnd}, the order of sensitivity was K_s, μ_{max}, r_b, and K_o; for S_{max} the order was K_s, r_b, K_o, and μ_{max}, and for S_{mass} the order was K_s, r_b, μ_{max}, and K_o.

Bar Graphs An easier way of depicting these results is to plot the difference between the predicted performance measures with the parameter at its minimum value and with the parameter at its maximum value, while all others were held constant at one particular combination. This was done for each parameter pair using t_{stnd} as the performance measure. The results are plotted as bar charts in Figures 6.20 - 6.25. In each, the straight line indicates $e_k^{t_{stnd}}$, the main effect, which is the average of all bars shown (and is given by example in Equation 6.3).

Several observations are made about these plots.

- The first 32 runs (16 pairs), corresponding to $\mu_{max} = 1.97\ \frac{1}{day}$, produced patterns that were nearly symmetric. See bars to the left of the vertical line in Figures 6.20, and 6.22 - 6.25. In these runs, there was almost no sensitivity to changes in Y or K_b.
- In the last 32 runs, however, where $\mu_{max} = 15.36\ \frac{1}{day}$ much more variation in the results was seen. See bars to the right of the vertical line in Figures 6.20, and 6.22 - 6.25. This was particularly noticeable for odd numbered runs, which correspond to $K_s = 1\ \frac{mg}{L}$. This was probably due to the combined effects of a high μ_{max} and a low K_s; both extremes cause faster degradation (equations 2.36 - 2.38).
- Runs 43, 45, 47 and 59 produced unexpected results. This was particularly noticeable as the extremely high or low bars in Figures 6.20 - 6.25. These pair numbers are highlighted on the bar charts. The common trait in each of these cases was a high μ_{max}, a low K_s, and a high r_b. Again, this corresponds to faster microbial kinetics.
- All plots were made with the same scale on the Y-axis, so that the relative sensitivity can be seen qualitatively by comparison of the bar graphs.
- K_o effects were drastically different for run pairs 4,2; 8,5; 20,18,; and 24,22 where $\mu_{max} = 1.97\ \frac{1}{day}$, $K_s = 266\ \frac{mg}{L}$ and $r_b = .001\ \frac{1}{day}$ (Figure 6.22). In these run pairs, the effect was negative, whereas in all other runs (of the first 32) the effect was positive. This effect wais also seen in pairs 44,42; 48,46; 60,58; and 64,62 where $\mu_{max} = 15.36\ \frac{1}{day}$, $K_s = 266\ \frac{mg}{L}$ and $r_b = .001\ \frac{1}{day}$. Thus, for low r_b, the main effect of K_o is opposite in direction to K_s ($-K_o$ at high K_s, and $+K_o$ at low K_s). But at high r_b, the main effect of K_o is positive regardless of K_s.

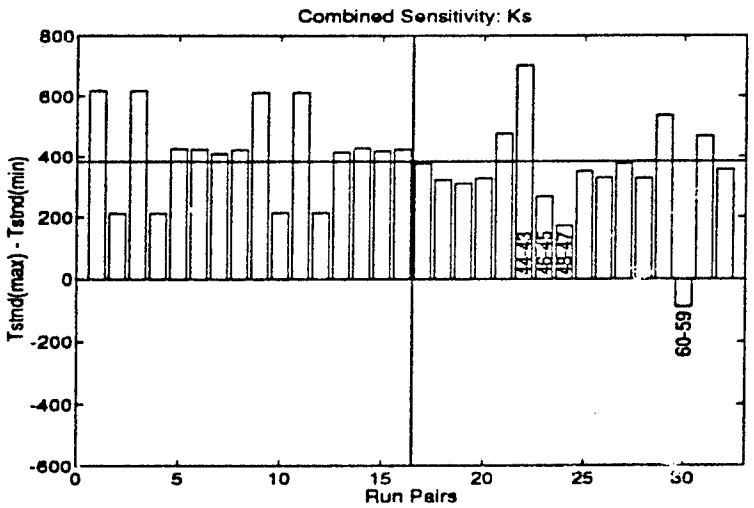

Figure 6.20: Combined Sensitivity: Differences in t_{stnd} for K_s Pairs, As Defined in Table D.4

Interactive Effects The main effects presented above calculate the *average* change of model output due to changes in uncertain biological parameters. This average is taken over all the various combinations of $k-1$ other parameters. It is possible to measure the degree of interaction between parameter k_1 and k_2 by the use of *two-way interaction effect*, $e_{k_1k_2}$. $e_{k_1k_2}$ is defined as one half the difference between the average effect of parameter k_1 when parameter k_2 is at its maximum level and the average effect of parameter k_1 when parameter k_2 is at its minimum level. Another way of defining the two-way interaction effect is the difference between the average effects of parameters k_1 and k_2 when both are at the same extreme (maximum or minimum), and the average effects when the are at opposite extremes. The two-way effects are symmetric ($e_{k_1k_2} = e_{k_2k_1}$). For example, the two-way interaction effect of K_s and

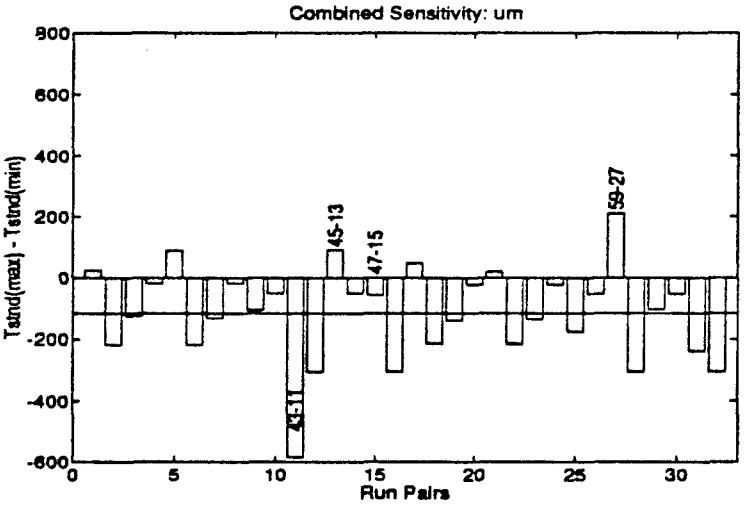

Figure 6.21: Combined Sensitivity: Differences in t_{stnd} for μ_{max} Pairs, As Defined in Table D.4

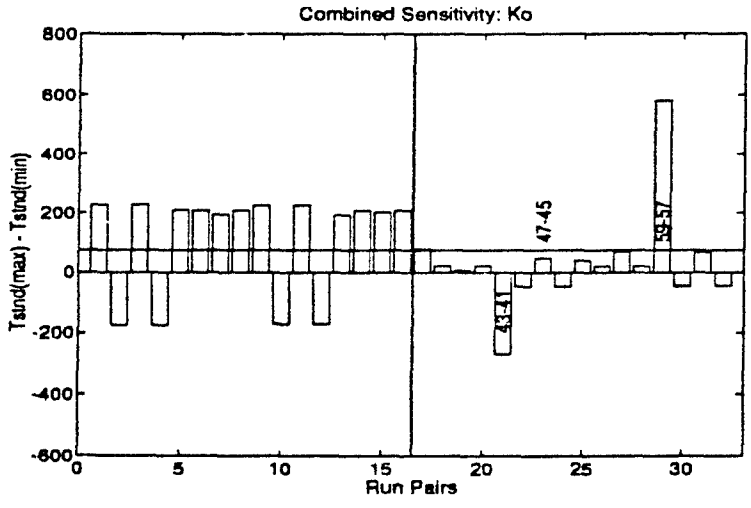

Figure 6.22: Combined Sensitivity: Differences in t_{stnd} for K_o Pairs, As Defined in Table D.4

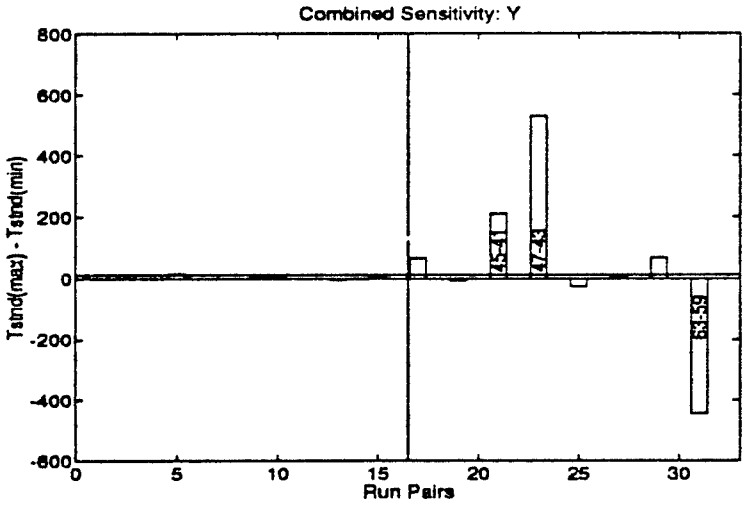

Figure 6.23: Combined Sensitivity: Differences in t_{stnd} for Y Pairs, As Defined in Table D.4

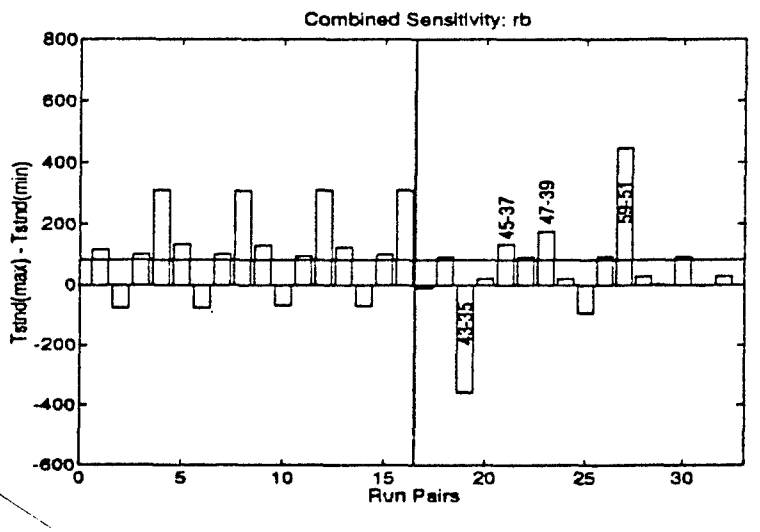

Figure 6.24: Combined Sensitivity: Differences in t_{stnd} for r_b Pairs, As Defined in Table D.4

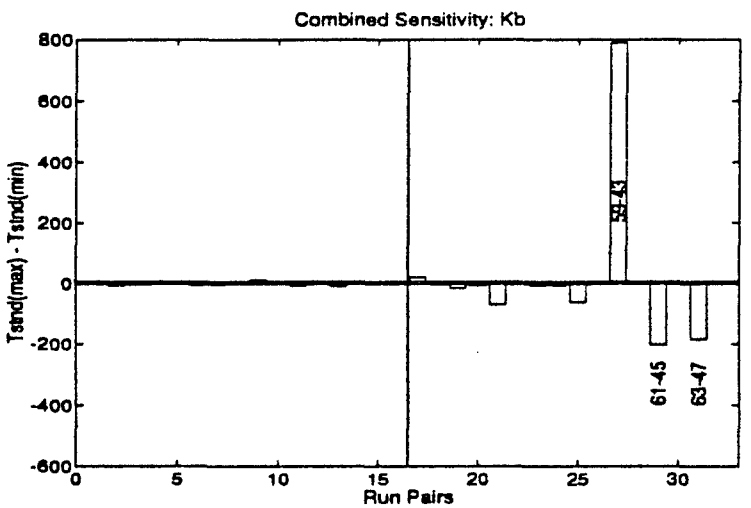

Figure 6.25: Combined Sensitivity: Differences in t_{stnd} for K_b Pairs, As Defined in Table D.4

μ_{max} using t_{stnd} as the measure of performance is:

$$e^{t_{stnd}}_{K_s\mu_{max}} = \frac{1}{2}\left[\frac{(t^{34}_{stnd} - t^{33}_{stnd}) + \cdots + (t^{64}_{stnd} - t^{63}_{stnd})}{16} - \frac{(t^{2}_{stnd} - t^{1}_{stnd}) + \cdots + (t^{32}_{stnd} - t^{31}_{stnd})}{16}\right] \tag{6.6}$$

where $1, 2, 3, \cdots, 64$ refer to the simulation run number (Appendix D). The interaction effect of K_s and K_o using S_{max} as the measure of performance is:

$$e^{S_{max}}_{K_sK_{o_t}} = \frac{1}{2}\left[\frac{(S^{4}_{max_t} - S^{2}_{max_t}) + \cdots + (S^{64}_{max_t} - S^{62}_{max_t})}{16} - \frac{(S^{3}_{max_t} - S^{1}_{max_t}) + \cdots + (S^{63}_{max_t} - S^{61}_{max_t})}{16}\right] \tag{6.7}$$

$$e^{S_{max}}_{K_sK_o} = \frac{\sum_{t=1}^{1500} e^{S_{max}}_{K_sK_{o_t}}}{1500} \tag{6.8}$$

Several of the various two-way interactive effects are shown in Table 6.7. For the performance measures of S_{max} and t_{stnd}, $K_s - K_o$ was the strongest two-way effect. For the performance measures of S_{mass}, however, the effects of K_s-μ_{max} and K_s-r_b were the most important. The magnitude of the two-way effects can be directly compared to the main effects calculated previously (Table 6.6). Observe that the two-way effects are in general smaller than the main effects.

Three-way effects were also computed in a manner similar to the two-way effects. The three-way effects are also symmetrical ($e_{k_1k_2k_3} = e_{k_3k_1k_2} = e_{k_2k_1k_3}$, etc.) Three-way effects for $K_s - \mu_{max} - r_b$ and $K_s - K_o - r_b$ were computed and are shown in Table 6.7. They are in general smaller than the main effects and two-way effects.

Table 6.7: Combined Sensitivity: Interactive Effects (Given by Example in Equations 6.6 - 6.8)

PARAMETERS	Interactive Effects:		
$k_1 - k_2$	$e^{S_{max}}_{k_1 k_2}$ $(\frac{mg}{L})$	$e^{S_{max}}_{k_1 k_2}$ (g)	$e^{t_{end}}_{k_1 k_2}$ $(days)$
$K_s - \mu_{max}$	-0.138	-264.5	-33
$K_o - \mu_{max}$	-0.019	-15.6	-42
$K_s - K_o$	-0.188	-41.0	-72
$K_s - Y$	0.026	-13.4	-13
$K_s - r_b$	-0.135	336.9	7
$K_s - K_b$	-0.063	-4.5	-10
$r_b - \mu_{max}$	-0.081	-196.4	-34
$K_o - r_b$	0.079	100.1	43
$K_s - \mu_{max} - r_b$	-0.038	-85.6	2
$K_s - K_o - r_b$	-0.007	29.9	22

6.4 Conclusions

The sensitivity analysis performed in this chapter yielded many new insights into BIO2D, and how its predictions of contaminant concentrations vary with uncertainty in biological parameters. These observations are summarized below:

- Individual sensitivity alone was insufficient in trying to assess the effects of uncertainty in BIO2D. Parameter-parameter interactions were found to be significant. As seen in Table 6.8, the effect of considering individual sensitivity alone would have been to misjudge K_o as the second most sensitive parameter and misjudge the direction of the sensitivity of K_o.
- A high coefficent of variation for an uncertain parameter does not necessarily lead to high sensitivity. For example, the coefficient of variation for K_i was 1.14, second only to K_s, but BIO2D was not sensitive to this parameter.

- The contaminant concentrations predicted by BIO2D were most sensitive to changes in K_s, the Monod half saturation constant. Model sensitivity to K_s is undoubtedly due in part to the variablity of this but this was true for both combined and individual sensitivity, and for all three performance measures. This observation is also consistant with what *Taylor* found in his study. Thus, in application of BIO2D, it is recommended that resources in parameter estimation be spent on determining K_s over any otner uncertain parameters.

- The contaminant concentrations predicted by BIO2D were not sensitive to changes in K_b, N_b, Y, nor K_i. Thus it is recommended that resources in parameter estimation not be spent determining these parameters. Values taken from literature (for the specific contaminant of interest) should be sufficient for these.

- The sensitivity of the predicted contaminant concentrations to K_o was quite variable, depending upon time, and the values of the other constants.

- Results of the sensitivity analysis differed with the performance measure of interest. For example, the importance of μ_{max} is greater when one is interested in estimating the time to meet a 1 ppm cleanup standard, than knowing K_o or r_b. However, if the total contaminant mass is chief concern, then it is more important to know r_b than μ_{max} or K_o.

- Combined effects of K_s-K_o were most significant of the parameter pairs when t_{stnd} or S_{max} was the performance measure. However, in estimating the total contaminant mass, the combined effects of K_s- μ_{max} and K_s-r_b were the most important.

Table 6.8: Comparison of Individual and Combined Sensitivity for t_{stnd} (Given by Example in Equation 6.3)

PARAMETER	Coefficient of Variation	Main Effect on t_{stnd} (days): Individual Sensitivity	Main Effect on t_{stnd} (days): Combined Sensitivity
K_s	1.32	186	384
μ_{max}	.55	-51	-115
r_b	1	51	81
K_o	1	-67	74
Y	.25	0	13
K_b	.50	6	7
N_b	.10	0	-
K_i	1.14	-1	-

Chapter 7

Summary

7.1 Conclusions

In this work an in-situ bioremediation model was tested and studied in great detail. Specifically, BIO2D was validated in its ability to model flow and transport using the IGWMC's Level 1 Testing Protocol. It was then compared to the better known and proven model BIOPLUME in its ability to model biodegradation. Two potential improvements to BIO2D were presented and evaluated. Finally, BIO2D was studied to determine which input biological parameters were most important in determining predicted concentrations. Based on this work, the following conclusions are made:

- BIO2D did an acceptable job modeling flow and transport for the five IGWMC test cases applied to it in Chapter 3. While there are certainly more sophisticated models available, BIO2D is a good, relatively straightforward model that allows the additional complications of degradation to be included without making it too cumbersome.
- As with many numerical codes, BIO2D is prone to numerical errors if the accuracy criteria given in equations 2.33 - 2.35 are not satisfied.

- BIO2D did a good job of modeling biodegradation in the four test cases evaluated. It predicted slightly less degradation than BIOPLUME in three of the four degradation tests performed in Chapter 4, as was expected.
- For the degradation test involving an injection-pumping well doublet, BIO2D actually outperformed BIOPLUME based on numerical dispersion and mass balance errors.
- The use of an iterative procedure to solve the nonlinear PDEs is recommended over a linearized solution. This method was proven as more efficient in Chapter 5.
- Individual sensitivity analysis alone was proven as insufficient for BIO2D. An more complete and accurate method was presented that included the effects of parameter-parameter interactions.
- BIO2D was most sensitive to the Monod half saturation constant, K_s. It was not sensitive to K_b, N_b, Y, nor K_i. Sensitivity to r_b, K_o, and μ_{max} was moderate and depended to some extent upon the performance measure of interest. Therefore, in application of BIO2D, it is recommended that resources in parameter estimation be spent on determining K_s over any other uncertain parameters.

7.2 Recommendations for Further Research

The following areas need further attention and are recommended for future research:

- The application of BIO2D to a real site is the only way to truly validate this model. It will also permit further evaluation of the choice of kinetics discussed in Chapter 5. The validation of BIO2D at one of the sites that BIOPLUME was applied is a reasonable possibility, although these two cases involve natural

degradation (no pumping) only. This is the best way to gain confidence in BIO2D's ability to model the complexities of biodegradation.

- Further sensitivity analysis should be performed using the combined approach presented in Chapter 6. It is recommended that an alternate selection of the two values used in 2^k factorial design be tested. In addition to the minimum and maximum, another measure related to the parameters' real distributions such as $\pm$one standard deviation should be tested. This will serve to verify the results of Chapter 6 and to avoid the problems associated with combinations of extremes.

- Sensitivity analysis of the optimization model would be an interesting and important work. It would be of great value to learn how the optimal cleanup strategy chosen changes with uncertainty in the parameters.

Appendix A

Definition of Variables Used

VARIABLE	DESCRIPTION	UNITS
T	transmissivity tensor	$[\frac{m^2}{day}]$
K	permeability tensor	$[\frac{m}{day}]$
h	vertically averaged hydraulic head	$[m]$
$\bar{S}$	storativity	[1]
b	saturated aquifer thickness	$[m]$
n	porosity	$[m]$
C	concentration of conservative tracer	$[\frac{mg}{L}]$
S	concentration of substrate (degradable contaminent)	$[\frac{mg}{L}]$
O	concentration of oxygen	$[\frac{mg}{L}]$
B	concentration of microbial biomass	$[\frac{mg}{L}]$
B_b	background concentration of biomass	$[\frac{mg}{L}]$
D	dispersion tensor	$[\frac{m^2}{day}]$
D_0	molecular dispersion	$[\frac{m^2}{day}]$

α_L	longitudinal dispersivity	$[m]$
α_T	transverse dispersivity	$[m]$
V	Darcy velocity	$[\frac{m}{day}]$
λ_{RS}	rate of substrate biodegradation	$[\frac{mg}{L-day}]$
λ_{RO}	rate of oxygen consumption	$[\frac{mg}{L-day}]$
λ_{RB}	rate of biomass growth (+) or decay (-)	$[\frac{mg}{L-day}]$
Q_w	injection (+) or extraction (-) rate in BIO2D	$[\frac{m^3}{day}]$
	injection (-) or extraction (+) rate in BIOPLUME	$[\frac{m^3}{day}]$
S_w	substrate concentration in water source/sink	$[\frac{mg}{L}]$
O_w	oxygen concentration in water source/sink	$[\frac{mg}{L}]$
B_w	biomass concentration in water source/sink	$[\frac{mg}{L}]$
R_s	substrate retardation factor = $\left(1 + \frac{\rho_b K_D}{n}\right)$	[1]
R_o	oxygen retardation factor = 1	[1]
R_b	biomass retardation factor = $\left(1 + \frac{1-n}{n}\rho_b K_b B^{\frac{1}{N_b}-1}\right)$	[1]
ρ_b	soil bulk density (taken as = 2.65)	$[\frac{g}{cm^3}]$
K_D	substrate partitioning coefficient	$[\frac{cm^3}{g}]$
K_b	Freundlich isotherm partitioning coefficient for bacteria adsoption	$[\frac{cm^3}{g}]$
N_b	Freundlich isotherm exponent for bacteria adsoption	[1]

F	ratio of oxygen to substrate used in degradation	$[\frac{mg}{mg}]$
F'	ratio of oxygen to background carbon used in degradation	$[\frac{mg}{mg}]$
Y	yield coefficient	$[\frac{mg}{mg}]$
μ_{max}	maximum specific growth rate for bacteria	$[\frac{1}{day}]$
μ_s	bacterial growth rate	$[\frac{1}{day}]$
r_b	bacterial decay rate	$[\frac{1}{day}]$
K_s	Monod half-saturation coefficient for substrate	$[\frac{mg}{L}]$
K_o	Monod half-saturation coefficient for oxygen	$[\frac{mg}{L}]$
K_i	Inhibition coefficient for substrate	$[\frac{mg}{L}]$
C_c	natural organic carbon in aquifer	$[\frac{mg}{L}]$
k_c	first order decay rate of organic carbon	$[\frac{1}{day}]$
$\delta_{i,j}$	Dirac delta function evaluated at (i,j)	$[\frac{1}{m^3}]$
K_o	vertical conductivity	$[\frac{m}{day}]$
w_i, w_j	finite element basis functions	[1]
$\vec{n}$	unit outward normal vector to finite element boundary	[1]
$\vec{n_x}$, $\vec{n_y}$	finite element directional cosines between unit normal to boundary and x,y coordinate axes	[1]
nfe	number of finite elements in aquifer mesh	[1]
nds	number of nodes in aquifer mesh	[1]
nbw	band width of finite element matrices	[1]

P_e	Peclet Number	[1]
C_r	Courant Number	[1]
S_{max}	maximum substrate concentration in aquifer	$[\frac{mg}{L}]$
S_{mass}	total substrate mass in aquifer	$[g]$
t_{stnd}	time to meet a $1[\frac{mg}{L}]$ standard	$[days]$
β	Convergence criterion for iterative procedure	[1]
δ_s	residual error in substrate equation	[1]
δ_o	residual error in oxygen equation	[1]
δ_b	residual error in biomass equation	[1]
$mxitr$	maximum number of iterations in iterative procedure	[1]
η	normalized sensitivity measure of S_{max}	[1]
γ	normalized sensitivity measure of S_{mass}	[1]
e_k	main effect of parameter k	variable

Appendix B

BIO2D Finite Element Equations

This appendix details the finite element equations used in the simulation model BIO2D. The equations are based on an unpublished manuscript by *Taylor [1991]*, and Taylor [1993]. All matrices and vectors are defined in Appendix A.

The hydraulic head equation derived from equation 3.1 is:

$$[A]\{h\} = [P_h]\{Q_w\} + \{F_h\} \tag{B.1}$$

where Q_{w_i} is the pumping rate vector as a function of time.

The elemental coefficient matrices are defined as follows:

$$[A]^e_{ij} = \left[\int\int \left(T_{xx}\frac{\partial w_i}{\partial x}\frac{\partial w_j}{\partial x} + T_{yy}\frac{\partial w_i}{\partial y}\frac{\partial w_j}{\partial y}\right) dx\, dy\right]^e \tag{B.2}$$

$$\{F_h\}^e_i = \left(\int_\Gamma w_i \cdot \sum_{j=1}^{4}\left(T_{xx}\frac{\partial w_j}{\partial x}\vec{n_x} + T_{yy}\frac{\partial w_j}{\partial y}\vec{n_y}\right) h_j \cdot d\vec{l}\right)^e \tag{B.3}$$

$$[P_h] = [e^1_h, ..., e^m_h] \tag{B.4}$$

where w_i is the weighting function at node i, $\vec{n_x}$ and $\vec{n_y}$ are directional cosines between the unit normal to the boundary and the x, y coordinate axes, e^i_h are binary vectors

denoting the location of the i^{th} well in the head vector, Γ is the surface of the element, and h_j is the specified boundary head. All other terms are defined as in Appendix A.

The substrate (contaminant) concentration equation derived from equation 3.2 using finite elements and a variably weighted backward difference scheme is

$$\begin{aligned}\left([M_s] + \Delta t\theta\left[[N] + [R_s^{t+1}] + \textstyle\sum_{i=1}^{m} Q_{w_{t,i}}[P_c]^i\right]\right)\{S\}^{t+1} \; = \\ \left([M_s] - \Delta t(1-\theta)\left[[N] + [R_s^{t}] + \textstyle\sum_{i=1}^{m} Q_{w_{t,i}}[P_c]^i\right]\right)\{S\}^{t} \; + \\ \textstyle\sum_{i=1}^{m} Q_{w_{t,i}}[P_c]^i S_w + \Delta t\theta\{F_s\}^{t+1} + \Delta t(1-\theta)\{F_s\}^{t}\end{aligned} \tag{B.5}$$

where $\{S\}^t$ and $\{S\}^{t+1}$ are substrate concentrations vectors at the beginning and end of the current time step respectively. Δt is the time step , and θ is the time weighting or implicitness factor ($0 \leq \theta \leq 1$). Equation B.5 is nonlinear because of $[R_s]\{S\}$. The matrices are defined as above and

$$\begin{aligned}[N]_{ij}^e \; = \Big[\int\int \Big(bD_{xx}\tfrac{\partial w_i}{\partial x}\tfrac{\partial w_j}{\partial x} \; + \; 2bD_{xy}\tfrac{\partial w_i}{\partial x}\tfrac{\partial w_j}{\partial y} \; + \\ bD_{yy}\tfrac{\partial w_i}{\partial y}\tfrac{\partial w_j}{\partial y} \; + \; bV_x w_i\tfrac{\partial w_j}{\partial x} \; + \; bV_y w_i\tfrac{\partial w_j}{\partial y}\Big)\,dx\,dy\Big]^e\end{aligned} \tag{B.6}$$

$$[M_s]_{ij}^e \; = \; \left[\int\int (bnR_s)\, w_i w_j dx\, dy\right]^e \tag{B.7}$$

$$[R_s^t]_{ij}^e = \left[\int\int \sum_{k=1}^{4} bnw_i w_k B_k^t R_b \frac{\mu_{max}}{Y}\left[\frac{1}{K_s + S_k^t + \frac{S_k^{t2}}{K_i}}\right]\left[\frac{O_k^t}{K_o + O_k^t}\right] w_j dx dy\right]^e \tag{B.8}$$

$$\{F_s\}_i^e = \left(\int_\Gamma (bD \cdot \nabla S) \cdot \vec{n} w_i dl\right)^e \tag{B.9}$$

$$[P_c]^i = e_{i,c} \cdot e_{i,c}^T \tag{B.10}$$

where $\vec{n}$ is a normal vector to the boundary, $e_{i,c}$ are binary vectors denoting the location of the i^{th} well in the concentration vector.

Similar to equation B.5, the oxygen concentration equation derived from equation 3.3 is:

$$\begin{aligned} &\left([M_o] + \Delta t\theta\left[[N] + [R_o^{t+1}] + \textstyle\sum_{i=1}^m Q_{w_{t,i}}[P_c]^i\right]\right)\{O\}^{t+1} = \\ &\left([M_o] - \Delta t(1-\theta)\left[[N] + [R_o^t] + \textstyle\sum_{i=1}^m Q_{w_{t,i}}[P_c]^i\right]\right)\{O\}^t + \\ &\textstyle\sum_{i=1}^m Q_{w_{t,i}}[P_c]^i O_w + \Delta t\theta\{F_o\}^{t+1} + \Delta t(1-\theta)\{F_o\}^t \end{aligned} \tag{B.11}$$

where $\{O\}^t$ and $\{O\}^{i+1}$ are oxygen concentrations vectors at the beginning and end of the current time step respectively. Equation B.11 is nonlinear because of $[R_o]\{O\}$. Additional matrices not defined above are:

$$[M_o]_{ij}^e = \left[\int\int (bn)\, w_i w_j dx\, dy\right]^e \tag{B.12}$$

$$[R_o^t]_{ij}^e = \left[\int\int \sum_{k=1}^{4} bn w_i w_k B_k^t R_b \frac{\mu_{max}}{Y}\left[\frac{S_k^t}{K_s + S_k^t + \frac{S_k^{t2}}{K_i}}\right]\left[\frac{1}{K_o + O_k^t}\right] w_j dx dy\right]^e \tag{B.13}$$

$$\{F_o\}_i^e = \left(\int_\Gamma (bD \cdot \nabla O) \cdot \vec{n} w_i dl\right)^e \tag{B.14}$$

Finally, the biomass equation derived from equation 3.4 is:

$$\begin{aligned} &\left(\theta[M_b]^{t+1} + (1-\theta)[M_b]^t \Delta t\theta\left[[N] + [R_b^{t+1}] + \textstyle\sum_{i=1}^m Q_{w_{t,i}}[P_c]^i\right]\right)\{B\}^{t+1} = \\ &\left(\theta[M_b]^{t+1} + (1-\theta)[M_b]^t + \Delta t(1-\theta)\left[[N] + [R_b^t] + \textstyle\sum_{i=1}^m Q_{w_{t,i}}[P_c]^i\right]\right)\{B\}^t + \\ &\textstyle\sum_{i=1}^m Q_{w_{t,i}}[P_c]^i B_w + \Delta t\theta\{F_b\}^{t+1} + \Delta t(1-\theta)\{F_b\}^t \end{aligned} \tag{B.15}$$

where $\{B\}^t$ and $\{B\}^{t+1}$ are biomass concentrations vectors at the beginning and end of the current time step respectively. Equation B.15 is nonlinear because of $[M_b]\{B\}$ whenever a nonlinear isotherm is used. Additional matrices not defined above are:

$$[M_b]^e_{ij} = \left[\int\int (bnR_b)\, w_i w_j dx\, dy\right]^e \tag{B.16}$$

$$[R^t_b]^e_{ij} = \left[\int\int \sum_{k=1}^{4} bnw_i w_k R_b \frac{\mu_{max}}{Y} \left[\frac{S^t_k}{K_s + S^t_k + \frac{S^{t2}_k}{K_i}}\right] \left[\frac{O^t_k}{K_o + O^t_k}\right] w_j dx dy\right]^e \tag{B.17}$$

$$\{F_b\}^e_i = \left(\int_\Gamma (bD \cdot \nabla B) \cdot \vec{n} w_i dl\right)^e + \left[\int\int (bnCYk_c w_i)\, dx\, dy\right]^e \tag{B.18}$$

Appendix C

Validation Testing: Problem Statements and Analytical Solutions

C.1 Validation Test 1: Transport in a Semi-Infinite Column

Problem Statement One-dimensional advective-dispersive transport of a conservative contaminant through a semi-infinite porous medium is given by the following equation *[Bear, 1979]*:

$$D\frac{\partial^2 C}{\partial x^2} - V\frac{\partial C}{\partial x} = R_s\, n\frac{\partial C}{\partial t} \tag{C.1}$$

where D is the coefficient of longitudinal dispersion, R_s is the retardation factor, and V is the velocity in the x-direction. The initial and boundary conditions are:

$$C(x,0) = 0 \tag{C.2}$$

$$C(0,t) = C_0 \tag{C.3}$$

$$C(\infty,t) = 0 \tag{C.4}$$

where C_0 is the constant concentration at the inlet boundary.

Analytical Solution *Ogata and Banks [1961]* give the anlytical solution of the problem as

$$\frac{C}{C_0} = \frac{1}{2}\exp\frac{Vx}{2D}\left[\exp\frac{-Vx}{2D}erfc\frac{R_s nx - Vt}{2\sqrt{R_s Dt}} + \exp\frac{Vx}{2D}erfc\frac{R_s nx + Vt}{2\sqrt{R_s Dt}}\right] \tag{C.5}$$

Input Specifications The physical parameters used in Validation Test 1 are shown in Table C.1 and Figure 4.1. The grid used in this problem consisted of 40 elements with nodal spacing of 10 meters in the x-direction. Thus, the overall length of the column was 400 meters. The simulation was conducted for 50 days at an initial time step of 2.5 days. Other time steps were considered in order to maintain the implicitness factor at 1.0. As shown in Table C.2, the simulation took 1.30 seconds on an IBM RS/6000 (Model 570) workstation.

Table C.1: Values of Physical Parameters Used in Validation Test 1

Parameter	Value
Darcy Velocity, V	1 $\frac{m}{d}$
Porosity, n	0.25
Longitudinal Dispersivity, α_L	5 m
Concentration at Boundary, C_0	1.0 $\frac{mg}{L}$
Δx	10.0 m
R_s for Case 1	1.0
R_s for Case 2	2.0
Δt (initially)	2.5 days
Implicitness Factor, θ	variable
Peclet number (P_{e_x})	2
Courant number (C_r)	0.4

Table C.2: Validation Test 1 Timing Results

		CPU Time (sec)	
No. of Elements	No. of Nodes	Per time step	For 20 time steps
40	82	0.065	1.3

C.2 Validation Test 2: Transport From A Continuous Point Source

Problem Statement This test involves the two-dimensional dispersion of a conservative solute injected from a point source in uniform areal groundwater flow. It is assumed that the injection rate is so small that the natural velocity of groundwater is unchanged. For transport of a conservative species, the governing equation is

$$D_{xx}\frac{\partial^2 C}{\partial x^2} + D_{yy}\frac{\partial^2 C}{\partial y^2} - V\frac{\partial C}{\partial x} = nR_s\frac{\partial C}{\delta t} - Q_c \tag{C.6}$$

where D_{xx} and D_{yy} are the coefficients of hydrodynamic dispersion in the x and y direction. Q_c is the mass injection rate of solute per unit volume of aquifer $\left[\frac{M}{L^3T}\right]$. It is also assumed that mechanical dispersion dominates over molecular diffusion. Thus, the coefficients become

$$D_{xx} = \alpha_L V \tag{C.7}$$
$$D_{yy} = \alpha_T V$$

where α_L and α_T are the coefficients of longitudinal and transverse dispersivity.

The initial and boundary conditions for this problem are:

$$C(x, y, 0) = 0 \tag{C.8}$$
$$Q_c(x, y, t) = QC_0\delta(x, y) \tag{C.9}$$
$$C(\pm\infty, \pm\infty, t) = 0 \tag{C.10}$$

where Q is the volumetric injection rate of fluid per unit aquifer thickness $\left[\frac{L^2}{T}\right]$, C_0 is the concentration of the injected fluid $\left[\frac{M}{L^3}\right]$ and δ is the Dirac delta function $[L^{-2}]$.

Analytical Solution Following the procedure described in *Bear [1979]*, the general solution may be written as

$$C = \frac{QC_0 \exp\frac{x}{B}}{4\pi\sqrt{D_{xx}D_{yy}}} W\left(u, \frac{r}{B}\right) \tag{C.11}$$

where

$$B = \frac{2D_{xx}}{V} \tag{C.12}$$

$$r = \sqrt{x^2 + \frac{D_{xx}y^2}{D_{yy}}} \tag{C.13}$$

$$u = \frac{R_s n r^2}{4D_{xx}t} \tag{C.14}$$

$$W\left(u, \frac{r}{B}\right) = \int_u^\infty \frac{1}{\theta} \exp\left[-\left(\theta + \frac{r^2}{4B^2\theta}\right)\right] d\theta \tag{C.15}$$

$W(u, \frac{r}{B})$ is commonly referred to as a *Hantush [1956]* well function for the problem of transient flow to a well in an infinite leaky aquifer. Thus, as $t \rightarrow \infty$, or $u \rightarrow 0$ a steady-state condition will be reached. This results in a balance between the rate of solute injection and dispersion. Equation C.11 becomes

$$C = \frac{QC_0 \exp\frac{x}{B}}{4\pi\sqrt{D_{xx}D_{yy}}} K_0\left(\frac{r}{B}\right) \tag{C.16}$$

where $K_0(\frac{r}{B})$ is the modified Besssel Function of the second kind, zero order.

Input Specifications Values of the physical parameters used in Validation Test 2 are shown in Table C.3 and Figure 4.5. As discussed in *Huyakorn et al. [1984]* the data represents a simulation of the hexavalent chromium contaminant reported by *Perlmutter and Lieber [1970]* and *Wilson and Miller [1978]*. This problem considered three different discretizations of the aquifer: fine, medium and coarse.

The problem is axisymetrical with respect to the x-axis, so it was possible to model the upper half of the aquifer only, saving on memory requirements and speeding

Table C.3: Values of Physical Parameters Used in Validation Test 2

Parameter	Value
Aquifer Thickness, b	33.5 m
Darcy Velocity, V	.161 $\frac{m}{d}$
Porosity, n	0.35
Longitudinal Dispersivity, α_L	21.3 m
Transverse Dispersivity, α_T	4.3 m
Contaminent mass flux, QC_0	704 $\frac{g}{m-day}$
R_s	1.0
Δt (initially)	100 days
Implicitness Factor, θ	variable

Selected Grid	Δx	Δy	P_{e_x}	P_{e_y}	C_r
Fine	10 m	10 m	.47	2.32	1.61
Medium	60 m	15 m	2.8	3.5	.27
Course	60 m	30 m	2.8	7.0	.27

calculations. The nodal spacing, and number of elements and nodes for each case are shown in Table C.4. The simulation took 86.8, 21.2, and 5.8 seconds on an IBM RS/6000 workstation for the fine, medium and coarse grids respectively.

Table C.4: Validation Test 2 Timing Results

			CPU Time (sec)	
Selected Grid	No. of Elements	No. of Nodes	Per time step	For 20 time steps
Fine	3000	3171	4.34	86.8
Medium	800	861	1.06	21.2
Coarse	400	451	0.29	5.8

C.3 Validation Test 3: Transport Of A Solute Slug In A Uniform Flow Field

Problem Statement This test involves the two-dimensional dispersion of a conservative solute slug injected in uniform, isotropic groundwater flow. It is assumed that the injection doesn't change the natural groundwater velocity. For transport of a conservative species, the governing equation is

$$D_{xx}\frac{\partial^2 C}{\partial x^2} + D_{yy}\frac{\partial^2 C}{\partial y^2} - V\frac{\partial C}{\partial x} = nR_s\frac{\partial C}{\partial t} - Q_c \qquad \text{(C.17)}$$

where D_{xx} and D_{yy} are the coefficients of hydrodynamic dispersion in the x and y direction. Q_c is the mass injection rate of solute per unit volume of aquifer $\left[\frac{M}{L^3T}\right]$. It is also assumed that mechanical dispersion dominates over molecular diffusion, and the coefficients are

$$D_{xx} = \alpha_L V \qquad \text{(C.18)}$$
$$D_{yy} = \alpha_T V$$

where α_L and α_T are the coefficients of longitudinaland transverse dispersivity.

The initial and boundary conditions for this problem are:

$$C(x,y,0) = 0 \tag{C.19}$$

$$Q_c(0,0,0) = \frac{m}{n}\delta(x,y) \tag{C.20}$$

$$C(\pm\infty,\pm\infty,t) = 0 \tag{C.21}$$

$$\tag{C.22}$$

where m is the solute mass injected per unit aquifer thickness $\left[\frac{M}{L}\right]$ and δ is the Dirac delta function $[L^{-2}]$.

Analytical Solution The general analytical solution was presented by *Sauty [1980]*, and using present notation:

$$c_R(a,t'_R) = \frac{t'_{RMAX}}{t'_R}\exp\left[\frac{a^2+t'^2_{RMAX}}{4t'_{RMAX}} - \frac{a^2+t'^2_R}{4t'_R}\right] \tag{C.23}$$

where

$$a = \sqrt{x_R^2 + \frac{y^2}{\alpha_L\alpha_T}} = \sqrt{x_R^2+y_R^2} \tag{C.24}$$

$$t'_R = \frac{Vt}{\alpha_L n} \tag{C.25}$$

$$t'_{RMAX} = \sqrt{a^2+4} - 2 \tag{C.26}$$

$$x_R = \begin{cases} \frac{x}{\alpha_L} & x > 0, \\ |x| + \frac{2Vt}{n} & x < 0. \end{cases} \tag{C.27}$$

The concentration C is calculated as a product of the dimensionless concentration C_R and the peak concentration C_{MAX}:

$$C_{MAX}(x_R,y_R) = \frac{M}{4\pi n\alpha_L\sqrt{\alpha_L\alpha_T}} f(x_R,y_R) \tag{C.28}$$

where

$$f(x_R,y_R) = \frac{1}{x_R t_{RMAX}}\exp - \left[\frac{x_R(1-t_{RMAX})^2}{4t_{RMAX}} + \frac{y_R^2}{4x_R t_{RMAX}}\right] \tag{C.29}$$

Table C.5: Values of Physical Parameters Used in Validation Test 3

Parameter	Value
Aquifer Thickness, b	1.0 m
Darcy Velocity, V	2 $\frac{m}{d}$
Porosity, n	0.35
Longitudinal Dispersivity, α_L	4 m
Transverse Dispersivity, α_T	1 m
Contaminent mass per unit thickness of aquifer	3500 $\frac{mg}{m}$
R_s	1.0
Δx	5 m
Δy	5 m
Δt (initially)	1 day
Implicitness Factor, θ	variable
Peclet number (P_{e_x})	1.25
Peclet number (P_{e_y})	5.00
Courant number (C_r)	0.40

with

$$t_{RMAX} = \sqrt{1 + \left(\frac{2}{x_R}\right)^2 + \left(\frac{y_R}{x_R}\right)^2} - \frac{2}{x_R} \tag{C.30}$$

Input Specifications Values of the physical parameters used in Validation Test 3 are shown in Table C.5 and Figure 4.8. A rectangular finite element grid was used in the simulation with $\Delta x = \Delta y = 5$m. The problem is axisymetrical with respect to the x-axis, so it was possible to model the upper half of the aquifer only, reducing memory requirements and speeding calculations. As shown in Table C.6, the simulation took 19.6 seconds on an IBM RS/6000 workstation.

Table C.6: Validation Test 3 Timing Results

		CPU Time (sec)	
No. of Elements	No. of Nodes	Per time step	For 15 time steps
960	1029	1.31	19.65

C.4 Validation Test 4: Transport In A Radial Flow Field

Problem Statement This validation test involves the two-dimensional dispersion of a solute injected from a fully penetrating well in a confined aquifer (Figure 4.12). It is assumed that the rate of injection is constant and that the background aquifer flow is negligible. The resulting flow field is assumed radial and steady-state. The following equation desribes the problem:

$$D\frac{\partial^2 C}{\partial r^2} - V\frac{\partial C}{\partial r} = n\frac{\partial C}{\partial t} \tag{C.31}$$

where r is the radial distance from the well and V is the Darcy velocity given by

$$V_r = \frac{Q}{2\pi r b} \tag{C.32}$$

where Q is the injection rate of the fluid $\left[\frac{L^3}{T}\right]$ and b is the aquifer thickness $[L]$.

The initial and boundary conditions for this problem are:

$$C(r,0) = 0 \tag{C.33}$$

$$C(r_w,t) = C_0 \tag{C.34}$$

$$C(\infty,t) = 0 \tag{C.35}$$

(C.36)

Analytical Solution The general analytical solution was derived by *Ogata [1958]* and presented by *Huyakorn et al. [1984].* Using present notation:

$$\frac{C}{C_0} = 1 + \frac{2}{\pi} exp\left[\frac{r - r_w}{2\alpha_L}\right] \int_0^\infty \frac{\exp\left(-\nu^2 t\right)}{\nu} \left[\frac{\nu^2 r - \frac{G}{4\alpha_L}}{\nu^2 r_w - \frac{G}{4\alpha_L}}\right] M(\nu)\, d\nu \qquad \text{(C.37)}$$

where

$$M(\nu) = \frac{J_{\frac{1}{3}}(\sigma) Y_{\frac{1}{3}}(\sigma') - Y_{\frac{1}{3}}(\sigma) J_{\frac{1}{3}}(\sigma')}{J^2_{\frac{1}{3}}(\sigma') + Y^2_{\frac{1}{3}}(\sigma')} \qquad \text{(C.38)}$$

$$G = \frac{Q}{2\pi b n} \qquad \text{(C.39)}$$

$$\sigma = \frac{2}{3\sqrt{\alpha_L G}} \frac{\left(\nu^2 r - \frac{G}{4\alpha_L}\right)^{\frac{3}{2}}}{\nu^2} \qquad \text{(C.40)}$$

$$\sigma' = \frac{2}{3\sqrt{\alpha_L G}} \frac{\left(\nu^2 r_w - \frac{G}{4\alpha_L}\right)^{\frac{3}{2}}}{\nu^2} \qquad \text{(C.41)}$$

and $J_{\frac{1}{3}}$ and $Y_{\frac{1}{3}}$ are Bessel functions of order $\frac{1}{3}$, of the first and second kinds respectively.

Equation A.35 is too complicated to evaluate analytically. *Huyakorn et al. [1984]* recommend using *Hoopes and Harleman's [1966]* approximate solution:

$$\frac{C}{C_0} = \frac{1}{2} erfc\left[\frac{\frac{r^2}{2} - Gt}{\sqrt{\frac{4}{3}\alpha_L r^3}}\right] \qquad \text{(C.42)}$$

where G is defined as above.

Input Specifications Values of the physical parameters used in Validation Test 4 are shown in Table C.7. The problem is axisymetrical, so that it was possible to model one quarter of the aquifer only, saving considerably on memory requirements

Table C.7: Values of Physical Parameters Used in Validation Test 4

Parameter	Value
Well Discharge, Q	25 $\frac{m^3}{day}$
Initial Concentration, C_0	$1\frac{mg}{L}$
Aquifer Thickness, b	10 m
Darcy Velocity, V	0 $\frac{m}{d}$
Porosity, n	0.25
Longitudinal Dispersivity, α_L	0.3 m
Transverse Dispersivity, α_T	0.0 m
R_s	1.0
Δx	1 m
Δy	1 m
Δt (initially)	1 day
Implicitness Factor, θ	variable
Peclet number (P_{e_x})	3.33
Courant number (C_r)	0.40

and speeding calculations. A rectangular finite element grid was used in the simulation with $\Delta x = \Delta y = 1m$. A total of 400 finite elements and 441 nodes were used. As shown in Table C.8, the simulation took 19.6 seconds on an IBM RS/6000 workstation.

Table C.8: Validation Test 4 Timing Results

		CPU Time (sec)	
No. of Elements	No. of Nodes	Per time step	For 40 time steps
400	441	0.49	19.60

C.5 Validation Test 5: Transport in a Non-Uniform Flow Field Caused by an Injection-Extraction Well Doublet

Problem Statement The final validation test used to evaluate BIO2D concerns solute transport between a pair of recharging and discharging wells operating at a constant flow rate. Both wells fully penetrate a uniform thickness confined aquifer that is assumed as infinite, homogeneous and isotropic (Figure 3.14). The flow field is assumed as steady-state. For transport of a conservative species, the governing equation is

$$\frac{\partial}{\partial x}D_{xx}\frac{\partial C}{\partial x}+\frac{\partial}{\partial y}D_{yy}\frac{\partial C}{\partial y}+\frac{\partial}{\partial x}D_{xy}\frac{\partial C}{\partial y}+\frac{\partial}{\partial y}D_{xy}\frac{\partial C}{\partial x}-V_x\frac{\partial C}{\partial x}-V_y\frac{\partial C}{\partial y}=nR_s\frac{\partial C}{\partial t} \quad \text{(C.43)}$$

where D_{xx},D_{xx}, and D_{xx} are the three components of the hydrodynamic dispersion tensor, and V_x and V_y are the components of the Darcy velocity in the x and y directions, respectively. For the well doublet, the values of V_x and V_y are given by

$$V_x=-\frac{Q}{2\pi b}\left[\frac{x-x_0}{(x-x_0)^2+y^2}-\frac{x+x_0}{(x+x_0)^2+y^2}\right] \quad \text{(C.44)}$$

$$V_y=-\frac{Q}{2\pi b}\left[\frac{1}{(x-x_0)^2+y^2}-\frac{1}{(x+x_0)^2+y^2}\right] \quad \text{(C.45)}$$

where Q is the well flow rate $[\frac{L^3}{T}]$, b is the aquifer thickness and x_0 is half the well spacing.

The initial and boundary conditions associated with equation C.43 are:

$$C(x, y, 0) = 0 \tag{C.46}$$

$$C(-x_0, y, 0) = C_0 \tag{C.47}$$

Analytical Solutions For the most general case involving the combined influences of advection and dispersion, an analytical solution does not exist *[Huyakorn et al., 1984]*. For a more limited case of pure advection, a solution was developed by *Hoopes and Harleman [1967] and Gringarten and Sauty [1975]*. For a second limiting case of advection and longitudinal dispersion only, an approximate analytical solution was developed by *Hoopes and Harleman [1967] and Grove and Beetem [1971]*. Both are presented in *[Huyakorn et al., 1984]*.

For the first case (pure advection), a semi-analytical solution was developed and programmed by *Javandel et al. [1984]*. The model, called RESSQ, uses the complex velocity potential to estimate the concentration distribution in the aquifer. Validation Test 5 utilized RESSQ, which assumes a confined aquifer of uniform thickness, infinite in extent, that is homogeneous and isotropic.

The technique used by *Javandel et al.* was to first identify simple flow components, such as sinks and sources. Then the overall complex velocity potential of the system is obtained by combining the expressions for each individual component. The velocity field is then identified by taking the derivative of the velocity potential. Locations of contaminant fronts and flow patterns are estimated at various values of time. Finally, stream function of the system is used to calculate the time variation of the rate at which a contaminant reaches any desired point *[El-Kadi, 1988]*.

Input Specifications Values of the physical parameters used in Validation Test 5 are given in Table C.8. The problem is axisymetrical with respect to the x-axis, so that it was possible to model one half of the aquifer only, saving considerably on memory requirements and speeding calculations. A rectangular finite element grid was used in the simulation with $\Delta x = \Delta y = 5$ m.

Table C.9: Physical Parameters For Validation Test 5

Parameter		Value
Injection and Extraction Rates, Q		$\pm 2.0\ \frac{m^3}{d}$
Injected Concentration, C_0		$100\ \frac{mg}{L}$
Darcy Velocity, V		$0.015\ \frac{m}{d}$
Porosity, n		0.29
R_s		1.0
Aquifer Thickness, b		1.0 m
Δx		5.0 m
Δy		5.0 m
Δt		1.0 day
Implicitness Factor, θ		1.0
Case 1	Dispersivities, $\alpha_L = \alpha_T$	.01 m
	Peclet number ($Pe_x = Pe_y$)	500
Case 2	Dispersivities, $\alpha_L = \alpha_T$	.1 m
	Peclet number ($Pe_x = Pe_y$)	50
Case 3	Dispersivities, $\alpha_L = \alpha_T$	1 m
	Peclet number ($Pe_x = Pe_y$)	5
Case 4	Dispersivities, $\alpha_L = \alpha_T$	5 m
	Peclet number ($Pe_x = Pe_y$)	1
Case 5	Longitudinal Dispersivity, α_L	9.1 m
	Tranverse Dispersivity, α_T	1.8 m
	Peclet number (Pe_x)	.55
	Peclet number (Pe_y)	2.78

Appendix D

Sensitivity Analysis Run Summaries

This appendix details the sensitivity analysis runs discussed in Chapter 6. The biological parameters are defined in Table 2.2, and the specific parameter ranges considered for phenol are found in Table 4.2.

Table D.1 contains the specific values of the biological parameters used for the individual sensitivity analysis presented in Section 6.2. A total of 17 runs were made in the individual sensitivity analysis. The results of these runs are found in Tables 6.1 - 6.2, and Figures 6.2 - 6.16.

Tables D.2 - D.3 contain the specific values of the biological parameters used for the combined sensitivity analysis presented in Section 6.3 A total of 64 runs were made in the individual sensitivity analysis. The results of these runs are found in Tables 6.3 - 6.5, and Figures 6.17 - 6.19.

Table D.4 contains the specific run numbers that comprise parameter run pairs used in Section 6.3 and Figures 6.20 - 6.25. For example, K_s run pair 1 consists of runs 2 and 1 from Table D.2. μ_{max} run pair 1 consists of runs 33 and 1, and μ_{max} run pair 2 consists of runs 34 and 2 from Tables D.2 and D.3.

Table D.1: Values of Biological Parameters Used in BIO2D Individual Sensitivity Runs (see Table 2.2 for parameter definitions).

RUN	μ_{max}	K_s	K_o	K_i	Y	r_b	K_b	N_b	F	C_c	k_c
1	6.36	49.6	1	356.8	.70	.05	15.26	1.0	3	715	.00001
2	15.36	49.6	1	356.8	.70	.05	15.26	1.0	3	715	.00001
3	1.97	49.6	1	356.7	.70	.05	15.26	1.0	3	715	.00001
4	6.48	266	1	356.8	.70	.05	15.26	1.0	3	715	.00001
5	6.48	1	1	356.8	.70	.05	15.26	1.0	3	715	.00001
6	6.48	49.6	1	1463	.70	.05	15.26	1.0	3	715	.00001
7	6.48	49.6	1	23	.70	.05	15.26	1.0	3	715	.00001
8	6.48	49.6	1	356.8	1.02	.05	15.26	1.0	3	715	.00001
9	6.48	49.6	1	356.8	.50	.05	15.26	1.0	3	715	.00001
10	6.48	49.6	1	356.8	.70	.10	15.26	1.0	3	715	.00001
11	6.48	49.6	1	356.8	.70	.001	15.26	1.0	3	715	.00001
12	6.48	49.6	2	356.8	.70	.05	15.26	1.0	3	715	.00001
13	6.48	49.6	.1	356.8	.70	.05	15.26	1.0	3	715	.00001
14	6.48	49.6	1	356.8	.70	.05	22.97	1.0	3	715	.00001
15	6.48	49.6	1	356.8	.70	.05	7.55	1.0	3	715	.00001
16	6.48	49.6	1	356.8	.70	.05	15.26	1.1	3	715	.00001
17	6.48	49.6	1	356.8	.70	.05	15.26	.9	3	715	.00001

Table D.2: Values of Biological Parameters Used in BIO2D For Combined Sensitivity Runs 1-32 (see Table 2.2 for parameter definitions).

RUN	μ_{max}	K_s	K_o	Y	r_b	K_b	K_i	N_b	F	C_c	k_c
1	1.97	1	.001	.5	.001	7.55	356.7	1	3	715	.00001
2	1.97	266	.001	.5	.001	7.55	356.7	1	3	715	.00001
3	1.97	1	2	.5	.001	7.55	356.7	1	3	715	.00001
4	1.97	266	2	.5	.001	7.55	356.7	1	3	715	.00001
5	1.97	1	.001	1.02	.001	7.55	356.7	1	3	715	.00001
6	1.97	266	.001	1.02	.001	7.55	356.7	1	3	715	.00001
7	1.97	1	2	1.02	.001	7.55	356.7	1	3	715	.00001
8	1.97	266	2	1.02	.001	7.55	356.7	1	3	715	.00001
9	1.97	1	.001	.5	.1	7.55	356.7	1	3	715	.00001
10	1.97	266	.001	.5	.1	7.55	356.7	1	3	715	.00001
11	1.97	1	2	.5	.1	7.55	356.7	1	3	715	.00001
12	1.97	266	2	.5	.1	7.55	356.7	1	3	715	.00001
13	1.97	1	.001	1.02	.1	7.55	356.7	1	3	715	.00001
14	1.97	266	.001	1.02	.1	7.55	356.7	1	3	715	.00001
15	1.97	1	2	1.02	.1	7.55	356.7	1	3	715	.00001
16	1.97	266	2	1.02	.1	7.55	356.7	1	3	715	.00001
17	1.97	1	.001	.5	.001	22.97	356.7	1	3	715	.00001
18	1.97	266	.001	.5	.001	22.97	356.7	1	3	715	.00001
19	1.97	1	2	.5	.001	22.97	356.7	1	3	715	.00001
20	1.97	266	2	.5	.001	22.97	356.7	1	3	715	.00001
21	1.97	1	.001	1.02	.001	22.97	356.7	1	3	715	.00001
22	1.97	266	.001	1.02	.001	22.97	356.7	1	3	715	.00001
23	1.97	1	2	1.02	.001	22.97	356.7	1	3	715	.00001
24	1.97	266	2	1.02	.001	22.97	356.7	1	3	715	.00001
25	1.97	1	.001	.5	.1	22.97	356.7	1	3	715	.00001
26	1.97	266	.001	.5	.1	22.97	356.7	1	3	715	.00001
27	1.97	1	2	.5	.1	22.97	356.7	1	3	715	.00001
28	1.97	266	2	.5	.1	22.97	356.7	1	3	715	.00001
29	1.97	1	.001	1.02	.1	22.97	356.7	1	3	715	.00001
30	1.97	266	.001	1.02	.1	22.97	356.7	1	3	715	.00001
31	1.97	1	2	1.02	.1	22.97	356.7	1	3	715	.00001
32	1.97	266	2	1.02	.1	22.97	356.7	1	3	715	.00001

Table D.3: Values of Biological Parameters Used in BIO2D For Combined Sensitivity Runs 33-64 (see Table 2.2 for parameter definitions).

RUN	μ_{max}	K_s	K_o	Y	r_b	K_b	K_i	N_b	F	C_c	k_c
33	15.36	1	.001	.5	.001	7.55	356.7	1	3	715	.00001
34	15.36	266	.001	.5	.001	7.55	356.7	1	3	715	.00001
35	15.36	1	2	.5	.001	7.55	356.7	1	3	715	.00001
36	15.36	266	2	.5	.001	7.55	356.7	1	3	715	.00001
37	15.36	1	.001	1.02	.001	7.55	356.7	1	3	715	.00001
38	15.36	266	.001	1.02	.001	7.55	356.7	1	3	715	.00001
39	15.36	1	2	1.02	.001	7.55	356.7	1	3	715	.00001
40	15.36	266	2	1.02	.001	7.55	356.7	1	3	715	.00001
41	15.36	1	.001	.5	.1	7.55	356.7	1	3	715	.00001
42	15.36	266	.001	.5	.1	7.55	356.7	1	3	715	.00001
43	15.36	1	2	.5	.1	7.55	356.7	1	3	715	.00001
44	15.36	266	2	.5	.1	7.55	356.7	1	3	715	.00001
45	15.36	1	.001	1.02	.1	7.55	356.7	1	3	715	.00001
46	15.36	266	.001	1.02	.1	7.55	356.7	1	3	715	.00001
47	15.36	1	2	1.02	.1	7.55	356.7	1	3	715	.00001
48	15.36	266	2	1.02	.1	7.55	356.7	1	3	715	.00001
49	15.36	1	.001	.5	.001	22.97	356.7	1	3	715	.00001
50	15.36	266	.001	.5	.001	22.97	356.7	1	3	715	.00001
51	15.36	1	2	.5	.001	22.97	356.7	1	3	715	.00001
52	15.36	266	2	.5	.001	22.97	356.7	1	3	715	.00001
53	15.36	1	.001	1.02	.001	22.97	356.7	1	3	715	.00001
54	15.36	266	.001	1.02	.001	22.97	356.7	1	3	715	.00001
55	15.36	1	2	1.02	.001	22.97	356.7	1	3	715	.00001
56	15.36	266	2	1.02	.001	22.97	356.7	1	3	715	.00001
57	15.36	1	.001	.5	.1	22.97	356.7	1	3	715	.00001
58	15.36	266	.001	.5	.1	22.97	356.7	1	3	715	.00001
59	15.36	1	2	.5	.1	22.97	356.7	1	3	715	.00001
60	15.36	266	2	.5	.1	22.97	356.7	1	3	715	.00001
61	15.36	1	.001	1.02	.1	22.97	356.7	1	3	715	.00001
62	15.36	266	.001	1.02	.1	22.97	356.7	1	3	715	.00001
63	15.36	1	2	1.02	.1	22.97	356.7	1	3	715	.00001
64	15.36	266	2	1.02	.1	22.97	356.7	1	3	715	.00001

Table D.4: Run Numbers Comprising BIO2D Combined Sensitivity Run Pairs Shown in Figures 6.20 - 6.25. For example, K_s run pair 1 consists of runs 2 and 1, and μ_{max} run pair 1 consists of runs 33 and 1.

	Runs from Tables D.2 - D.3 In Pair					
PAIR	K_s	μ_{max}	K_o	Y	r_b	K_b
1	2- 1	33- 1	3- 1	5- 1	9- 1	17- 1
2	4- 3	34- 2	4- 2	6- 2	10- 2	18- 2
3	6- 5	35- 3	7- 5	7- 3	11- 3	19- 3
4	8- 7	36- 4	8- 6	8- 4	12- 4	20- 4
5	10- 9	37- 5	11- 9	13- 9	13- 5	21- 5
6	12-11	38- 6	12-10	14-10	14- 6	22- 6
7	14-13	39- 7	15-13	15-11	15- 7	23- 7
8	16-15	40- 8	16-14	16-12	16- 8	24- 8
9	18-17	41- 9	19-17	21-17	25-17	25- 9
10	20-19	42-10	20-18	22-18	26-18	26-10
11	22-21	43-11	23-21	23-19	27-19	27-11
12	24-23	44-12	24-22	24-20	28-20	28-12
13	26-25	45-13	27-25	29-25	29-21	29-13
14	28-27	46-14	28-26	30-26	30-22	30-14
15	30-29	47-15	31-29	31-27	31-23	31-15
16	32-31	48-16	32-30	32-28	32-24	32-16
17	34-33	49-17	35-33	37-33	41-33	49-33
18	36-35	50-18	36-34	38-34	42-34	50-34
19	38-37	51-19	39-37	39-35	43-35	51-35
20	40-39	52-20	40-38	40-36	44-36	52-36
21	42-41	53-21	43-41	45-41	45-37	53-37
22	44-43	54-22	44-42	46-42	46-38	54-38
23	46-45	55-23	47-45	47-43	47-39	55-39
24	48-47	56-24	48-46	48-44	48-40	56-40
25	50-49	57-25	51-49	53-49	57-49	57-41
26	52-51	58-26	52-50	54-50	58-50	58-42
27	54-53	59-27	55-53	55-51	59-51	59-43
28	56-55	60-28	56-54	56-52	60-52	60-44
29	58-57	61-29	59-57	61-57	61-53	61-45
30	60-59	62-30	60-58	62-58	62-54	62-46
31	62-61	63-31	63-61	63-59	63-55	63-47
32	64-63	64-32	64-62	64-60	64-56	64-48

Bibliography

[1] Alder Schaller, S.E., and P.B. Bedient. 1989. Evaluation of the Hydraulic Effect of Injection and Pumping Wells on In-Situ Bioremediation. In *Proceedings of the Petroleum Hydrocarbons and Organic Chemicals in Ground Water: Prevention, Detection and Restoration.* 191-201. Houston, Texas.

[2] Alexander, M., and K.M. Scow. 1989. Kinetics of Biodegradation in Soil. In *Reactions and Movement of Organic Chemicals in Soils.* 243-269. Madison, WI: Soil Science Society of America.

[3] Anderson, M.P., and W.W. Woessner. 1992. *Applied Groundwater Modeling: Simulation of Flow and Advective Transport.* San Diego, CA: Academic Press.

[4] Baehr, A., and M.Y. Corapcioglu. 1984. A Predictive Model for Pollution From Gasoline in Soils and Groundwater. In *Proceedings, NWWA Conference-Petroleum Hydrocarbons and Organic Chemicals in Groundwater.* 144-156. Houston, Texas: National Well Water Association.

[5] Baker, K.H., and D.S. Herson. 1994. *Bioremediation.* New York: McGraw Hill.

[6] Bear, J. 1979. *Hydraulics of Groundwater.* New York: McGraw Hill.

[7] Bear, J., M.S. Beljin, and R.R. Ross. 1992. *Fundamentals of Groundwater Modeling.* U.S. Environmental Protection Agency. EPA/540/S-92/005.

[8] Bedient, P.B., and H.S. Rifai. 1992. Groundwater Contaminant Modeling For Bioremediation: A Review. *Journal of Hazardous Materials,* 32 : 225-243.

[9] Bedient, P.B., G.P. Long, and H.S. Rifai. 1992. Modeling Natural Biodegradation with BIOPLUME II. In *Proceedings 5th International Conference on Solving Groundwater Problems with Models.* 699-714. Dallas, Texas.

[10] Beljin, M.S. 1988. *Testing and Validation of Groundwater Models for Simulating Solute Transport in Groundwater: Code Intercomparison and Evaluation of Validation Methodology.* International Groundwater Modeling Center. GWMI 88-11.

[11] Borden, R.C., and P.B. Bedient. 1986. Transport of Dissolved Hydrocarbons Influenced by Oxygen Limited Biodegradation: 1. Theoretical Development. *Water Resources Research,* 22 : 1973-1990.

[12] Borden, R.C., and P.B. Bedient. 1986. Transport of Dissolved Hydrocarbons Influenced by Oxygen Limited Biodegradation: 2. Field Application. *Water Resources Research,* 22 : 1973-1990.

[13] Borden, R.C., and P.B. Bedient. 1987. In-Situ Measurement of Adsorption and Biotransformation at a Hazardous Waste Site. *Water Resources Bulletin,* 23 : 629-636.

[14] Celia, M.A., J.S. Kindred, and I. Herrera. 1989. Contaminant Transport and Biodegradation. *Water Resources Research,* 25 : 1141-1159.

[15] Charbeneau, R.J., P.B. Bedient, and R.C. Loehr. 1992. *Groundwater Remediation.* Lancaster, Pennsylvania: Technomic Publishing Co.

[16] Chen, Y., L.M. Abriola, P.J.J. Alvarez, P.J. Anid, and T.M. Vogel. 1992. Modeling Transport and Biodegradation of Benzene and Toluene in Sandy Aquifer Material: Comparisons With Experimental Measurements. *Water Resources Research,* 28 (7) : 1833-1847.

[17] Chiang, C.Y., C.N. Dawson, and M.F. Wheeler. 1990. Modeling of In-situ Biorestoration of Organic Compounds in Groundwater. *Transport in Porous Media,* 6 (5-6) : 667-702.

[18] Corapcioglu, M.Y., and A. Haridas. 1985. Microbial Transport in Soils and Groundwater: A Numerical Model. *Advances in Water Resources,* 8 : 188-200.

[19] Culver, T.B., and C.A. Shoemaker. 1992. Dynamic Optimal Control for Groundwater Remediation with Flexible Management Periods. *Water Resources Research,* 29 : 823-831.

[20] El-Kadi, A.I. 1988. Applying the USGS Mass-Transport Model (MOC) to Remedial Actions by Recovery Wells. *Groundwater,* 26 (3) : 281-288.

[21] Fjeld, R.A., and B.B. Looney. 1987. The Sensitivity Index as a Screening Tool in the Analysis of Ground-Water Contaminant Transport. In *Geostatistical Sensitivity and Uncertainty Methods for Ground-Water Flow and Radionuclide Modeling.* Edited by B. E. Buxton. 323-325. Columbus, OH: Battelle Press.

[22] Frind, E.O., W.H.M. Duynisveld, O. Strebel, and J. Boettcher. 1990. Modeling of Multicomponent Transport With Microbial Transformation in Groundwater: The Fuhrberg Case. *Water Resources Research,* 26 (8) : 1707-1719.

[23] Garder, A.O., D.W. Peaceman, and A.L. Pozzi. 1964. Numerical Calculation of Multidimensional Miscible Displacement by the Method of Characteristics. *Society of Petroleum Engineers Journal*, 4 (1) : 26-36.

[24] Gringarten, A.C. and J.P. Sauty. 1975. A Theoretical Study of Heat Extraction from Aquifers with Uniform Regional Flow. *Journal of Geophysical Research*, 80 : 4856 - 4962.

[25] Gupta, A.D., and P.R. Onta Shrestha. 1986. Contaminant Movement Under Pumpage-Recharge Condition in Steady Ground-Water Flow System. *Groundwater*, 24 (3) : 342-350.

[26] Hantush, M.S. 1956. Analysis of Data From Pumping Tests in Leaky Aquifers. *Transactions of the American Geophysical Union*, 37 (6) : 702-714.

[27] Hobson, M.J., and N.F. Mills. 1990. Chemostat Studies of a Mixed Culture Growing on Phenolics. *Research Journal WPCF*, 62 (5) : 684-691.

[28] Hoopes, J.A., and D.R. Harleman. 1967. Wastewater Recharge and Dispersion in Porous Media. *Journal of the Hydraulics Division, ASCE*, 93 (HY5) : 51-71.

[29] Huyakorn, P.S., and G.F. Pinder. 1983. *Computational Methods in Subsurface Flow.* New York: Academic Press.

[30] Huyakorn, P.S. et al. 1984. *SEFTRAN: A Simple and Efficient Flow and Transport Code.* GeoTrans, Inc., Reston, VA. 142 pp.

[31] Huyakorn, P.S. 1985. *Testing and Validation of Models for Simulating Solute Transport in Groundwater: Development, Evaluation, and Comparison of Benchmark Techniques.* International Groundwater Modeling Center. GWMI 84-13.

[32] Javandel, I., C. Doughty, and C.F. Tsang. 1984. *Groundwater Transport: Handbook of Mathematical Models.* American Geophysical Union. Water Resources Monograph 10.

[33] Kindred, J.S., and M.A. Celia. 1989. Contaminant Transport and Biodegradation: 2. Conceptual Model and Test Simulations. *Water Resources Research*, 25 : 1141-1159.

[34] Kinzelbach, W. 1986. *Groundwater Modeling: An Introduction with Sample Programs in BASIC.* Developments in Water Science. Amsterdam, The Netherlands: Elsevier Science Publishers.

[35] Kinzelbach, W. 1987. Methods for the Simulation of Pollutant Transport in Groundwater - A Model Comparison. In *Proceedings NWWA Conference on Solving Problems with Models.* 656-674. Denver, Colorodo: National Well Water Association.

[36] Kinzelbach, W., W. Schafer, and J. Herzer. 1991. Numerical Modeling of Natural and Enhanced Denitrification Processes in Aquifers. *Water Resources Research,* 27 (6) : 1123-1135.

[37] Konikow, L.F., and J.D. Bredehoeft. 1978. *Computer Model of Two-Dimensional Solute Transport and Dispersion in Groundwater.* Techniques of Water-Resources Investgations of the United States Geological Survey. United States Geological Survey.

[38] Konikow, L.F., and J. Mercer. 1988. Groundwater Flow and Transport Modeling. *Journal of Hydrology,* 100 : 379-409.

[39] LaGrega, M.D., P.L.Buckingham, and J.C. Evans. 1994. *Hazardous Waste Management.* New York: McGraw Hill.

[40] Law, A.M., and W.D. Kelton. 1991. *Simulation Modeling and Analysis.* New York: McGraw Hill.

[41] Lee, M.D., J.M. Thomas, R.C. Borden, P.B. Bedient, C.H. Ward, and J.T. Wilson. 1988. *Biorestoration of Aquifers Contaminated with Organic Compounds.* National Council of Ground Water Resources. R.S. Kerr Environmental Research Laboratory, U.S. Environmental Protection Agency, Ada, OK. 18 : 29-89.

[42] Lin, W. 1992. *Dynamic Modeling of the Biological Activated Carbon (BAC) Process and its Experimental Corroboration.* Ph.D. Dissertation, State University of New York at Buffalo.

[43] MacQuarrie, K.T.B., E.A. Sudicky, and E.O. Frind. 1990. Simulation of Biodegradable Organic Contaminants in Groundwater: 1. Numerical Formulation in Principal Directions. *Water Resources Research,* 26 : 207-239.

[44] MacQuarrie, K.T.B., E.A. Sudicky, and E.O. Frind. 1990. Simulation of Biodegradable Organic Contaminants in Groundwater: 2. Plume Behavior in Uniform and Random Flow Fields. *Water Resources Research,* 26 : 207-239.

[45] Minsker, B.S., and C.A. Shoemaker. Submitted 1994. Dynamic Optimal Control of In Situ Bioremediation of Groundwater. *Water Resources Research.*

[46] Molz, F.J., M.A. Widdowson, and L.D. Benefield. 1986. Simulation of Microbial Growth Dynamics Coupled To Nutrient and Oxygen Transport in Porous Media. *Water Resources Research,* 22 : 1207-1216.

[47] Molz, F.J., and M.A. Widdowson. 1988. Internal Inconsistancies in Dispersion-Dominated Models That Incorporate Chemical and Microbial Kinetics. *Water Resources Research,* 24 (4) : 615-619.

[48] National Research Council (NRC). 1992. *A Review of Groundwater Modeling Needs for the U.S. Army.* Washington, D.C.: National Academy Press.

[49] Neidhardt, F.C., J.L. Ingraham, and M. Schaechter. 1990. *Physiology of the Bacterial Cell.* Sunderland, MA: Sinauer Associates Inc.

[50] Oak Ridge National Laboratory. 1989. *The Installation Resoration Program Toxicology Guide.* Volume 2. Biomedical and Environmental Information Analysis Health and Safety Research Division. Oak Ridge, TN.

[51] Odencrantz, V., and B. Rittman. 1990. Modeling Two-Dimensional Solute Transport With Different Biodegradation Kinetics. In *Proceedings of the Petroleum Hydrocarbons and Organic Chemicals in Ground Water: Prevention, Detection and Restoration.* 355-368. Houston, Texas.

[52] Ogata, A. 1958. *Dispersion in Porous Media.* Ph.D. Dissertation, Northwestern University.

[53] Ogata, A., and R.B. Banks. 1961. *A Solution of the Differential Equation of Longitudinal Dispersion in Porous Media.* U.S. Geological Survey. 411-A.

[54] Perlmutter, N.M., and M. Lieber. 1970. *Dispersal of Plating Wastes and Sewage Contaminants in Groundwater and Surface Water.* U.S. Geological Survey. 1879-G.

[55] Pinder, G.F., and J.D. Bredehoeft. 1968. Application of the Digital Computer for Aquifer Evaluation. *Water Resources Research,* 6 (3) : 875-882.

[56] Pinder, G.F., and W.G. Gray. 1977. *Finite Element Simulation in Surface and Subsurface Hydrology.* New York: Academic Press.

[57] Pinder, G.F. 1979. *Galerkin Finite Element Models for Aquifer Simulation.* Princeton University. 76-WR-5.

[58] Remson, I., G.M. Hornberger, and F.J. Molz. 1971. *Numerical Methods in Subsurface Hydrology with an Introduction to the Finite Element Method.* New York: Wiley.

[59] Rifai, H.S., and P.B. Bedient. 1987. BIOPLUME II: Two-Dimensional Modeling for Hydrocarbon Biodegradation and In-Situ Restoration. In *Proceedings National Water Well Association Conference on Petroleum Hydrocarbons and Organic Chemicals in Groundwater.* 431-450. Houston, Texas: National Well Water Association.

[60] Rifai, H.S., P.B. Bedient, R.C. Borden, and J.F.Haasbeek. 1987. *BIOPLUME II: Computer Model of Two-Dimensional Contaminant Transport Under the Influence of Oxygen Limited Biodegradation in Groundwater, User's Manual, Version 1.0.* National Center for Groundwater Research, Rice University, Houston, TX, October, 1987.

[61] Rifai, H.S., P.B. Bedient, J.T. Wilson, K.M. Miller, and J.M. Armstrong. 1988. Biodegradation Modeling at a Jet Fuel Spill Site. *ASCE Journal of Environmental Engineering,* 114 : 1007-1019.

[62] Rifai, H.S., and P.B. Bedient. 1990. Comparison of Biodegradation Kinetics With an Instantaneous Reaction Model for Groundwater. *Water Resources Research,* 26 (4) : 637-645.

[63] Rifai, H.S., G.P. Long, and P.B. Bedient. 1991. Modeling Bioremediation: Theory and Field Application. In *Proceedings In-Situ Bioreclamation, Applications and Investigations for Hydrocarbon and Contamininated Site Remediation.* 535-541. Boston, MA: Butterworth Heinemann.

[64] Rozich, A.F., A.F. Gaudy, and P.D. D'Adamo. 1983. Predictive Model for Treatment of Phenolic Wastes by Activated Sludge. *Water Research,* 17 (10) : 1453-1466.

[65] Rozich, A.F., A.F. Gaudy, and P.D. D'Adamo. 1985. Selection of Growth Rate Model for Activated Sludges Treating Phenol. *Water Research,* 19 (4) : 481-490.

[66] Sauty, J.P. 1980. An Analysis of Hydrodispersive Transfer in Aquifers. *Water Resources Research,* 16 (1) : 145-158.

[67] Schafer, W., and W. Kinzelbach. 1992. Stochastic Modeling of an In-Situ Bioremediation in Heterogeneous Aquifers. *Journal of Contaminant Hydrology,* 10 : 47-73.

[68] Segerlind, A.E. 1985. *Applied Finite Element Analysis.* 2 ed. New York: Wiley.

[69] Semprini, L., and P.L. McCarty. 1992. Comparisons Between Model Simulations and Field Results for In-Situ Biorestoration of Chlorinated Aliphatics: Part 2. Cometabolic Transformations. *Groundwater,* 39 (1) : 37-44.

[70] Sims, J.L., J.M. Sufita, and H.H. Russell. 1992. *In-Situ Bioremediation of Contaminated Groundwater.* U.S. Environmental Protection Agency. EPA/540/S-92/003.

[71] Speitel, G.E., K. Dovantzis, and F.A. DiGiano. 1987. Mathematical Modeling of Bioregeneration in GAC Columns. *ASCE Journal of Environmental Engineering,* 113 (1) : 32-48.

[72] Srinivasan, P., and J.W. Mercer. 1988. Simulation of Biodegradation and Sorption Processes in Groundwater. *Groundwater,* 26 (4) : 475-487.

[73] Taylor, S., and P. Jaffe. 1990. Substrate and Biomass Transport in a Porous Media. *Water Resources Research,* 26 (9) : 2181-2194.

[74] Taylor, S., and P. Jaffe. 1991. Enhanced In-Situ Biodegradation and Aquifer Permeability Reduction. *ACSE Journal of Environmental Engineering,* 117 : 25-46.

[75] Taylor, S. 1993. Modeling Enhanced In-Situ Biodegradation in Groundwater: Model Response to Biological Parameter Uncertainty. In *Proceedings, 1993 Groundwater Modeling Conference. Golden, CO: International Groundwater Modeling Center.*

[76] Trescott, P.C., G.F. Pinder, and S.P. Larson. 1976. *Finite Difference Model for Aquifer Simulation in Two-Dimensions with Results of Numerical Experiments.* Techniques of Water Resources Investigations. U.S. Geological Survey.

[77] U.S. Environmental Protection Agency. March 1992. *Bioremediation Case Studies.* EPA/600/R-92/044.

[78] U.S. Environmental Protection Agency. August 1992. *Bioremediation of Hazardous Wastes.* EPA/600/R-92/126.

[79] van der Heijde, P.K.M., P.S. Huyakorn, and J.W. Mercer. 1985. Testing and Validation of Groundwater Models. In *Proceedings, Conference on Practical Applications of Groundwater Models.* 14-31. Columbus, Ohio: National Well Water Association.

[80] van der Heijde, P.K.M., and O.A. Einawawy. 1991. *Compilation of Groundwater Models.* International Groundwater Modeling Center. GWMI 91-06.

[81] van der Heijde, P.K.M., and O.A. Einawawy. 1992. *Quality Assurance and Quality Control in the Development and Application of Groundwater Models.* International Groundwater Modeling Center. GWMI 92-03.

[82] Wagner, D.M. 1990. *Biological and Physical Factors Affecting Sorption of Bacteria to Subsurface Particles.* M.S. Thesis, State University of New York at Buffalo.

[83] Widdowson, M.A., F.J. Molz, and L.D. Benefield. 1987. Development and Application of a Model for Simulating Microbial Growth Dynamics Coupled to Nutrient and Oxygen Transport in Porous Media. In *Proceedings AGWSE/IGWMCH Conference on Solving Groundwater Problems with Models.* 28-51. Denver, Colorado: National Well Water Association.

[84] Widdowson, M.A., F.J. Molz, and L.D. Benefield. 1988. A Numerical Transport Model For Oxygen and Nitrate Based Respiration Linked to Substrate and Nutrient Availability in Porous Media. *Water Resources Research,* 24 : 1553-1565.

[85] Widdowson, M.A. 1991. Comment on "An Evaluation of Mathematical Models of the Transport of Biologically Reacting Solutes in Saturated Soils and Aquifers" by P. Baveye and A. Valocchi. *Water Resources Research*, 27 (6) : 1375-1378.

[86] Wilson, J.L., and P.J. Miller. 1978. Two-Dimensional Plume in Uniform Groundwater Flow. *Journal of Hydraulics Division, ASCE*, 104 (HY4) : 503-514.